Nitrogen and Noble Gases in Carbonatites of India

A THESIS

submitted for the Award of Ph. D. degree of

Mohan Lal Sukhadia University

in the

Faculty of Science

BY

Sudeshna Basu

Under the Supervision of

Prof. S. V. S. Murty

PLANETARY AND GEOSCIENCES DIVISION
PHYSICAL RESEARCH LABORATORY, AHMEDABAD

MOHANLAL SUKHADIA UNIVERSITY, UDAIPUR

Year of submission: 2004

To

my dear grandmother, Didan

CERTIFICATE

This is to certify that the thesis entitled "Nitrogen and Noble Gases in Carbonatites of India" submitted for the award of the degree of Doctor of Philosophy of Mohanlal Sukhadia University in the faculty of Science is a record of bonafide investigations carried out by Ms. Sudeshna Basu under my supervision and guidance.

This is an original piece of work on which no one has been awarded a degree in this University or in any other University.

The literary presentation of the thesis is satisfactory and it is in a form suitable for publication. The work presented in the thesis has been done after registration in this University.

Further the candidate has put in attendance of more than 200 days in my institution as required under rule 7(b) and thus completed the residential requirement.

Professor S.V.S. Murty
(SUPERVISOR)

March 2004

Contents

Chapter 6

Acknowledgement

It has been quite sometime since 1998 when I joined PRL and, March 1999 when I joined the noble gas and nitrogen mass spectrometry lab here. Today when I sit to reflect the past few years, all I can say is that they were a mixture of good and bad as I think life should exactly be. But overall, the experiences have been very pleasant and I consider the years to be very fruitful for me. The present thesis work would not have been possible without the constant support and cooperation of a number of people. I would like to take this opportunity to thank all of them.

I love my lab, and learning here has been a great experience. I owe almost all of it to Dr. Murty, my supervisor. He guided me wonderfully giving me enough space so as not to curb my individuality, but at the same time propelling me forward. The world of noble gases and nitrogen is too vast, and maybe it requires a lifetime to master it. However Murty has opened the door to that intriguing world for me and I hope to make the most of it in future in terms of understanding this big Universe to which we all belong. I must also mention here that during my association with him I have never thanked him with formal words of 'Thank you' every time I should have. I thought it would have to be too many times a day anyway! Today I thank him with all my heart for his patience and encouragement all along.

I was lucky enough to have Ratan, Vinai, Ramakant and Jayesh as colleagues in my lab. Their cooperation and friendliness added to the enjoyment of my work. During high and low (like the leak problems!), they were always there to listen, understand and help out.

I am indebted to the faculties of PGSDN here for their comments and suggestions during various phases of my work that certainly added to its quality. I was lucky to have Dr. J. S. Ray as my expert during synopsis. His suggestions were of immense value to me at various points during the last two years. I must thank Dr. Kanchan Pande for his constant assistance and interest in my work and for accompanying me to the fields of Sung Valley and Ambadongar. I am grateful to Dr. P.N. Shukla for his invaluable suggestions on many occasions. Special thanks are also due to Dr. Ramesh, my expert in the second year review, Dr. Goswami, Dr. Bhattacharya, Dr Krishnaswami, Dr. Somayajulu, Dr Sarin, Dr Singhvi, Dr Venkatasen, Dr Trivedi and Dr Gupta for their inputs during various area seminars. I must also mention the cooperation of Dr. M. Yadava and Mr. N.B. Vaghela in whose lab I packed and weighed my samples before analyses. Besides the regular area seminars of the division, the informal Friday talks among the small group of 'TGIF gang' were extremely beneficial for me.

I am indebted to Dr. Sarin for my chemical analysis. I express my heartfelt gratitude to Sudheer for his utmost cooperation and help rendered during the period. Special thanks are also due to Anirban for helping me with the chemical analyses of my samples. Also, I would like to thank Mr. J. P. Bhausar for his assistance on numerous occasions.

I must extend my thanks to Dr. Bhandari for allowing me to use the Logitech facility in PLANEX for making thin sections. I acknowledge Deepak for helping me with the sections.

I express my thanks to Mr. V.G. Shah for his help during XRD analysis of the samples. In this regard I also thank Mr. Pratipal of IPR where the XRD studies had been done.

My sincere appreciation to Mr. M.P. Kurup and Mr. K.K. Sivasankaran (for glass blowing), Mr. M. L. Mathew and Mr. J.A. Patel (liquid nitrogen) and Mr. Ubale and his team for their excellent support and expertise. Without any one of them, it would be impossible to keep the instrument running in the lab. I gratefully acknowledge the library and computer staff for their assistance. I extend my thanks to the electronics staff members Mr. V.G. Shah and Pandianji for their help in maintaining the instrument in proper working conditions in the lab. I should also thank Arjun bhai for his assistance during my experiments in fetching liquid nitrogen from the plant. I express my gratitude to various PGSDN office staff members especially Thomas, Nambiar and Pauline for their cooperation.

My sample collection during various occasions in the field would not have been possible without the cooperation of GMDC (Ambadongar) and organizers of the 'Symposium of Carbonatite and Alkaline Magmatism' (2001, Chennai). My sincere thanks to all of them including the various rock cutters and porters who had helped me greatly. Also I profoundly thank Dr. A. Kumar for providing me some of the samples from Hogenakal, Khambamettu and Sevattur. I must also thank Dr. J. S. Ray for providing some samples from Ambadongar and Oldoinyo Lengai, and Dr. F. Wall for sending me samples from Kola carbonatites.

I would like to thank Prasanta, Alok, Tarak and Lokesh who had helped me on numerous occasions during my stay here. I express my heartfelt gratitude to all of my friends in PRL for making my stay here so lovely. The list is too long to name each of them individually, but all of them here today and those earlier have contributed to make this stay worthwhile. The formal and informal discussions over breakfast, lunch tea and dinner made life entertaining and worth every minute of it. I thank the great PRL family back in our hostel for being what it is and each member for just being what they are, each one special and unique in their own way.

The biggest debt I owe to my family. The affections showered on me by my Baromama, Chotomama, Maima, Mamin, Chotto Bubka and Rolla, Dibhai, Paludada, Ronnie, Mejomoni, Botumoni transgresses the distance and keep me going. My parents-in-law and Calisto have been a constant source of encouragement and affections. I believe the blessings of my grandparents Didan and Mummum keep me insulated from all evils. My loving 'little brother' Dipan has been always there to listen, understand and help out. The constant unconditional love and support of my best friend, my husband, the very anchorage of my life had kept me going even during those 'thesis blue' periods. Finally, for my parents, I am at a loss for words as I owe it all to them.

Abstract

The Earth's mantle constitutes 82% of the total volume and 65% of the mass of the Earth. It is the dynamism of the mantle that accounts for the various magmatic processes we see on the surface of the Earth. In fact, it is definitely known today that degassing of the mantle has formed our atmosphere. The earth's atmosphere and the mantle behave as a coupled system interacting with each other continuously via the processes of magmatism that transfers volatiles and materials from the interior to the surface. On the other hand, materials from the surface are transported to the interior by the process of subduction. Thus there is a continuous exchange between the two.

It is well known that nitrogen makes up to 78% of the atmosphere. What is interesting is the fact that the interior of the Earth (upper mantle) and the atmosphere are in isotopic disequilibrium. Since N makes up the bulk of the atmosphere, and since its isotopic signature is distinct between the atmosphere and the mantle, it can be very useful as tracer to understand the interaction between the two, and hence for better understanding the evolution of the atmosphere and the mantle.

However, our understanding of the mantle N is constrained by the lack of estimate of $\delta^{15}N$ and $N_2/^{36}Ar$ for the lower mantle. Constraining the lower mantle $\delta^{15}N$ signatures can provide better understanding regarding evolution of terrestrial N. They can answer important questions like if N is still locked up in the mantle, or if it has escaped by hydrodynamic escape. The parameters will also provide answers to the nature of N in the mantle, if it is in the pristine or recycled form. Our understanding on mantle depends on samples brought to the surface by various magmatic processes.

Carbonatites are magmatic rocks with more than 50% of carbonate minerals in them. These rocks are extremely rich in volatiles and span over a range in age from late Archean to very recent. Found mostly in continental settings, they can help in better understanding of the evolution of the subcontinental mantle. Since these rocks are derived from a volatile enriched source, they have been selected for the study of noble gases and N in them. Many isotopes of noble gases have distinct signatures for upper and lower mantle. The main objective of studying noble gases in these samples was to constrain their source region in the mantle. If indeed they were derived from the lower mantle, they would be appropriate to constrain the lower mantle $\delta^{15}N$. But, till date,

there are very few studies on volatiles in carbonatites due to the difficulties involved in separating the trace amount of the gases of interest from the high amount of other volatiles. This is the first attempt to study N and noble gases in carbonatites of India.

The volatiles in the samples are likely to have more than one component present in them. In addition to the trapped gases, they would also have contribution from nucleogenic/radiogenic/fissiogenic sources produced in the samples after their crystallization. In order to minimize contribution of these later produced gases, experiments have been carried out where mineral separates (carbonates, apatites and magnetites) have been analyzed for noble gases and N by vacuum crushing. In this process, preferentially the gases residing in the vesicles, which are of trapped origin, are released when they are ruptured on crushing. It is clearly seen from our study that all the carbonatites are multicomponent systems, and no unique source region in the mantle may be ascribed to them. The Sung Valley and Ambadongar carbonatites are dominated by lower mantle volatiles while the South Indian carbonates studied have considerable fraction of upper mantle volatiles in them. However, the apatites from the South Indian carbonatites, in contrast to their carbonates are dominated by lower mantle component. This indicates that carbonatite formation was much more complex and related to more than one generations of magma. In fact, the evolution of magma is recorded in the fluid inclusions where different generations of inclusions, having different sizes have different isotopic composition depending on its interaction with the evolving magma. Such evidences are apparent from both N and noble gases. It is clearly seen from the present study that the samples have recycled volatiles, incorporated at shallow depths in addition to mantle volatiles. Probably because the recycled volatiles were incorporated at a shallow depth, the duration of time was not adequate for its complete homogenisation with the mantle gases. This is especially true for N where the recycled form of N is likely to be dominantly of some solid, inorganic form residing in the lattice of the mineral. A small fraction of gas that resides in the fluid inclusions still preserved its mantle signature. The distinction between the two N components, the recycled one in the lattice released during pyrolysis, and the pristine mantle component in the inclusions released during crushing is clearly seen for the apatites for which both pyrolysis and vacuum crushing have been done. From our study it has been possible to constrain the $\delta^{15}N$ of the lower

mantle to be ~ -20‰. From our work it is also seen that atleast 5 ppm of N in its pristine form is locked up in the lower mantle.

The in situ noble gases present in the U,Th rich apatites released during pyrolysis of the samples have been used as geological clocks. For the first time, the U,Th-^{21}Ne systematic has been used along with the already existing U,Th-^{4}He and U-^{136}Xe dating tools. In conjunction, the three tools prove to be very informative in delineating the thermal history of the terrain.

List of Tables

List of Figures

Chapter 1

Introduction

1.1 Interior of the Earth

Evidences from seismology indicate that the earth has a layered structure (Fig. 1.1). According to chemical composition, the layers consist of the crust, mantle and the core. The uppermost layer comprises the crust that is variable in thickness as well as in composition. The continental crust is *andesitic* in composition, and 10-70 km thick while the oceanic crust is only 8-10 km thick and *basaltic* in composition. Of the total silicate present in the earth, ~0.6% is concentrated in the crust. The rest of the silicate mass of the earth is concentrated in the underlying layer, the mantle. The mantle constitutes the major portion of the earth accounting for 82% of its volume and 65% of its mass (Helffrich and Wood, 2001), and extends from the base of the crust to a depth of ~2700 km. In terms of physical properties, the mantle is further divided into the lithosphere (brittle), 100-200 km thick, comprising of the crust and part of the upper mantle, and the asthenosphere (solid but capable of flowing) (Hoffman, 1997). Beneath the mantle, lies the core that is essentially Fe-Ni in composition and concentrates most of the siderophile elements of the earth. At the core-mantle-boundary (CMB), seismic evidences suggest the presence of the D" layer that is about 200 km thick, with the thickness varying at various points (Brandon et al., 1998). The region shows discrete discontinuous scattering features, which in conjunction with other evidences indicate it to be a layer with lateral chemical heterogeneities that differ chemically from the overlying mantle. Besides the seismic discontinuity at D" layer, a look at the seismic structure of the mantle indicate major discontinuities at 410 km and 660 km. These discontinuities can be related to phase transformations of olivine to *wadsleyite* at 410 km, and *ringwoodite* to *perovskite* and oxide at 660 km (Helffrich and Wood, 2001).

The interior of the earth has always been of much interest as many of the different processes on the surface of the earth like earthquakes and volcanoes are manifestation of occurrences within the mantle. These processes are a direct consequence of thermal convection in the mantle induced when the thermal gradient is high enough, for

example due to the transfer of heat from the earth's core to the mantle. This causes the material at depth to expand so that its density becomes lower than the material above it. As a result of this unstable situation, the hotter, lower density material from depth

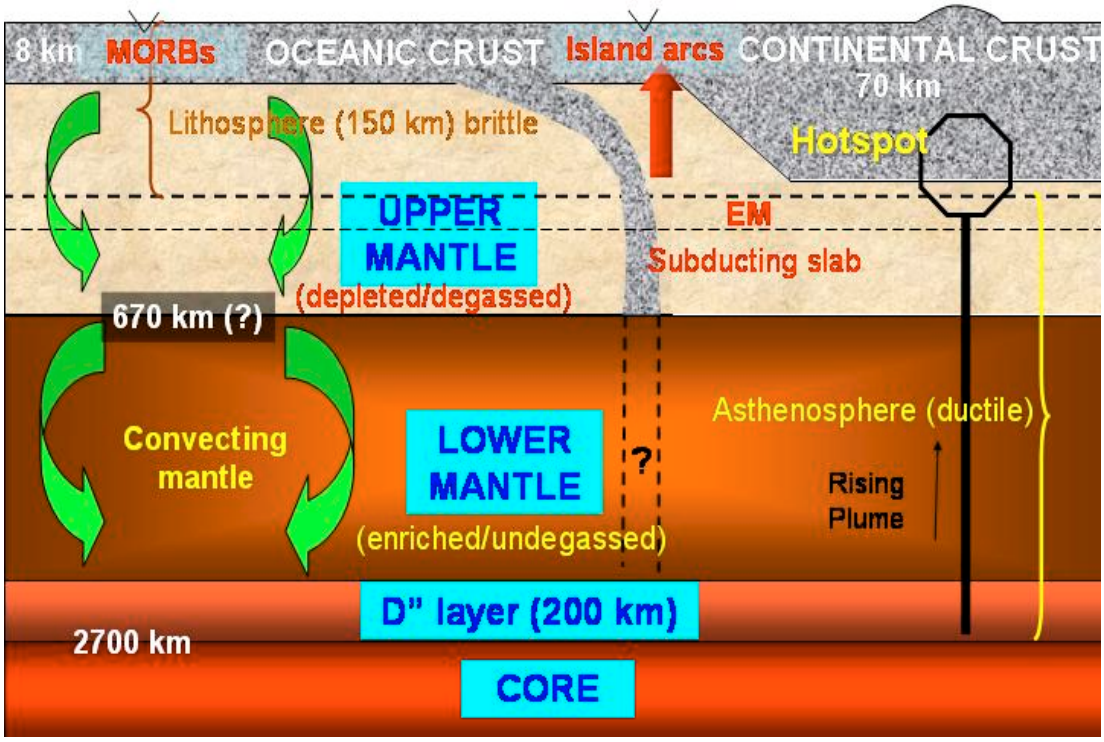

Fig. 1.1 The stratified, heterogeneous interior of the earth (not to scale). See text for discussion

will rise up and get replaced by the descending cooler material in a convecting cell. Relative motions of the continents, the formation of new crust and volcanism are all related to the process of convection in the mantle. At oceanic ridges where mantle ascends due to rising convection currents, followed by decompression melting, magmas are generated that erupt to form the MORBs (Mid-oceanic-ridge-basalts). Then when oceanic lithosphere, owing to convection runs into another oceanic lithospheric plate and subducts beneath it, the ensuing volcanism results in island arcs. Often, there are long lines of ocean island volcanoes as in Hawaii of progressively increasing ages (Oceanic-Island-basalts or OIBs). They are formed by stationary heat source or hot spot, which causes thin plumes of mantle materials to rise along narrow zones from the deeper mantle. The hot spot remains stationary in the mantle while the plate moves over it.

1.2 Mantle samples

Although the earth's interior is of tremendous interest to geoscientists, it is still not directly accessible. The deepest borehole so far has been only 12 km. Thus most of

our understanding of the mantle has depended on indirect means like seismic studies, modeling and laboratory simulation experiments, as well as from the studies of samples brought from the mantle to the surface of the earth by various volcanic processes. Such commonly studied mantle samples are MORBs, OIBs, diamonds and xenoliths. MORBs and OIBs are basalts that pour out on the surface of the Earth in the oceanic environments. Conventionally, the MORBs are believed to be samples from the upper mantle while OIBs are extracted from the deeper levels of the mantle, probably the lower mantle. Diamonds are mantle samples that come from depths in excess of 150 km and are present as inclusions in the kimberlites and lamproites in ancient cratons. On the other hand, the mantle xenoliths are fragments of the mantle accidentally entrained in the rising magma.

1.3 The heterogeneous mantle

Evidences for the heterogeneous nature of the mantle come from geochemical studies of various trace elements. When a mantle region melts, it loses its incompatible elements to the melt that is concentrated in the oceanic or continental crust that forms. Sr and Nd isotopes have been used to characterize the mantle into enriched and depleted regions (Hoffmann, 1997). Since Rb is less compatible than Sr, and Sm is more compatible than Nd, in general $^{143}Nd/^{144}Nd$ correlates negatively with $^{87}Sr/^{86}Sr$. The MORBs that are depleted in incompatible elements have lower Rb/Sr and therefore lower $^{87}Sr/^{86}Sr$ ratios coupled with higher Sm/Nd and consequently higher $^{143}Nd/^{144}Nd$ ratio. Continental crust, which is enriched in incompatible elements, shows just the reverse trend. In the array of Sr and Nd isotopic data, the position of the OIBs are between the depleted MORB source and the continental crust suggesting that the OIBs could simply be the result of recycling of various types of crustal material into the mantle. The isotopic variability for the OIBs indicates strongly the presence of extreme end member components preserved in the mantle namely *HIMU, EM-I* and *EM-II* (See Appendix for explanations).

Some people advocate the presence of a shallow enriched mantle layer just below the lithosphere (EM in Fig. 1.1). This zone is believed to be a buoyant mobile layer being continuously nourished by subducting N and noble gases (Mohapatra, 1998; Mohapatra and Murty, 2000a). Presence of such a layer in the mantle, enriched by recycled gases introduced by subducting slab in a mantle wedge setting is not unlikely (Matsumuto et al., 2001).

1.4 Noble gases in the mantle

Evidences for the heterogeneous nature of the mantle also come from noble gas studies in various mantle samples. The earth's mantle is stratified into the degassed upper mantle and the less degassed lower mantle based on noble gas isotopic systematics of MORBs and OIBs that are believed to represent the upper and lower mantle respectively. Since the noble gases are chemically inert and only experience weak Van der Waals interactions, they act as excellent tracers to understand the evolution of the mantle. Various noble gas isotopic ratios of different reservoirs of the earth are summarized in Table 1.1. Some noble gas isotopic ratios like $^{22}Ne/^{20}Ne$ and $^{129}Xe/^{132}Xe$ are characteristic of mantle regions and are very different from air. Then there are other isotopic ratios like that of $^{3}He/^{4}He$, $^{21}Ne/^{20}Ne$ and $^{40}Ar/^{36}Ar$ that are not only different for air and the mantle, but have different value for the lower and upper mantle as well. These various isotopes can be used to trace the source of the sample and its subsequent evolution.

Samples like the popping rock 2πD43 dredged from North Atlantic from a considerable depth of 3510 m have been studied extensively and are considered to be good representative samples of the upper mantle (Moreira et al., 1998). Very precise measurements of noble gases in these samples have been possible owing to the high vesciculariy (16 to 18%) and therefore high gas concentrations in these samples. The Hawaiian and Icelandic basalts are considered to be good representative samples of the LM. Table 1.2 lists the various noble gas isotopes found in different mantle samples. The different isotopes may be only primordial, or may be generated by other radioactive processes. Accordingly, they will evolve in the various mantle reservoirs. Because the He content in the atmosphere is very low, it acts as an excellent tracer for mantle sources and yield evidences for two distinct mantle reservoirs. The popping rock and most other ridge basalts have $^{3}He/^{4}He$ value between 6.5-9.5 R_A, while that of the Hawaiian and Icelandic plumes lie between 35-43 R_A (Graham, 2002).

From some recent studies, the $^{20}Ne/^{22}Ne$ ratio in different mantle plumes and MORB reservoirs has been constrained to be ~ 12.5 which can be considered the end member ratio in the mantle (Moreira et al., 1998; Honda et al., 1991; Trieloff et al., 2000; Trieloff et al., 2002). This value is close to Ne-B that is the typical signature of solar neon implanted as solar corpuscular radiation. Analyses of Popping rock have

demonstrated a good correlation between $^{40}Ar/^{36}Ar$ versus $^{20}Ne/^{22}Ne$ ratios where the best hyperbolic fit is achieved for r = 1.6±0.1[r defined as $\{(^{22}Ne/^{36}Ar)_{mantle}/(^{22}Ne/^{36}Ar)_{air}\}$] (Moreira et al., 1998). The maximum $^{40}Ar/^{36}Ar$ measured is 28000, that is in agreement with value obtained from correlation of $^{20}Ne/^{22}Ne$ and $^{40}Ar/^{36}Ar$. Analyses of single vesicles from the same sample have expanded the range of $^{40}Ar/^{36}Ar$ up to 40000 in the UM.

Table 1.1. Some isotopic and elemental ratios for different reservoirs of Earth
[Ozima and Podosek 2002, Mohapatra and Murty 2002, Mohapatra and Murty 2004].

Isotopic ratio	UM	LM	Air	Recycled
$^{3}He/^{4}He$	≈8.5R_A	≈(12 to52)R_A	1R_A	≤1R_A
$^{21}Ne/^{20}Ne$	0.0048	0.0032	0.00296	0.00296
$^{22}Ne/^{20}Ne$	0.08	0.08	0.1020	0.1020
$^{40}Ar/^{36}Ar$	≥40000	≤8000	295.5	≈375
$^{129}Xe/^{132}Xe$	1.12	1.12	0.9832	0.9832
$\delta^{15}N$(‰)	-5 to -15	?	0	+5 to +19
$N_2/^{36}Ar(10^6)$	5	?	0.0249	16.67
	200	12	≅1	670

$R_A = (1.4x10^{-6}) = (^{3}He/^{4}He)_{air}$

For LM, from measurements of Loihii basalts the ratio has been constrained to be ~ 8000. The $^{129}Xe/^{130}Xe$ ratio of the upper mantle is derived from the correlation of $^{129}Xe/^{130}Xe$ vs. $^{20}Ne/^{22}Ne$ in popping rock 2πD43 (Moreira et al., 1998). For a mantle ratio of ~ 12.5 for $^{22}Ne/^{20}Ne$, the corresponding $^{129}Xe/^{130}Xe$ is ~ 7.5. However similar estimates of LM could not be made as Xe isotopic ratios for OIBs are atmospheric. But Brazilian carbonatites, that originate from the less degassed LM, have $^{129}Xe/^{130}Xe$ ratios similar to that of UM (Sasada et al., 1997). For Kr, isotopic composition in mantle samples is identical to that of the atmosphere.

The isotopic compositions of the noble gases are closely related to the geochemical processes controlling the distribution of K, U and Th (Graham, 2002). The isotopic make up of every noble gas is modified by the radioactive decay of these elements. The geochemical distribution of He is directly related to α-particle-production by U and Th. As a result of both outgassing and the subsequent decay of U and Th, the $^{3}He/^{4}He$ ratio in the upper mantle is significantly lower than in lower mantle. For Ne,

while ^{20}Ne is a primordial isotope, both ^{21}Ne and ^{22}Ne are produced in the mantle from the reactions $^{18}O(\alpha,n)^{21}Ne$, $^{19}F(\alpha,n)^{22}Ne$ and $^{25}Mg(n,\alpha)^{22}Ne$ where α particles are generated from the decay of U and Th (Leya and Weiler, 1999). Like in case of $^{3}He/^{4}He$ ratios, the same process of outgassing and subsequent decay controls the $^{21}Ne/^{20}Ne$ and $^{22}Ne/^{20}Ne$ ratios in the mantle. Similarly radioactive decay of ^{40}K controls the Ar isotopic composition. In the more degassed upper mantle where K/Ar ratio is higher, subsequent decay of ^{40}K to ^{40}Ar raises the $^{40}Ar/^{36}Ar$ ratio to much higher values of ~40000 as compared to lower mantle $^{40}Ar/^{36}Ar$ ratio of ~ 8000.

Table 1.2. Noble gases and nitrogen and their stable isotopes. Primordial isotopes in the mantle are indicated in bold. Others may be generated by radiogenic/nucleogenic/fissiogenic processes

Element	Isotopes								
He	**^{3}He**	^{4}He							
N	**^{14}N**	**^{15}N**							
Ne	**^{20}Ne**	^{21}Ne	^{22}Ne						
Ar	**^{36}Ar**	^{38}Ar	^{40}Ar						
Kr	**^{78}Kr**	**^{80}Kr**	**^{82}Kr**	^{83}Kr	^{84}Kr	^{86}Kr			
Xe	**^{124}Xe**	**^{126}Xe**	**^{128}Xe**	^{129}Xe	**^{130}Xe**	^{131}Xe	^{132}Xe	^{134}Xe	^{136}Xe

Noble gases isotopic ratios can be thus very useful to identify trapped components in the samples since they are distinct for air and different mantle components. The trapped gases essentially would reflect the source region of the samples, and hence may throw a light on the genesis of the rocks. The trapped gases present in the samples may be a mixture of air and/or mantle gases. The air like signatures may reflect air contamination or the presence of air like gases in the source region introduced into the mantle by recycling (Mohapatra and Murty, 2000a; Matsumoto et al., 2001). Mantle gases may be tapped from the lower or upper mantle or have a mixture of gases from both the regions depending on the origin of their magma, its subsequent migration and history before crystallization.

Subsequent to crystallization, *in situ* noble gases may be generated in the samples by fissiogenic, nucleogenic and radiogenic processes. This will depend on the concentration of the parent elements like U, Th and K in the samples, as well as the target element concentration of O and F for the generation of nucleogenic Ne. Presence of any such *in situ* component in a sample may be identified from the deviations of the isotopic ratios from that expected for mantle and/or air. Thus all the

isotopic ratios have been normalized to a primordial isotope. In order to identify contribution from any post crystallization produced nucleogenic ^{21}Ne or ^{22}Ne in the samples, the primordial isotope ^{20}Ne has been used for normalization in the present study, contrary to the widely used practice of normalizing the ratios to ^{22}Ne.

Besides isotopic ratios, elemental ratios of noble gases can also be very useful to understand various magmatic processes. Noble gas elemental fractionation during magmatic processes shows a coherent light-to-heavy noble gas trend that reflects the physical processes at hand. For example, degassing of melts will lead to enrichment of the heavier noble gases like Ar and Xe in the exsolved (volatile) phase compared to the lighter species like He and Ne. The residual melt will show the opposite effect with a preferential depletion in the heavier species compared to the lighter ones.

1.5 Nitrogen in the earth's mantle

The study of nitrogen in various mantle samples is of considerable interest as it commonly occurs as an inert diatomic gas and therefore, like noble gases should be very useful tracers for understanding the mantle evolution. Also, nitrogen is the dominant constituent of the atmosphere accounting for ~ 78% of it. The nitrogen in the earth's atmosphere is derived by catastrophic degassing of the earth's mantle like the rare gases (Sano et al., 2001). This conclusion has been reached following the estimate of the total N flux that amounts to 2.8 x 10^9 mol/yr considering the output from MORBs, hot spots and subduction zones. Considering a constant flux for the 4.55 billion years, the total N can account for an order of magnitude less than the present inventory of N at the Earth's surface. Thus understanding the mantle N becomes very important for better understanding of the evolution of the earth's atmosphere also.

The nitrogen isotopic composition is highly variable among the different reservoirs of the earth as seen from Table 1.1. To some extent this isotopic imbalance can be accounted for by the evolution of terrestrial N since the accretion of the earth from E-chondritic material (Javoy and Pineau, 1983; Javoy, 1997). The mantle isotopic composition is being continuously modified by sedimentary rocks and basalts involved in subduction metamorphism that release nitrogen and increase the $\delta^{15}N$ in the residual N towards more positive values. An intriguing question at this juncture is the depth to which N may be recycled. Addition of sediment-derived N to the mantle sources is expected to result in higher N_2/He ratio and more positive $\delta^{15}N$ values.

Positive value of $\delta^{15}N$ up to ~6.3‰ and N_2/He ratio as high as 25000 in the Central American volcanic arc of Guatemala suggests shallow hemipelagic sediments as the transporting medium for the heavy nitrogen (Fischer et al., 2002). Mass balance calculations show that the subducted N is efficiently recycled to the atmosphere by arc volcanism indicating the presence of subduction barrier for the deep recycling of N. It is however important to keep in mind that the modification of N isotopic composition during subduction as well as to the depth to which it may be recycled depends on the prevailing geothermal gradient. Studies of metasediments from the Western Alps show an excellent correlation between N and K content (Busigny et al., 2003). From the K content of average oceanic subducted sediments, the N content can be estimated. Considering the total flux of subducted sediments the flux of recycled N has been estimated to be 7.6×10^{11} g/yr. From the N output flux estimates available, it can be deduced that 60-100% of the sedimentary N is recycled back to the deep mantle. Also the constancy of K/N ratio, along with that of K/Rb and K/Cs indicate that none of these fluid mobile elements were lost in the process of devolatilization during subduction atleast to a depth of island arc magmatism. $\delta^{15}N$ value of ~+3‰ for Kola carbonatites which are believed to be related to a LM source is clear evidence of recycled nitrogen into the deep mantle (Dauphas and Marty, 1999).

Study of N in the mantle is still at a stage of infancy and there are still many unanswered questions. An important question is the amount of N locked up in the mantle, and whether it is in the pristine or recycled form. Estimation of N locked up in the mantle, as well as understanding the nature of N in the mantle, pristine and/or recycled remain incomplete without better understanding and constraining the lower mantle for N concentration and isotopic signatures. The present thesis work ***'Nitrogen and Noble Gases in Carbonatites of India'*** is carried out with the objectives of constraining the $\delta^{15}N$ and $N_2/^{36}Ar$ of the lower mantle, and estimating the N that may be locked up in the deeper mantle of the earth.

A vital question is whether the nitrogen cycle of the past was identical to the present day nitrogen cycle on earth. Important consideration is the evolution of the convection regime of the Earth, and hence subduction through time. Also the higher heat flow might affect recycling during the Archean. Some authors argue that formation of a thicker basaltic crust during the Archean would prohibit subduction and recycled material has been able to penetrate into the deep mantle only as recently as $\leq$ 500 Ma

(Vlaar et al., 1994; Allegre, 1997). However there are experts who believe that subduction occurred even during the Archean and probably at a much faster rate based on the fact that the Archean crust has been formed by melting of subducted material (Martin, 1986). Again Late Archean Re-Os model ages of sulphide inclusions from eclogitic diamonds of Kaapvaal craton speak for subduction of oceanic crust at that time (Richardson et al., 2001; Pearson et al., 1998). Studies from Isua supracrustal belt of West Greenland is believed to suggest plate tectonics including subduction operating as early as 3.8 Ga (Komiya et al., 1999).

The biologic process controlling the surface N isotopic signature in the present day was different during the early history of the earth as indicated from some studies. Light nitrogen with $\delta^{15}N$ value of ~-7.4‰ has been identified from metasediments of Pilbara craton, 3.8 to 2.8 Ga accompanied by non atmospheric Ar and released at 1000°C (Pinti et al., 2001). The light nitrogen signature observed has been attributed to metabolic isotopic fractionation induced by chemosynthetic bacteria using inorganic NH_4^+. This is probably related to changes in the redox potential of the Earth, which had a much lower fO_2 during the Archean. The study of Moine metasediments (Peters et al., 1978) also show the $\delta^{15}N$ value to change in the kerogens from –6.2 to +10‰ from the Early Archean to Late Proterozoic (Beaumont and Robert, 1999). However, as implied from the study, as early as the Late Proterozoic a modern like nitrogen cycle dominated by nitrate species had already come into existence, and thus the effect of the different biological process during the Archean and Early Proterozoic on surface N must have been very limited.

1.6 Carbonatites as mantle representatives

One of the challenges of analyzing N in different mantle samples lie in the presence of very low amounts of N (mostly a few ppm) in them. This also makes them very prone to surficial contamination (both atmospheric and organic). However, the study of N in mantle samples has become feasible with the recent advent of highly sensitive, static mass spectrometry that circumvents many of the experimental problems otherwise faced (Frick and Pepin, 1981).

Recently, carbonatites are largely being analyzed as representatives of the mantle. These rocks by definition, are igneous rocks with >50% by volume of carbonate minerals. Their peculiar chemistry is believed to be the result of immiscibility reactions between CO_2 rich fluids and alkaline melts (Brooker, 1998) or more rarely

as primary melts (Wyllie and Lee, 1998). A rather debatable question about the carbonatites is the source of the huge amount of C present in these rocks. C in the mantle occurs in trace amounts while it is present at several per cent level in the carbonatites. While some advocate a recycled origin for the huge amount of C (Ray et al., 1999), others propose its derivation from primordial sources (Sasada et al., 1997). Advantages of carbonatites as mantle representatives lie in their low viscosity, and therefore their interaction with large volumes of the mantle. The petrology and trace element geochemistry of carbonatites indicates their derivation from a metasomatically processed volatile element enriched mantle source (Anderson, 1987; Hawkesworth et al., 1990; Kramm and Kogarko, 1994). Thus they can be expected to contain large amount of volatile elements like noble gases and N and must be very appropriate for the present study. They also show considerable similarities both isotopically as well as chemically with oceanic islands or sea mounts (Grunnenfelder et al., 1986; Nelson et al., 1988; Bell and Bleckinsop, 1989; Kwon et al., 1989) indicating probably common sources and processes. Since these oceanic island basalts are believed to originate probably from the lower mantle, there is every possibility that the carbonatites too sample the deep mantle regions of the earth. Indeed, some recent analyses of He and Ne isotopes from carbonatites of Kola Peninsula suggest their origin to be plume related from the lower mantle (Marty et al., 1998). However, now there seems to be general agreement that carbonatites can be produced in different ways, thus all carbonatites need not be related to plumes or originate from the deep mantle. Rather the controlling factors for the generation of carbonatitic melts is high fugacity of CO_2 and undersaturated alkaline magma composition (Wyllie, 1989).

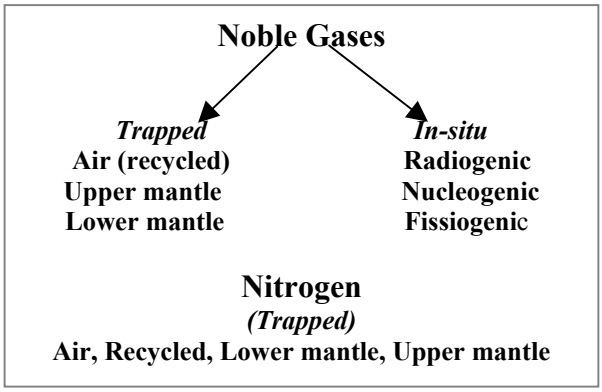

Fig. 1.2. The various components expected for noble gases and N in carbonatites

Except two known oceanic carbonatites, all other carbonatites are found in continental settings. Thus study of carbonatites can help us to understand better the evolution of the sub-continental mantle over atleast 2.7 Ga.

1.7 Experimental approach

A coupled N and noble gas study on carbonatites was undertaken for the present thesis and the experimental approach was designed keeping in mind the various components expected in the samples. The analyses of carbonatites by melting the bulk samples to extract the gases present in them is not possible as it would be impossible to separate the trace amount of noble gases and N from the huge amount of CO_2 that would be liberated in the process. Keeping this in mind, minerals like carbonates, apatites and magnetites were separated from the bulk rocks and analyzed by vacuum crushing. As seen from Fig. 1.2, noble gases consist of two components, namely the trapped gases incorporated from the source mantle region, and the *in situ* gases generated in the samples after their crystallization. The trapped gases are mainly hosted in the vesicles and released during crushing when they are ruptured. During vacuum crushing, only the fluid inclusions present in the samples are ruptured so as to preferentially release the gases trapped in them with minimum damage to the lattice structure of the minerals. The trapped noble gases may be air-like, or from the upper or lower mantle as the case may be. On the other hand the *in situ* gases remain exclusively in the lattice of the mineral and may be extracted on melting the sample so that the lattice structure is damaged. Only apatites have also been analyzed by vacuum crushing as well as by completely extracting the gases by melting the samples by pyrolysis. Unlike noble gases, N does not have any *in situ* component present, and the trapped gases may be air-like or from the mantle. N incorporated from subducted component may also be present in the samples as seen from Fig. 1.2. The carbonatites studied for the present thesis belong to Hogenakal, Sevattur, Khambamettu, Sung Valley and Ambadongar. The sample locations are shown on the Indian map in Fig. 1.3.

1.8 Objectives of the present study

- Noble gas isotopic systematics can be very useful to identify the trapped components in any mantle sample. In the present study, they will be useful to look for the presence of lower mantle and/or upper mantle volatiles as the case may be in the samples and therefore identify the source of the carbonatitic melts.
- If the carbonatites indeed come from the lower mantle, they may be ideal samples to constrain the lower mantle $\delta^{15}N$ and $N_2/^{36}Ar$ ratios, as well as estimate the N concentration in the lower mantle.

- Both $\delta^{15}N$ and $N_2/^{36}Ar$ values are very distinct between air and recycled components. They can act as excellent tracers to look for the presence of any recycled component that may be present in carbonatites.
- Since carbonatites cover a broad range of age, they have been analyzed from diverse locations covering a range of age from 2400 Ma (Hogenakal) to 65 Ma (Ambadongar), they can help to understand the temporal evolution of the mantle in terms of volatiles.
- Minerals like apatites analyzed from these carbonatites are rich in U and Th. Also, apatites have abundant O and F present in them, and *in situ* production of nucleogenic Ne in the apatites from the reactions $^{18}O(\alpha,n)^{21}Ne$ and $^{19}F(\alpha,n)^{22}Ne$ are expected. This is the first attempt to check the feasibility of using U,Th-^{21}Ne and U,Th-^{22}Ne as dating tools in such samples along with the already existing dating systematics of U,Th-^{4}He and U-^{136}Xe.

1.9 The samples

The samples analyzed, as mentioned earlier have been selected from both temporally as well as spatially varied settings. Fig. 1.3 shows the various sample locations of the present study. This section is a brief coverage of each studied carbonatite, its geological settings and the important information available from previous studies.

1.9A Hogenakal: The Hogenakal carbonatitic complex is emplaced into a series of deep NNE to NE trending fracture zones in the southern Indian craton (Grady, 1971) where low grade metamorphic Peninsular Gneiss to the north grades into granulite facies rocks to the south (Condie et al., 1982). Both Rb-Sr and Sm-Nd isochron ages for Hogenakal indicates its emplacement into the crust at 2.4 Ga (Kumar et al., 1998). The C and O isotopic signatures of the Hogenakal carbonatites are typically mantle like ($\delta^{13}C$ = ~-6 ‰ and $\delta^{18}O$ ~ 8 ‰) (Pandit et al., 2002). From Nd and Sr isotopic data, while Kumar et al., (1998) infer an enriched mantle source for the Hogenakal carbonatite, Pandit et al., (2002) suggest a depleted source for the same.

1.9B Sevattur: The Sevattur carbonatite is spatially associated with the Hogenakal carbonatite and located only 70 km ENE of it. However it is a much younger complex as compared to Hogenakal, its age being 0.77 Ga as implied by the mica-whole rock Rb-Sr isochrons for the carbonatites (Kumar et al., 1998). The Sr-Nd isotopic data are compatible with an enriched mantle source for the Sevattur carbonatites (Kumar et al., 1998; Pandit et al., 2002). C isotopic signatures indicate these carbonatites to be

relatively enriched ($\delta^{13}C$ = -5.3 to -3.3‰) as compared to Hogenakal (Pandit et al., 2002). Its O isotopic signature also shows a range of value ($\delta^{18}O$ = 7.3 to 15.4‰) indicating variable degree of post-magmatic low-temperature alteration (Pandit et al., 2002).

1.9C Sung Valley: The Sung valley carbonatitic complex occur in a horst like feature called the Assam-Meghalaya Plateau and are bounded by two E-W trending faults namely the Brahmaputra fault to the north and Dauki fault to the south (Kumar et al., 1996; Veena et al., 1998). The age of this carbonatite, as constrained by $^{40}Ar/^{39}Ar$ dating is 107.2±0.8 Ma (Ray et al., 1999). Nd-Sr-Pb isotopes show HIMU and EM-I/EM-II mantle signatures (Veena et al., 1998; Ray et al., 1999). The $\delta^{18}O$ value of the complex is consistent with its derivation in equilibrium with mantle silicates whereas higher than 'normal' mantle $\delta^{13}C$ ratio (-5 to -8‰) has been advocated to recycling of inorganic C (Ray et al., 1999).

1.9D Ambadongar: The sub-volcanic alkaline ring complex of Ambadongar consists of carbonatites, nephelinites and phonolites located at the northern periphery of the Deccan flood basalts at the western edge of the Narmada Rift Zone of central-west India (Viladkar, 1981). The complex has been dated precisely to be 65.0±0.3 Ma by $^{40}Ar/^{39}Ar$ dating method (Ray et al., 2000). From the same study, Sr isotopic data suggest an enriched source for these carbonatites. Incorporation of ^{13}C enriched subcontinental lithospheric mantle by the plume has also been inferred. Extensive C and O isotopic study indicates a moderate rise in ^{13}C coupled with an increase in ^{18}O from early to late stages of carbonatite formation (Viladkar and Schidlowski, 2000). The apparent correlation between $\delta^{13}C$ and $\delta^{18}O$ over the $\delta^{18}O$ range of 7-13‰ has been advocated to Rayleigh fractionation process, while the upsurge of ^{18}O in the late stage phases has been related to low temperature hydrothermal activity involving ^{18}O depleted groundwater.

Additionally, from South India, carbonatites have been analyzed from Khambamettu, associated with the Western Ghat faults. However, this carbonatite still needs to be analyzed for various isotopes and dated precisely. To date, the only available age of the complex has been proposed to be 523 Ma (Kumar, unpublished data).

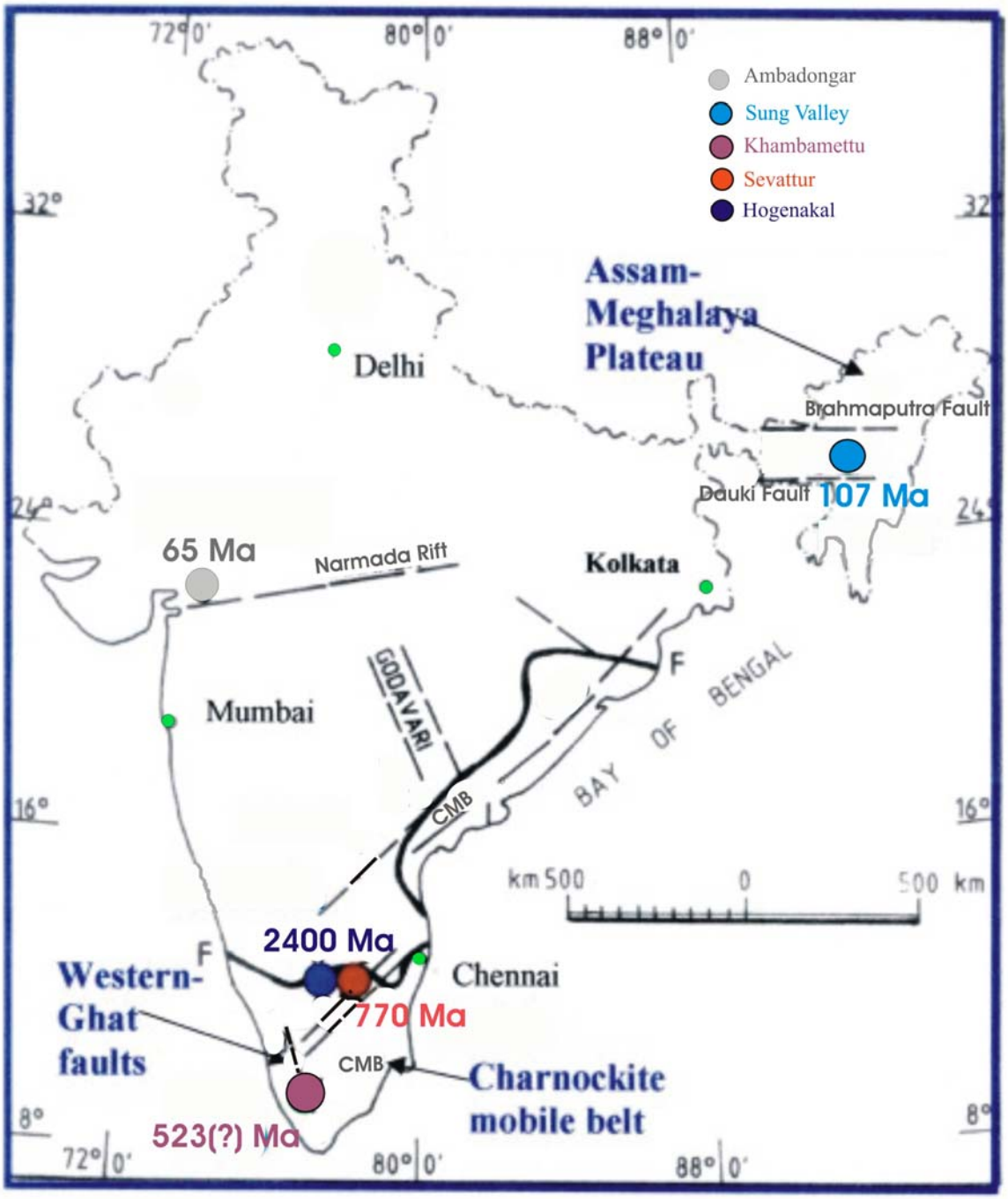

Fig. 1.3 Location map of carbonatites studied. The associated structures are also shown. Ages of each carbonatite indicated.

1.10 Outline of the thesis

The thesis consists of six chapters. The first two chapters contain a brief introduction to the study (Chapter 1) and the experimental procedures in general (Chapter 2). In chapter 3, the prospect of using *in situ* produced He, Ne and Xe for dating apatites in carbonatites has been investigated. In Chapter 4, an account of the noble gas results and their implication for the carbonatites has been discussed. Chapter 5 deals with N

and Ar results for these carbonatites and their implications for mantle N. The thesis ends with Chapter 6 where the overall implications of the present study in terms of N in the mantle as well as some futuristic aspect that may be explored have been discussed briefly.

Chapter 2

Experimental details

2.1 Introduction

The experimental techniques involved in studying carbonatites for noble gases and nitrogen have to consider the trace amount of these volatiles present in the samples, as well as the huge amount of CO_2 that may be released during their pyrolysis as compared to the gases of interest. In this chapter, the various experimental techniques employed for gas extraction, purification and measurement techniques during mass spectrometry are briefly described. A brief discussion on sample selection and characterization has also been given.

When a gram of carbonatite (dominantly carbonate) is melted and the gas present in it is completely extracted, N is unlikely to be more than 5 ppm and the ^{132}Xe is not expected to exceed 35 x 10^{-12} cc STP/g. Thus the N_2/CO_2 and $^{132}Xe/CO_2$ ratios will be unfavorably small like 1.8 x 10^{-5} and 1.6 x 10^{-13} respectively in total pyrolysis. The tolerable levels of CO_2 should be at least ~1000 to 10000 times lower for N_2 and Xe respectively. Our experimental techniques were designed appropriately to counteract this problem. Also the mass spectrometer used for the analysis is the VG Micromass 1200 that operates in the static mode and is capable of measuring these trace gases in the samples. In the present work mineral separates of carbonates, apatites and magnetites were analyzed to determine the concentration and isotopic composition of nitrogen and noble gases in these minerals.

Mass spectrometry

2.2 VG Micromass 1200

This is a commercially available gas source mass spectrometer from the Vacuum Generators Ltd. U.K and is operated in the static mode. Its sensitivity allows measurement of small amount of inert gases. The operating resolution of 170 gives flat topped xenon peaks. As all mass spectrometers, the operation involves ionization, acceleration and analyses of the different m/e signals. The ionization is achieved by a Nier type ion source with a source magnet to increase the ionization efficiency. A trap current of 100 μA is used in the emission control unit that maintains the controlled

electron beam for ionization. The ionized species is accelerated by electrostatic potential of 4KV. The VG Micromass 1200 is a magnetic deflection mass spectrometer with a 60º electromagnetic sector that acts as a mass analyzer. The different m/e signals are measured by varying the magnetic field. A Faraday cup and an electron multiplier, used for ion detection makes possible the measurement of a wide range of signals varying over more than six orders of magnitude. Ultra high vacuum (UHV) of ~10^{-9} torr is maintained in the mass spectrometer with an ion pump for evacuation that is connected to the mass spectrometer through all UHV valves. During sample analyses the pump is isolated from the mass spectrometer. A SAES™ getter attached to the mass spectrometer keeps the hydrogen background to a minimum and also helps in turn to reduce the hydrocarbon background. However, during analyses of nitrogen the getter has to be isolated as it acts as a chemical getter for nitrogen. The mass spectrometer has an external oven to bake it up to 300ºC during degassing.

2.3 Gas extraction units

Mainly two gas extraction units are connected to the mass spectrometer via the main lines used for purification and separation of the gases. One unit comprises of a combustion finger and an extraction bottle connected to the mass spectrometer via a glass line. The second extraction unit is the vacuum crusher connected to the mass spectrometer via a metal line. Both the extraction systems have been used for different purposes during the experiments. The extraction bottle and the combustion finger have been used for stepwise heating of the apatites till they melt while the vacuum crusher has been used to simply crush the samples (apatites, carbonates and magnetites) in vacuum and rupture the fluid inclusion to release the gases trapped in them.

2.4 Vacuum crusher

The main units of the vacuum crusher (Fig. 2.1) consist of:

A) A stainless steel (SS) well where the sample of known weight to be crushed is loaded. To avoid directly hitting the sample while crushing and preventing it from splashing, after the sample is placed in the SS well it is covered with a SS anvil. The anvil is removed during loading/unloading the sample. At the base of the structure there is a thick aluminum plate on which the sample well is mounted. It is in turn fixed to another heavy base plate at the bottom through shock absorbers, for

stabilization of the entire setup and prevents any misalignments due to vibrations while crushing.

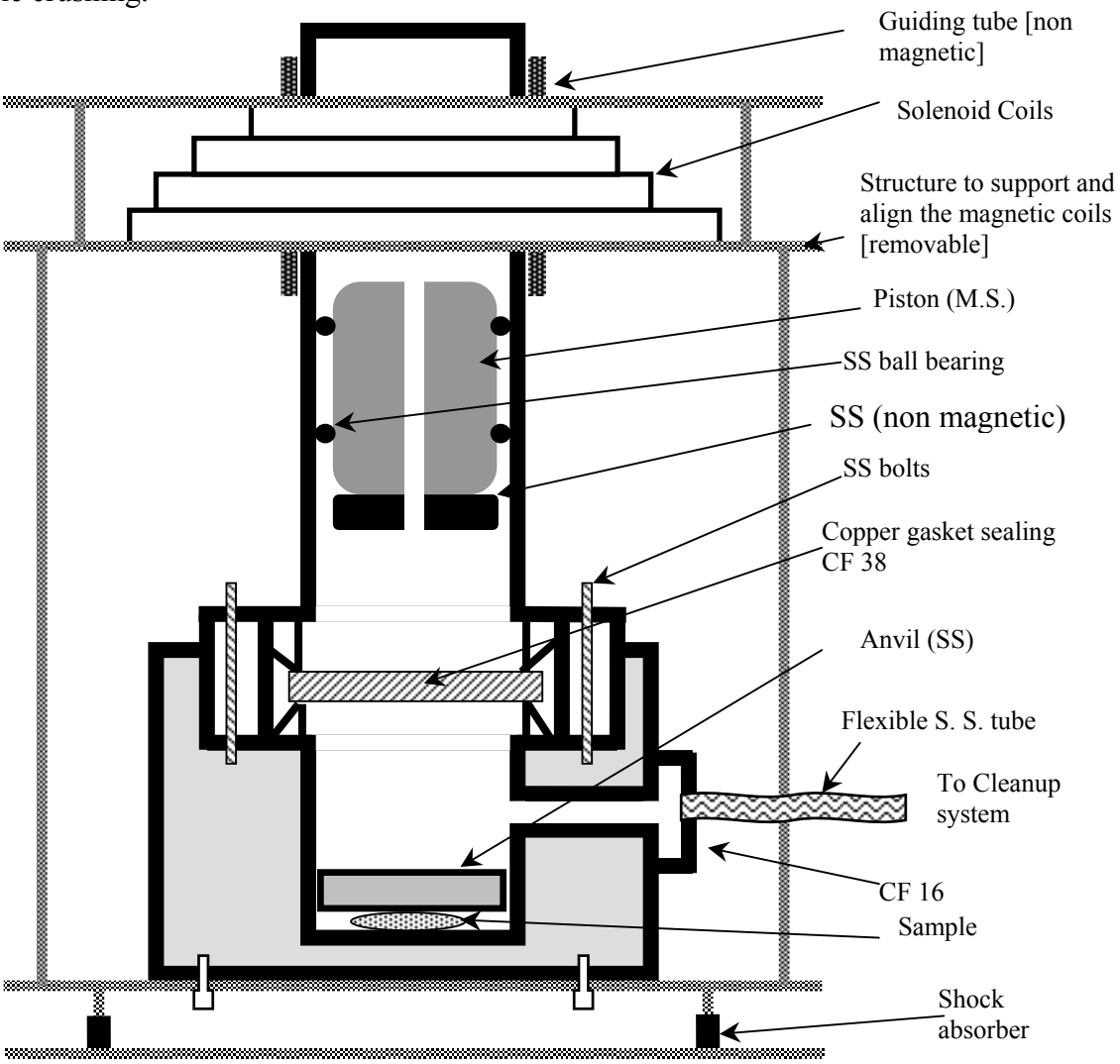

Fig. 2.1 Schematic diagram of the vacuum crusher. Dimensions are not to scale (Murty and Mahajan, 2003).

B) A magnetic piston (SS) weighing about 500g is used for crushing the sample. The magnetic piston is lifted to a height of 12 cm using an external magnet, and then dropped on the anvil covering the sample to crush it. The piston is fitted snugly in an external (SS) tube, but is provided with ball bearings at the sides for smooth lifting and falling during crushing. It also has venting ports for smooth evacuation. The SS tube is fixed to the well through a conflat flange and a copper gasket so as to maintain ultra-high vacuum in this region. The tube and the piston, like the anvil, are removed during loading/unloading of the samples.

C) To provide the necessary magnetic field for the action of the piston to be lifted and dropped on the anvil covering the sample, there are four solenoid coils that operate sequentially with a fixed time delay to lift the piston and then switched off to let it

fall. The frequency of this cycle of lifting the piston and free fall maybe varied using the time delay between each cycle. Generally about 30 cycles per minute is used. The solenoid coils are mounted in an aluminum frame that is precisely guided onto the tube of the crusher and firmly mounted without causing any strain on the tube that may result in leaks. This is a removable structure that supports and keeps the magnetic coils perfectly aligned with the tube, and hence the piston.

2.5 The gas cleaning and separation line (metal)

Subsequent to its extraction in the vacuum crusher, the sample gas passes through a series of separation and clean-up procedures in the main line (Fig. 2.2). The sample gas is introduced into this metal line from the vacuum crusher via a flexible (SS) tube that does not permit any vibrations to be communicated to the vacuum line. At the bottom of the cleanup system are placed two pumps that are connected to the cleanup system to generate and maintain UHV in the crusher and the line. The turbomolecular pump is used to remove the gases in line from atmospheric pressure level to 10^{-7} torr. The ion pump is then used to bring down the vacuum to 10^{-9} torr level. The turbomolecular pump is backed by oil free diaphragm pump to obtain a hydrocarbon free clean UHV.

The different components of the clean up system are two SSM (stainless steel mesh) fingers, two charcoal fingers, one CuO finger, one cold trap finger, one Ti-getter finger and another TiZr getter finger. The purposes of each of them have been discussed in the subsequent sections. All the fingers, except CuO and the cold trap fingers can be isolated from the main line by UHV valves. Although the main line and the components are basically an all-metal system, a separate pyrex glass branch line is used for nitrogen processing as metal extraction system does not give low and reproducible blanks for nitrogen. This glass line has been integrated to the system in such a way that after extraction of the gas, a volume split is isolated into the glass line very quickly (within a minute) for analyses of nitrogen, while the rest of the gas is processed in the metal line for noble gases. The glass line is provided with a CuO finger for clean up purposes.

The various units present in the main line are described briefly below.

2.5A The line fingers: The gas separations are mainly based on the principle of differential adsorption and desorption properties of the various noble gases. But prior to separation and purification the gases are collected on suitable fingers in the main

line. There are two stainless steel mesh (SSM) fingers in the main line, namely SSM2 and SSM6 that basically contain meshes made up of stainless steel powder of 2 μm size. They are used for collecting the gases and may be isolated from the main line by using valves V2 and V6 respectively. While SSM2 is used for the initial collection of the gases, SSM6 is used for finally collecting the sample gas just prior to introduction into the mass spectrometer. The adsorption/desorption properties of the SSM fingers are identical to that of the activated charcoal. However the advantage of the SSM fingers lie in their bakability up to 800°C unlike that of the conventional charcoal and zeolite which undergo structural damages if baked beyond 400°C. Also, for nitrogen, charcoal fingers may lead to carbon monoxide (CO) contamination and therefore cannot be used for its collection. During the present study, a small split of the total gas was isolated for nitrogen at the initial stage right after gas extraction and the charcoal finger (CH-4) used for collecting all the noble gases (except He and Ne that are non condensable) with liquid nitrogen. In addition to CH-4, there is another charcoal finger, the CH-5 in the main line. Both the charcoal fingers can be isolated from the main line with valves V4 and V5. For gauging the pressure in the system and hence the vacuum level, there are two convectron pressure gauges connected to the main metal line and one to the branch glass line.

2.5B CuO finger*:* Both the main line and the glass branch line have a CuO finger each for clean up procedures. They are also provided with a cold finger each for trapping unwanted condensables like H_2O and CO_2 with liquid nitrogen. Since gases extracted from the samples contain other species in addition to our gases of interest, it is essential to get rid of these species as they may not always be resolvable in the mass spectrometer leading to interferences. The CuO fingers contain wires (≈0.65 x 6 mm) of copper oxide (MERCKTM) wrapped in Pt-foil. They are contained in a single walled quartz finger in the glass line, and a stainless steel finger in the metal line. The sample gas is cleaned by CuO cycle wherein the unwanted species (CO, hydrocarbons, H_2 etc) are converted into condensable oxides like CO_2 and H_2O that can be separated cryogenically from the gas (generally nitrogen fraction) by the cold trap using liquid nitrogen. The oxygen required to convert the carbon etc into condensables is generated by heating the CuO getter to 750°C so as to break down CuO to Cu_2O and O_2. After the condensables have formed, the residual oxygen is taken back at a lower temperature of 600°C when Cu_2O recombines with oxygen to

form CuO again. The Pt foil remains unreactive up to 750°C and it acts as a catalyst for the reaction that takes place. Also it reduces direct contact between the CuO/ Cu_2O formed and the glass/SS finger preventing any reactions between them.

2.5C TiZr/Ti getters: The extraction line is also provided with two getters, a Ti-getter finger and another TiZr getter in the same volume as the charcoal fingers. Like the charcoal fingers, the isolation of both the Ti and TiZr getter can be easily achieved by valves V4 and V5 respectively. These are materials that chemically react with the reactive species like N_2, CO_2, O_2, H_2 and hydrocarbons to form refractory compounds. Thus noble gas fraction can be effectively cleaned off these species by exposing them to these getters. However they have a gettering effect on nitrogen too, and have to be completely isolated from the nitrogen fraction.

Basically, at temperatures > 700°C, Ti continuously reacts with N_2, O_2, CO_2, CO and decomposes hydrocarbons by taking up C from them, and leaving behind the H_2 that is sorbed at temperatures below 400°C. For the TiZr getter which is an alloy of Ti and Zr, Zr also helps to get rid of H_2O vapour by decomposing it into H_2 and O_2. It reacts with O_2 to form refractory oxide and sorbs H_2 at temperatures ≈300°C. After each experiment the getters are degassed at 800°C before further use, to pump off the exsolved H_2.

2.6 Glass extraction system

The glass extraction system, that is, the combustion finger and bottle is connected to an online sample tree where the samples are kept prior to gas extraction. For gas extraction the samples are maneuvered into the combustion finger or the bottle with the help of external magnet and nickel pieces (that are loaded into the sample tree). Known weight of samples are packed in aluminum or gold foils and then loaded into the sample tree. The choice of these foils depends on a number of factors like low blanks for noble gases and nitrogen, and no gettering effect of these materials for nitrogen. Sometimes gold foil is preferred over aluminum, as while aluminum melts at a temperature of 600°C or so, gold can survive up to 1000°C. Therefore the sample wrapped in gold can be maneuvered from the combustion finger after heating it up to 950°C to the extraction bottle (discussed later).

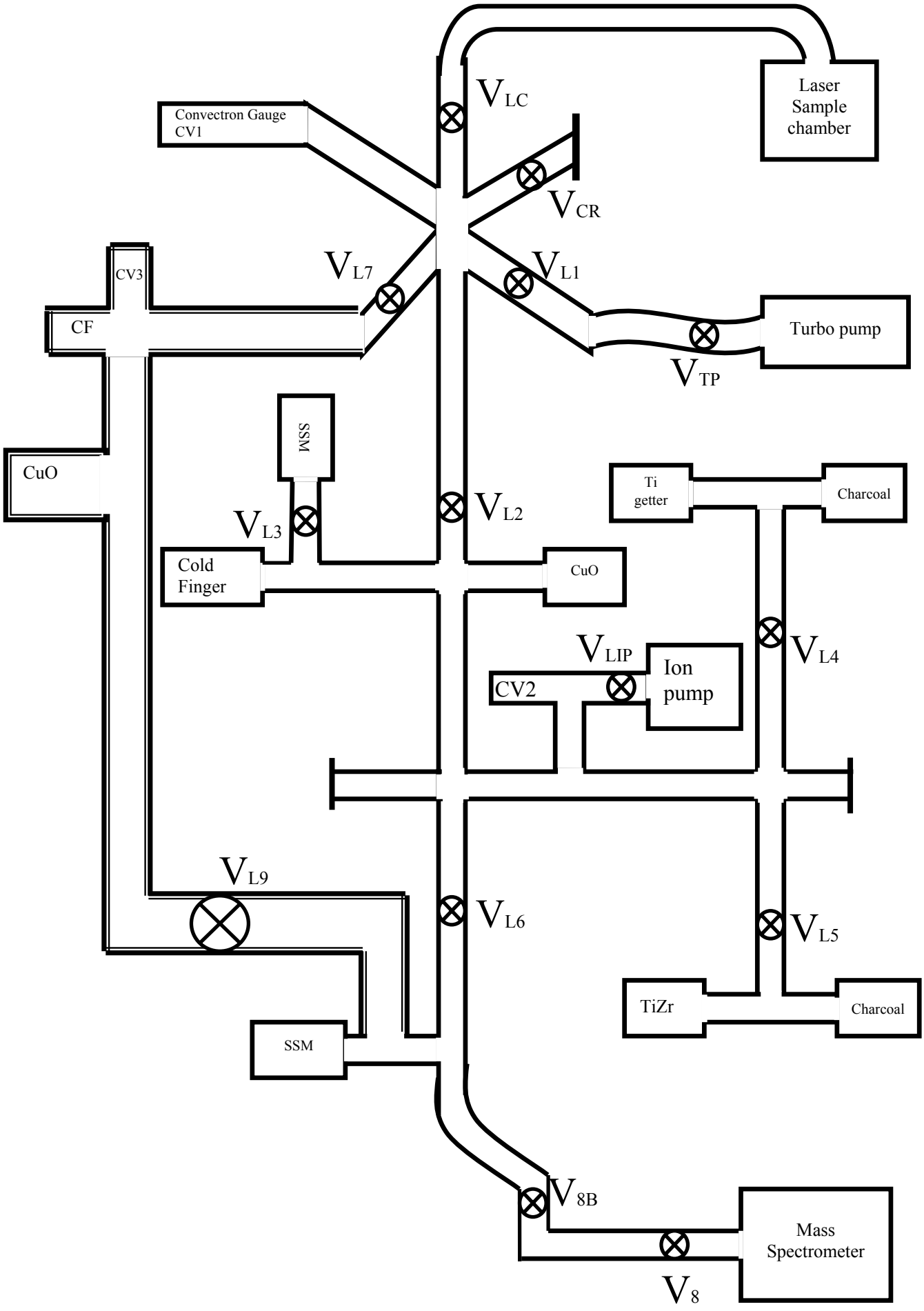

Fig. 2.2 Schematic diagram of the metal line

2.6A Combustion finger: The extraction system is attached to a double-walled (vacuum jacketed) quartz finger that can be heated up to 1050°C (the safe limit without collapsing the quartz) by means of an external resistance heater. The outer vacuum line of this finger is connected to the diffusion pump. Sample is introduced from the sample tree into this finger by means of a quartz boat that can be maneuvered with an external hand magnet. For combustion purposes, samples are heated within this finger in an environment of oxygen generated from an inline CuO getter.

2.6B Extraction bottle: The extraction bottle (Fig. 2.3) is used for the extraction of gases from the solid samples by heating them in temperature steps up to 1850°C. It is a double vacuum jacket that is cooled externally by a water jacket. The bottle is partly made of quartz and rest with pyrexTM. Only the innermost wall of the bottle that is subjected to higher temperatures is made of quartz that has a high melting temperature of > 2000°C. The extraction bottle contains a Mo crucible (melting point >2500°C) that is suspended through a funnel shaped quartz tube and is heated inductively by RF power. An outer chilled water jacket provides cooling to the pyrex layer that is subjected to high temperatures due to radiation heating from the crucible. The intermediate vacuum layer between the water jacket and the quartz wall is intended to serve two purposes:

- Once the quartz wall is degassed, there is no constant loading of gases into quartz since there is vacuum on both sides, and thus it remains clean.
- The diffusion of helium through quartz is also minimized due to the vacuum outside

Both these factors reduce blank levels considerably, thus enabling analyses of even small amounts of He. The optically flat view glass, at the top of the bottle allows viewing the crucible bottom for temperature calibration using an optical pyrometer, and also to confirm sample melting by visual inspection. A magnetic ball and the seating prevent vapour deposit on the view glass.

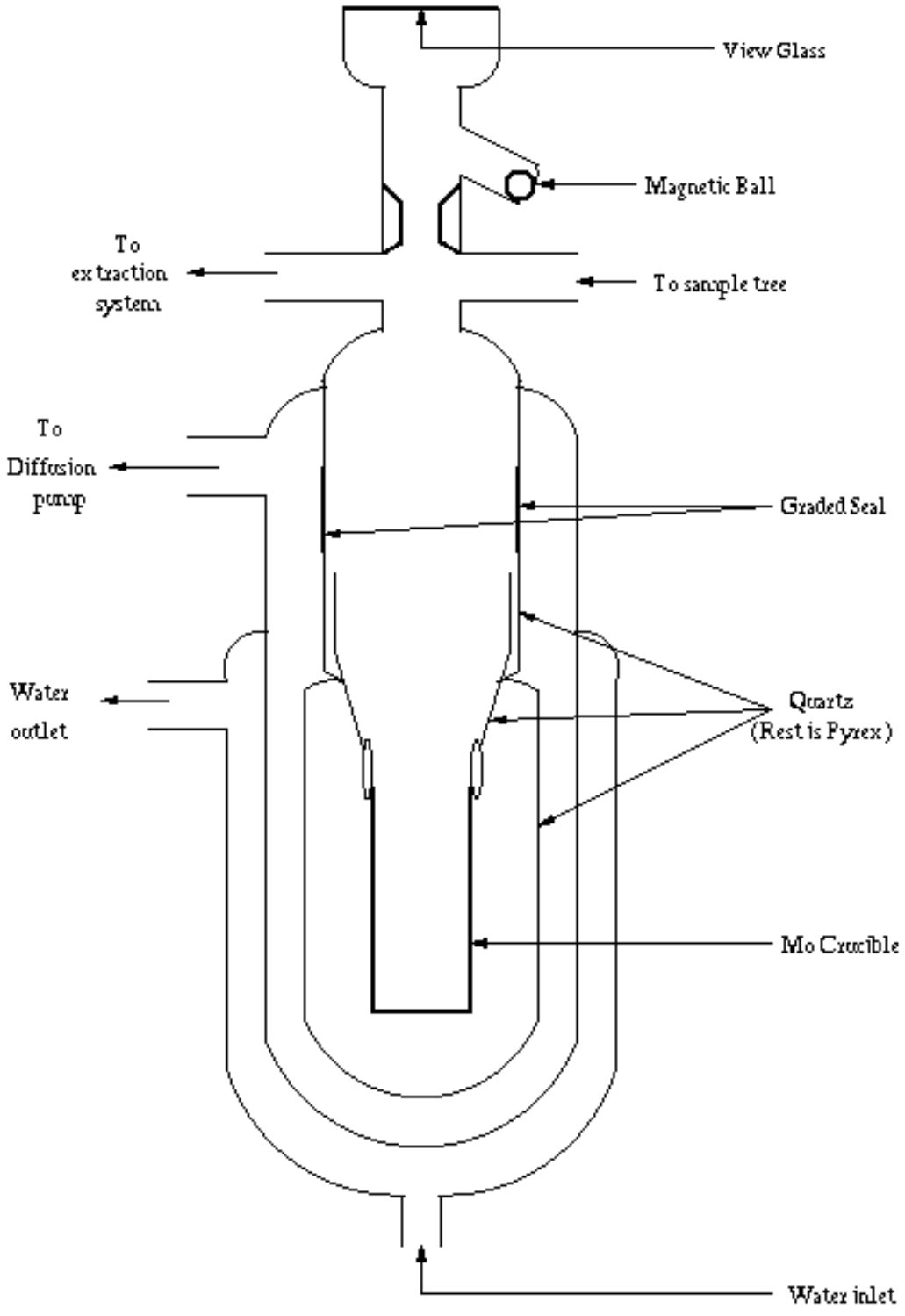

Fig. 2.3. Extraction bottle

2.7 The main line (glass)

Subsequent to extraction of the sample gases, they are passed onto the main line (Fig. 2.4) where the gases are cleaned up and separated. The basic units of the main line are similar to that of the metal line connected to the vacuum crusher discussed above, only with slight differences. The glass line also has two SSM fingers (SSM2 and SSM4) and two pyrex fingers containing charcoal (CH-3 and CH-6). All of them can be isolated from the mainline with UHV valves V2, V4, V6 and V3 respectively.

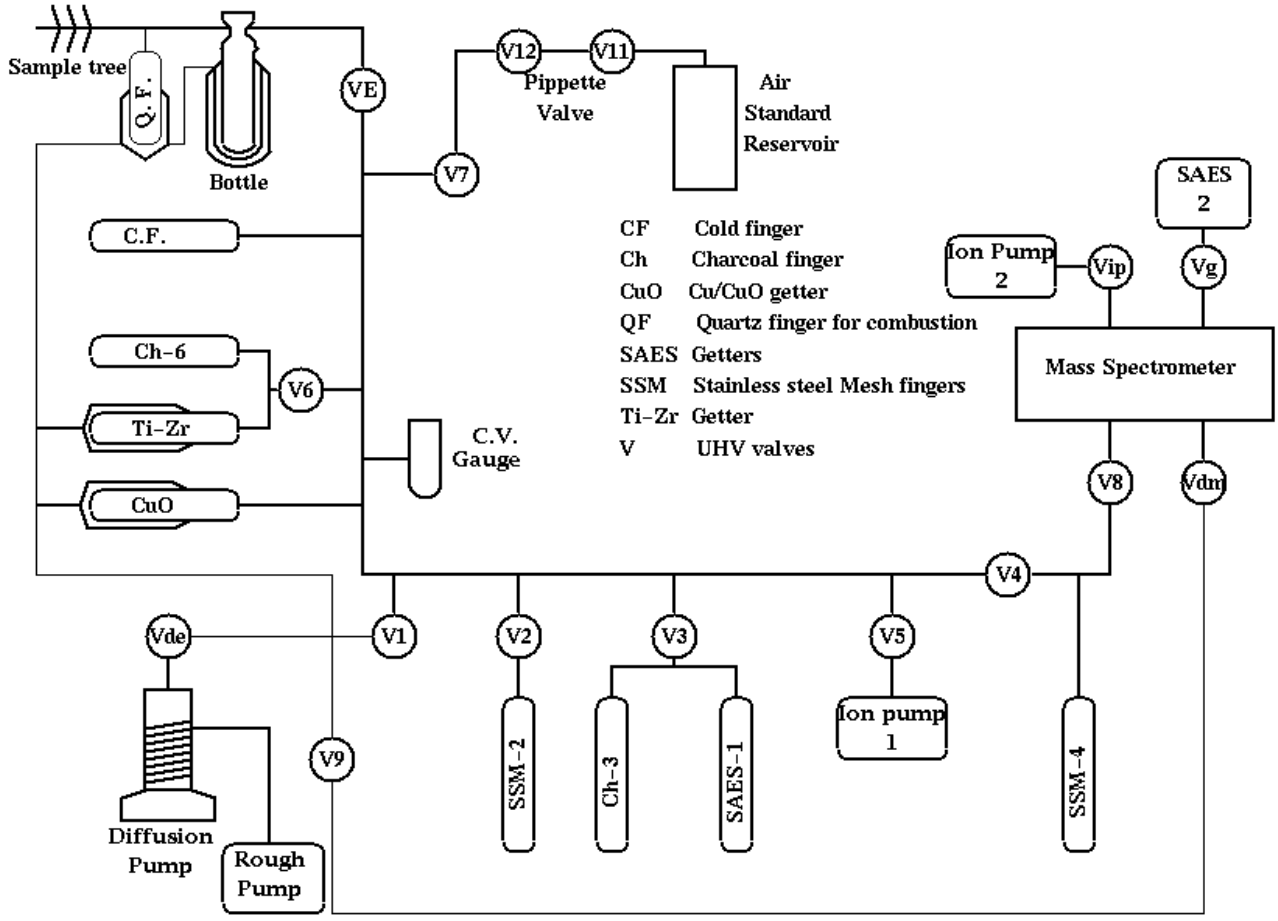

Fig. 2.4 Schematic diagram of the glass line

There is a pyrex cold finger in the main line to separate the condensables from the gases of interest. The extraction line is provided with a CuO getter that is a double walled quartz finger containing copper oxide. In addition to generating ultra-pure O_2 used for purification, of the sample gases, in the glass system the generated O_2 at 850°C is also used for combusting the samples in the combustion finger (discussed later).

There are two getters namely the TiZr and the SAES getters for cleaning up the noble gas fractions and connected to the mainline via V6 and V3 respectively. The SAES getter (AP-10GJ) has a gettering action similar to that of the TiZr and contains a non-evaporating getter material (ST 101 Zr Al alloy). It is used for a finer cleaning of noble gases that have already been cleaned by the Ti-Zr getter to remove further traces of impurities. During clean up the SAES getter is usually heated to 750°C and then cooled to 300°C in slow steps. Like the TiZr getter, after each experiment, the SAES getter is also degassed at 800°C.

The diffusion pump backed by a rotary pump and an ion pump achieves UHV in the unit. To gauge the level of vacuum in the system there are convectron pressure gauges to monitor the pressure in the line. Initially, before introduction of any gas that is to be analyzed the system pressure and hence the level of vacuum can be monitored by the ion pump also.

2.8 Standard procedures

The standard procedures involved in the experiments, in both glass and metal system is shown in the flow diagram (Fig. 2.5). The steps include first extraction of the sample gas followed by clean up and separation into individual gas fraction. This is followed by subsequent analysis in the mass spectrometer and the data acquisition.

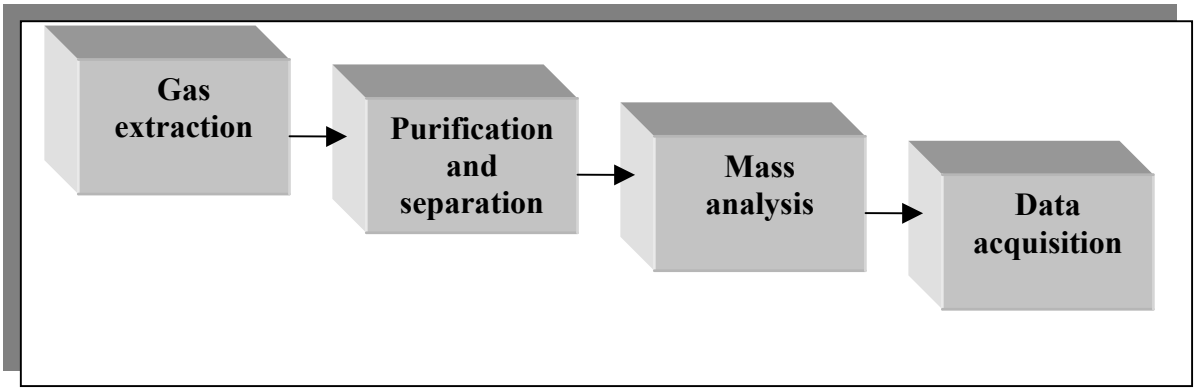

Fig. 2.5 Flow diagram of the standard experimental procedures

2.8A. Gas extraction:

- **Vacuum crushing in the metal system**

In the vacuum crusher, the sample gas is extracted by stepwise crushing. Prior to crushing, and after loading the sample, the system is baked at 150°C. After the system vacuum (10^{-9} torr) is achieved, a cold blank is done to ensure leak tightness, before crushing the sample. Generally the crushing sequence involves

three steps of 15, 300 and 300 strokes for carbonates and 15, 500 and 500 strokes for apatites and magnetites. The procedure has been adopted after some trial runs on some samples and by varying the number of strokes. The initial step of crushing is mainly to get rid of any surficial adsorbed contaminant gas. The second step is the main extraction step, while the third step is to ascertain that the gas to be extracted by crushing is already released.

During crushing, the crusher volume is isolated from the main line. Only after the gas has been extracted by crushing for that step it is introduced into the main line and the branch glass line for the noble gases and nitrogen respectively.

- **Stepped heating in the glass system**

In the glass extraction system gases are extracted from the apatites by stepwise heating of the samples up to their melting temperature of 1850°C. However an initial step of combustion is done in the combustion finger where the sample is combusted at 400°C in 2 torr of oxygen to remove the surficial contaminants. Combustion is generally carried out for 45 minutes during which the combustion finger is isolated from the main line by an UHV valve. Only after the heating is over the gas is expanded to the main line and processed for analyses.

The combustion step is followed by stepped pyrolysis that involves heating the sample in the combustion finger up to 1000°C but in the absence of oxygen, and then introducing it to the predegassed Mo crucible. Because they had to be transferred from the combustion finger to the crucible after heating up to 1000°C, the samples had to be wrapped in gold foils so as to keep the packing intact till the transfer. In the Mo crucible it is heated in temperature steps up to 1850°C using RF heater. At each step, the sample is heated for 45 minutes (30 minutes for the melting step), the gases released being simultaneously adsorbed on a stainless steel mesh (SSM) maintained at liquid nitrogen temperature. Subsequent to heating, the main line is isolated from the extraction bottle and the gases from the stainless steel mesh are desorbed for their processing.

2.8B Cleaning and separation: The extracted gas, whether by crushing or combustion/pyrolysis contains many unwanted species in addition to nitrogen and noble gases. These may contaminate the mass spectrometer and lead to mass interference. It is very important to remove or minimize these species in the sample gas at various stages of cleanup. During pyrolysis/combustion, the gases are cleaned

up by exposing them to the CuO getter that is heated to 700°C for 20 minutes followed by cooling to 400°C in steps. During heating, the non-condensable species like hydrocarbons, CO and H_2 are oxidized to condensable species like H_2O and CO_2 that are isolated from the sample gas by using liquid nitrogen trap. A portion of this clean sample gas (≈10%) that is free from the interfering species is isolated for the analysis of nitrogen before collecting the rest of the fraction on charcoal finger for exposure to getters for noble gas study. As clean up with CuO is the only way of cleaning the nitrogen fraction**,** this is an essential procedure for nitrogen processing. Very often when these unwanted species generated are large, more than one cycles of CuO clean up is done. During crushing, only the fraction of the gas (≈12%) that is isolated after extraction in the branch glass line for nitrogen analyses is cleaned by CuO, very often more than once to get rid of the various interfering species. Another known fraction of the gas is collected on a charcoal finger for noble gas analyses in both cases of crushing and pyrolysis/combustion. During crushing, considering the huge amount of CO_2 that may be liberated from the inclusions present in the carbonates being crushed, and the distance of the flexible tube in the crusher volume from the nearest charcoal finger (CH-4), the fraction of the gas in the tube and the crusher volume is not utilized for our analyses. This is partially to reduce the load on the getters. The fraction for noble gases is cleaned by TiZr getter in the glass system and the Ti getter in the metal system. The split of noble gas fraction collected in the charcoal finger is a mixture of xenon, krypton and argon. These are separated in two steps by allowing selective adsorption of the species on a charcoal finger at suitable temperature (-108°C for Xe and -154°C for Kr) using a variable temperature probe.

A known fraction of the total gas during pyrolysis/combustion is analyzed for helium-neon. This fraction is exposed to both TiZr and SAES getters before being introduced into the mass spectrometer. Also, during He-Ne analysis, liquid nitrogen traps constantly maintained on the SSM (SSM-4) and the charcoal finger(CH-3) nearest to the mass spectrometer to adsorb any H_2O, CO_2 or Ar that might have escaped the cleaning stages and interfere with the Ne isotopes. Also, it prevents these background species to build up in the mass spectrometer during the course of the analyses.

During crushing, it is to be kept in mind that the fraction used for helium-neon is isolated before its exposure to the glass branch line used for nitrogen. This is to

minimize the blank contribution for helium-neon that is very much higher for glass as compared to metal system.

2.8C Mass analysis: Each of the separated fractions from the extraction line is introduced into the mass spectrometer through an UHV valve, and analyzed for the masses by scanning the peaks manually in a number of cycles. In addition to the masses of interest, peak signals at masses 2(H_2^+), 18(H_2O^+), 40($^{40}Ar^{++}$) and 44(CO_2^{++}) in the He-Ne fraction are monitored regularly to assess the background contributions (discussed later). The noble gases are usually measured on the electron multiplier except for mass 4 and 40 in some samples that are measured on the Faraday cup. Nitrogen is measured in the molecular form on the Faraday cup for mass 28, 29 and 30. For smaller nitrogen amount in some samples, 29 and 30 were run on the multiplier after scanning 28 and 29 mass peaks on Faraday. Measuring mass 30 in the nitrogen fraction allows a precise estimation and correction for the interference from CO (discussed later).

2.8D Data acquisition and reduction: The signals from the mass spectrometer are acquired and recorded on an on-line computer by using suitable interface and programs. A parallel XY recorder gives a graphic view of the scan and helps in the identification of the peaks. The digitized 'time vs. signal' data is processed for the time and peak-heights. The time zero (T_0 = Time of sample introduction into mass spectrometer) value for the peak height and the isotopic ratios are found out from this data by offline data reduction. The data thus acquired is corrected for the blanks, backgrounds and the instrumental mass discrimination.

2.9 Blanks

Blanks are performed in identical fashion to the sample steps both for crushing as well as pyrolysis/combustion. However, since in the case of crusher it has to be exposed to the atmosphere every time a new sample is loaded after removing the crushed powder of the previous one, it is baked each time before the analyses of the new sample to minimize the blank. Then a leak test is done before taking a cold blank to check if the system has reached working vacuum conditions. For blank corrections, blanks that have been done for 15, 300 and 500 strokes on an empty crushing unit before analyses of the samples are used .It is observed that the 300 and 500 stroke blanks are almost identical for all gases.

During pyrolysis/combustion, blank is taken before analyses of each sample to monitor if the system is in good vacuum conditions. At the end of each sample the system is baked at 150°C to remove any traces of gas from the previous sample and to minimize blank. Blank corrections for each temperature step are done by taking into account the corresponding blank of the system for that temperature during the measurement of the sample.

Some typical blank concentrations for both the metal and glass systems are listed below for the 500 strokes step in case of crushing, and the 1800°C for pyrolysis (Table 2.1). In both cases, the blank concentrations are < 5% for nitrogen and seldom exceed 10% for noble gases (except for helium and neon where it is ~30%). During pyrolysis, blanks generally show an increase with temperature. Blanks can vary with the conditions of sample, but such variations are within a factor of two. It is to be noted here that blank compositions have also been corrected for interference effects. Isotopic compositions of the blanks are $\delta^{15}N = 5\pm1‰$ for nitrogen and almost atmospheric for the noble gases.

Table 2.1. Some typical blank concentrations in metal (500 strokes) and glass (1800°C) systems

System	^{4}He	^{22}Ne	^{36}Ar	^{84}Kr	^{132}Xe	N
	← 10^{-12} →					
metal	0.2	4.5	8	1	0.3	390
glass	62	235	22	0.6	0.1	440

Concentrations are in cc STP except N which is in picogram

2.10 Interference corrections

The measured signals often have a contribution from the interfering species. With the usual resolving power of the mass spectrometer, it is not possible to resolve these masses. In some cases, it is however possible to identify and thus correct for the contributions from these interfering species as outlined below.

2.10A Interference at mass 3: The molecular ion of hydrogen (H_3^+) is an interfering species for the ^{3}He mass. The peak for these two masses cannot be resolved with the resolving power of 170 of the mass spectrometer. The contribution of H_3^+ at mass 3, however can be assessed and corrected for, by measuring the peak at mass 2(H_2^+) and estimating the corresponding H_3^+ contribution using a predetermined H_3^+/H_2^+ ratio of 4.62×10^{-4} (using pure H_2). The corrected ^{3}He measurement has only been considered

for the metal system where the blank of helium is low. The contribution of H_3^+ at mass 3 can be considerable, generally ~20% or less (only in one case up to 75% in a carbonate sample), and therefore the correction has been routinely done in all samples where ^3He has been detected.

2.10B Interference at masses 20 and 22: Contributions from $H_2{}^{18}O^+$ and $^{40}Ar^{++}$ at mass 20 and $^{44}CO_2{}^{++}$ at mass 22 cannot be resolved from the neon peak signals by the mass spectrometer. The neon data is, therefore, corrected for these background contributions from the measured peak heights of the masses 18, 40 and 44 and the $^{18}O/^{16}O$(normal isotopic ratios), $40^{++}/40^+$ and $44^{++}/44^+$ abundance ratios respectively. The abundance ratios $40^{++}/40^+$ and $44^{++}/44^+$, in the above correction are periodically determined for the operating conditions of the mass spectrometer from the air standard. The typical values of $40^{++}/40^+$ and $44^{++}/44^+$ are 0.06 and 0.01 respectively. The ratio of H_2O_{18}/P_{18} is a defined ratio of 0.00204 where P_{18} denotes the peak at mass 18.

2.10C CO correction: Peak height at mass 30 can have contributions from $^{15}N^{15}N$, $^{12}C^{18}O$ and possibly also from the hydrocarbons. Assuming that all the hydrocarbon contribution at masses 30 and 31 would be comparable, and considering the near absence of any 31 peak in the spectra, it is considered that the hydrocarbon peak at mass 30 is negligible. Therefore, the excess over $^{15}N^{15}N$ at mass 30 is assigned wholly to CO contribution. The effect of CO contribution which shifts the $\delta^{15}N$ to more positive value, is corrected for by routinely measuring mass 30 along with masses 28 and 29 in the nitrogen fraction. The correction procedure is as follows: (ex, meas, exp and corr denotes excess, measured, expected and corrected respectively)

i. Estimate excess at mass 30: As a first approximation, the $(28/29)_{meas}$ is assumed to be correct and the $(30/29)_{exp}$ is calculated. Then,

$30_{ex} = [(30/29)_{meas} - (30/29)_{exp}] \times 29_{meas}$

where $(30/29)_{exp} = (1/4) \times (29/28)_{meas}$

ii. Contribution at mass 29 from CO (^{29}CO) is now estimated from the amount of ^{30}CO derived in the previous step, using the $^{29}CO/^{30}CO$ ratio of 5.711 for normal C, O isotopic compositions.

$(28/29)_{corr} = [\{(28/29)_{meas}\} - \{85.939 \times X_i\}]/[1-X_i]$

where $^{28}CO/^{29}CO = 85.939$ and $X_i = {}^{29}CO/29_{meas}$

Then using the $(28/29)_{corr}$ the steps i. and ii. are repeated. In less than five iterations the (28/29) value converges and this is used as the CO-corrected value. The CO correction on $\delta^{15}N$ is usually less than 1‰.

2.11 Calibration of the mass spectrometer

Known amounts of air standards, processed in a fashion similar to the samples, are run periodically to calibrate the mass spectrometer, for its sensitivity and mass discrimination. The reservoir containing standard air is connected to the main glass line through a pipette valve (V11 and V12, Fig. 2.4). An air standard is also used to find out the separation efficiency of Ar, Kr, and Xe is a mixture of these gases. Typical values of the air standard parameters that are used in calibration are given in Table 2.2. The sensitivities lie within 10% between standards analyzed over two years. For a particular experiment, the closest air standard parameters are used. The mass discrimination is more reproducible for long periods of time.

2.12 Mass discrimination

The sensitivity of the mass spectrometer for different isotopes of an element is not the same and this causes a systematic difference in measured isotopic ratios and actual isotopic ratios. The correction factor for mass discrimination can be calculated using reference gas (air) with known isotopic composition using the following equation (R_m, R_t and R_s stand for measured, true and standard ratios respectively):

$$m.d(\%/amu) = (100/m_j - m_i) \times [(R_m/R_s) - 1]$$

where $Ratio = [m_i]/[m_j]$

$$mdf = [1 - \{m.d \times (m_j - m_i)\}/100)]$$

$$R_t = R_m \times mdf$$

So by multiplying the R_m by mdf factor the true ratio R_t is obtained.

For He, the sensitivity and the mass discrimination is determined by an artificial mixture of He, which is cross calibrated using Bruderheim standard.

2.13 Reproducibility of measurement

To check the reproducibility of our experiments, repeat analyses of a few carbonates and one magnetite (vacuum crushing) have been done. Here we report the result for the two sets of analyses from one carbonate (H-C1A and H-C1B), and one magnetite

(SV-M1A and SV-M1B). It is to be remarked here that reproducibility for vacuum crushing experiments as in the present case is difficult to achieve. This is because concentrations may show considerable variations depending upon the fluid inclusion distribution that may vary between individual grains. Also different generations of fluid inclusions may host gases of different compositions (see Chapters 3 and 4). Therefore depending on the fluid inclusion being ruptured and its magmatic history (for example variable equilibration with crustal fluids), there might be some variation in the isotopic composition. Another cause of variability may be the differential atmospheric contribution during the two sets of experiments for the same sample and also the variability of adsorbed gases on the surface of individual grains. The variable *in situ* contribution during crushing may also result in some difference in isotopic composition and concentration for the same sample during two sets of experiments. For magnetites some difference may also result from carbonate contamination in the separates. Taking into account all the above factors, our results are reasonably reproducible as seen from Table 2.3. Table 2.3A lists the comparisons for He and Ne, 2.3B for N and Ar and 2.3C for Xe and Kr.

Table 2.2 Typical values of air standard parameters used in calibration

Species	Detector and Resistance(ohms)used	Sensitivity (cc STP/Counts)	Yield (%)	M.D* % .amu^{-1}
^{4}He	M, 10^{8}	1.6 x10^{-13}		12(3)
^{22}Ne	M, 10^{8}	0.9 x10^{-13}		2.1(.04)
$^{28}N_2$	F, 10^{10}	5.9 x 10^{-8}♣		2.2(.01)
^{36}Ar	M, 10^{8}	1.6 x 10^{-14}		0.91(.10)F 1.30(.02)M
^{40}Ar	F, 10^{10}	4.7 x 10^{-11}	85	
^{84}Kr	M, 10^{9}	1.4 x 10^{-15}	74	0.98(.09)
^{132}Xe	M, 10^{9}	10.9 x 10^{-16}	92	0.40(.12)

100 counts/sec ≡ 1 mV; M.D* ≡ mass discrimination ♣ Sensitivity of N_2 is in micrograms/count

Table 2.3A Some concentrations and isotopic ratios for He and Ne for repeat samples (t, n and m stands for trapped, nucleogenic and measured respectively). The $^{21}Ne_n$ and $^{22}Ne_n$ have been derived from the $(^{21}Ne/^{20}Ne)_m$ and $(^{22}Ne/^{20}Ne)_m$ ratios after correcting for trapped values assuming all $^{20}Ne_m$ to be trapped(lower mantle-like). Concentrations are in cc STP/g

	^4He_m (10^{-6})	$^{20}Ne_t$	$^{21}Ne_n$	$^{22}Ne_n$	$(^{21}Ne/^{20}Ne)_m$	$(^{22}Ne/^{20}Ne)_m$	$(^3He/^4He)_m$
		(10^{-10})					
H-C1A	30.1	11.5	0.02	0.37	0.0047 ±.0002	0.1123 ±.0008	
H-C1B	22.0	7.4	0.01	0.17	0.0052 .0001	0.1026 .0006	
SV-M1A	6.8	8.4	0.02	0.34	0.0051 .0002	0.1202 .0032	7.08 ±.66
SV-M1B	4.2	5.1	0.01	0.10	0.0057 .0002	0.0989 .0011	7.99 .71

Table 2.3B Some concentrations and isotopic ratios for N and Ar for repeat samples, N in ppb while Ar is in cc STP/g.

	N	$\delta^{15}N$ (‰)	^{36}Ar (10^{-10})	$^{40}Ar/^{36}Ar$
H-C1A	1505	4.70 ±.44	27.4	8367 78
H-C1B	451.2	4.99 .28	21.3	11392 104
SV-M1A	519.2	3.32 .20	16.4	1743 28
SV-M1B	417.3	-1.69 .72	8.6	1386 13

Table 2.3C Some concentrations and isotopic ratios for Xe for repeat carbonate samples. ^{84}Kr concentration is also given. Concentrations are in cc STP/g.

	^{84}Kr (10^{-12})	$^{132}Xe_m$ (10^{-12})	$^{132}Xe_f$ (10^{-12})	$^{129}Xe/^{132}Xe$	$^{131}Xe/^{132}Xe$	$^{134}Xe/^{132}Xe$	$^{136}Xe/^{132}Xe$
H-C1A	63.3	4.5	-	1.07 .01	0.84 .01	0.45 .01	0.37 .01
HC-1B	40.2	18.6	-	1.16 .01	0.81 .01	0.38 .01	0.33 .01

Reproducibility check for pyrolysis analyses had also been done, but the second sets of pyrolysis experiments were conducted on already vacuum crushed powders. This resulted in considerable discrepancy due to loss of *in situ* gases from the powders as

well as surface adsorbed gases on the powdered grains (see Chapter 2) and has not been considered for reproducibility check. To check the accuracy of the instrument, carbonatite of Oldanyo Lengai has been analyzed for nitrogen and noble gases. The $^{20}Ne/^{22}Ne$, $^{40}Ar/^{36}Ar$ and $\delta^{15}N$ values of 9.2±.08, 356±3 and 1.03±.52 for our analyses are in agreement with reported (Javoy et al., 1989) values.

2.14 Characterization of samples

For the present noble gas and nitrogen studies, only fresh and unaltered samples have been selected. Mainly, thin sections and elemental analyses have been done for characterization of samples, so as to aid in their proper selection. However initially, before any elemental analysis or thin section studies, solely on the basis of visual inspection only interior chunks of clean and fresh samples had been selected.

Thin section studies under optical microscope was mainly done at the preliminary stage to distinguish between early and late stages of carbonatites. Typical minerals in the early stages of carbonatites like calcite and dolomites, silicates (forsteritic olivine, monticellite, nepheline, phlogopite/biotite, clinopyroxene and amphibole) and oxides (magnetite, perovskite) tend to react with water at low temperatures to form the assemblage of dolomite or ankerite, quartz, zeolites, fluorite, chlorite, rutile and haematite. Thus rocks whose thin sections show the presence of quartz, chlorite and oxides (rutile, haematite) have been ignored for our analyses. Some typical sections that have been considered for our studies as well as those that have been discarded are shown in Fig. 2.6.

For the study, minerals (carbonates, apatites and magnetites) have been separated under optical microscope for analyses. To confirm mineral identification XRD studies have been done on the carbonates and apatites. The XRD spectrum of the minerals when compared to standards indicate that most of the carbonates separated are calcitic and a very few of them are dolomitic as well. Typical diffraction angles and the corresponding intensities for standard calcites, dolomites and apatites (that is equated to the characteristic d-spacing of a mineral by Bragg's Law, provided the wavelength is known which will depend on the type of X-ray tube being used. In the present case Cu tube had been used) are shown in Table 2.4. The diffraction angles and the corresponding intensities for the samples analyzed conform to that of the standards.

Trace elemental analyses can be very informative about the characterization of the samples. Analyses of elements like K, Na and Fe done by AAS (Atomic-adsorption-spectrometry) and Ca and Mg by ICPAES on the samples (Inductively-coupled-plasma-atomic-emission-spectrometry) are given in Table 2.5.

The elemental analyses confirm that the carbonates separated are generally calcitic to dolomitic in composition. However, for SE-C7, where the composition deflects from that of an ideal carbonate, it is likely that some other phases like fluorite is present in the sample. With progressive carbonatitic magmatism, the composition changes from calcitic to dolomitic and finally to ankeritic (Fe-rich) (Viladkar and Schidlowski, 2000). In general the Fe content in the samples is negligible implying that the carbonates are derived from relatively early stages of magma genesis

For the apatites, elemental analysis conforms to that of ideal apatites. Iron and Mg substitutes for Ca in the apatite structure and are present as 0.01 to 0.09% Fe and 0.01-0.9% Mg. Certain other trace elements including REES (rare-earth-elements) have been analyzed by ICPMS (Inductively-coupled-plasma-mass-spectrometry) on the apatite separates. Apatites from carbonatites normally have characteristically high ratio of LREE/HREE. Most apatite specimens have La/Yb ratio as high as 150-200 and in some cases the ratios may be as high as 300. But apatites may form early in carbonatites and can persist to late stages of development. From early to middle stages of development, apatites show an increase in HREE. A typical secondary apatite can even have a La/Yb ratio as low as 0.03.Thus La/Yb ratio can be used to distinguish between early and late stages of carbonatites.

Table 2.4 XRD spectrum of diffraction angles for standard calcite, dolomite and apatite. I represents the intensity measured in linear counts/sec

2θ	I	2θ	I	2θ	I
Calcite		Dolomite		Apatite	
29.71	**100**	24.04	4	29.66	16
36.31	12	**30.94**	**100**	**31.03**	**100**
39.81	22	33.54	4	32.45	20
43.60	13	37.38	7	33.03	10
47.62	7	41.13	19	32.45	20
48.13	28	44.95	10	33.48	8
49.06	21	50.53	10	34.37	65
58.01	9	51.07	13	35.12	8

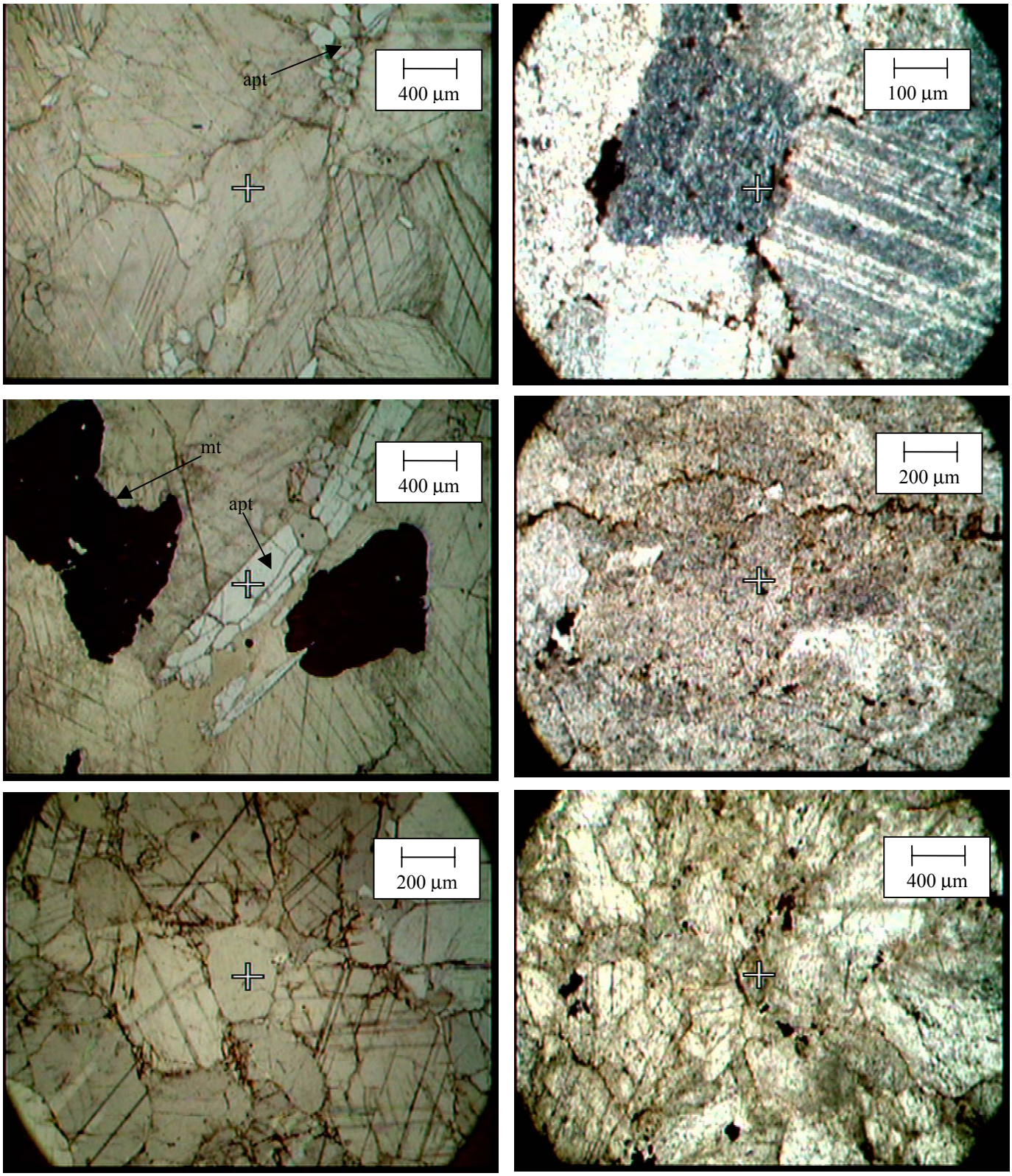

Fig.2.6A Typical photomicrographs of thin sections of carbonatites under plane polarized light that have been selected for noble gases and nitrogen analyses. Carbonates are the dominant phase, some apatites(apt) and magnetites(mt) also present.

Fig.2.6B Typical photomicrographs of thin sections of carbonatites under plane polarized light that have not been selected for present analyses as they show the effect of late stage alteration along grain boundaries. The sections show the formation of secondary Fe oxides(brownish in the pictures) along the margins of the grains.

Table 2.5 Elemental analyses of different mineral separates from carbonatites

	Ca	Mg	Fe	K	Na
Hogenakal					
H-C1A	41.1	0.44	0.49	19.4	96
H-C1B	40.2	0.42	0.36	18.0	69.3
H-C2	40.4	0.51	0.45	29.5	85
H-C4	40.9	0.43	0.27	18.1	324
H-A	40.0	0.04	0.05	36.5	1752
Sevattur					
SE-C3	38.0	1.81	1.03	18.6	182
SE-C4	37.3	2.20	1.18	20.4	176
SE-C7	61.0	0.66	0.43	27.3	343
SE-A1	42.3	0.04	0.08	11.4	1731
Khambamettu					
K-C1	38.2	0.22	0.21	44.7	411
K-C3	32.9	0.45	0.56	0.9	268
K-A1	38.4	0.02	0.03	16.1	2408
K-A2	41.0	0.03	0.06	7.6	1841
Sung valley					
SV-C1	39.7	1.11	0.05	21.5	354
SV-C2	40.3	1.40	0.15	8.3	230
SV-C4	37.9	0.91	0.09	4.6	228
SV-A1	42.1	0.10	0.02	9.3	257
SV-M1A	12.32	3.01	29	21.4	242

K and Na are in ppm, Ca, Mg and Fe in %. Errors are ± 5%.

Table 2.6 Elemental analyses of different apatite separates of carbonatites

	La/Yb	Ba	Sr	Na
			(ppm)	
H-A	55	125	5213	1752
SE-A1	80	163	1930	1731
K-A1	270	1124	15858	2408
K-A2	173	128	12727	1841
SV-A1	105	18.8	1684	257

The errors involved are within ±5%

Other elements like Sr, Ba and Na also show a trend in apatites from carbonatites during the course of their crystallization. Na decreases from 0.1 to 0.9% in the primary apatites to 0.01 to 0.09% in the secondary apatites. Ba, on the other hand increases from early to late carbonatites from 0.04% to 0.19%. Sr that enters calcite in the early carbonatites but are later concentrated in fluroapatite, barite and strontianite increases from an average of 0.33 to 0.90% from early to late stages of apatite. Table 2.6 is a tabulation of these results in the apatites that help us to conclude about their primary/secondary nature.

Taking into account all these parameters into consideration, it is likely that the apatites analyzed have formed during the primary or intermediate stages of carbonatite crystallization.

Chapter 3

Noble gases in carbonatites - *In situ* produced components

3.1 Introduction

Noble gases in carbonatites essentially have two components, namely a trapped and an *in situ* component. The trapped component basically represents the source region from where the sample has trapped its gases, while the *in situ* component is that produced in the sample after its crystallization. Owing to the incompatible nature of both noble gases and nitrogen the trapped gases are mostly expected to be present in

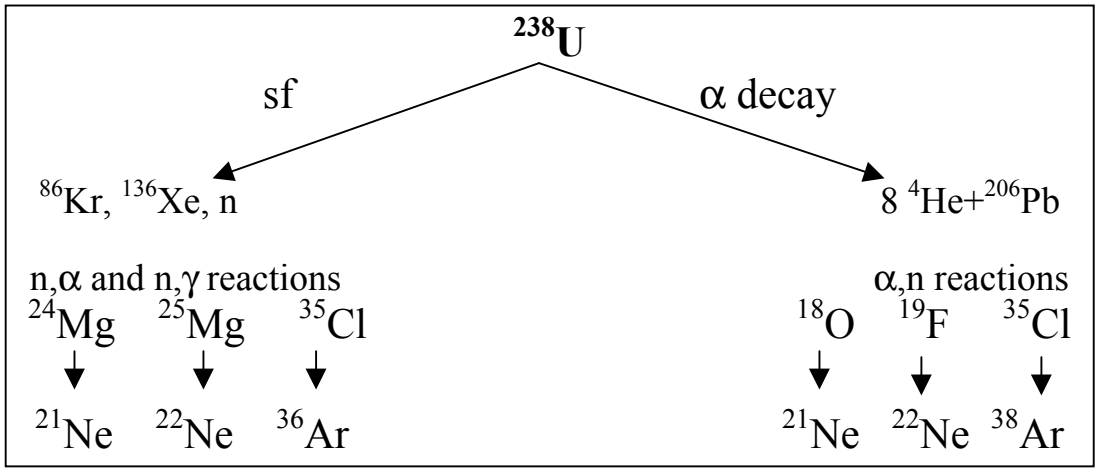

Fig. 3.1 Schematic representation of various in situ noble gases that are produced in U, Th rich minerals like apatites

the fluid inclusions while the *in situ* gases are hosted in the lattice structure. Thus total release of *in situ* gases is only possible when samples are melted completely, while vacuum crushing (VC) preferentially release the trapped gases from the fluid inclusions with possibly a small fractional release of *in situ* gases from the lattice. Here, in order to derive the concentration of *in situ* isotopes of noble gases in the samples, only pyrolysis (P and VC+P') analyses of apatites have been considered where the total gas has been released.

Fig. 3.1 schematically represents the production of *in situ* noble gases in the apatites. ^{238}U decays to produce alpha particles (α) while spontaneous fission produces ^{86}Kr and ^{136}Xe. Both the α particles, that have energies between 4.01 MeV and 8.75 MeV

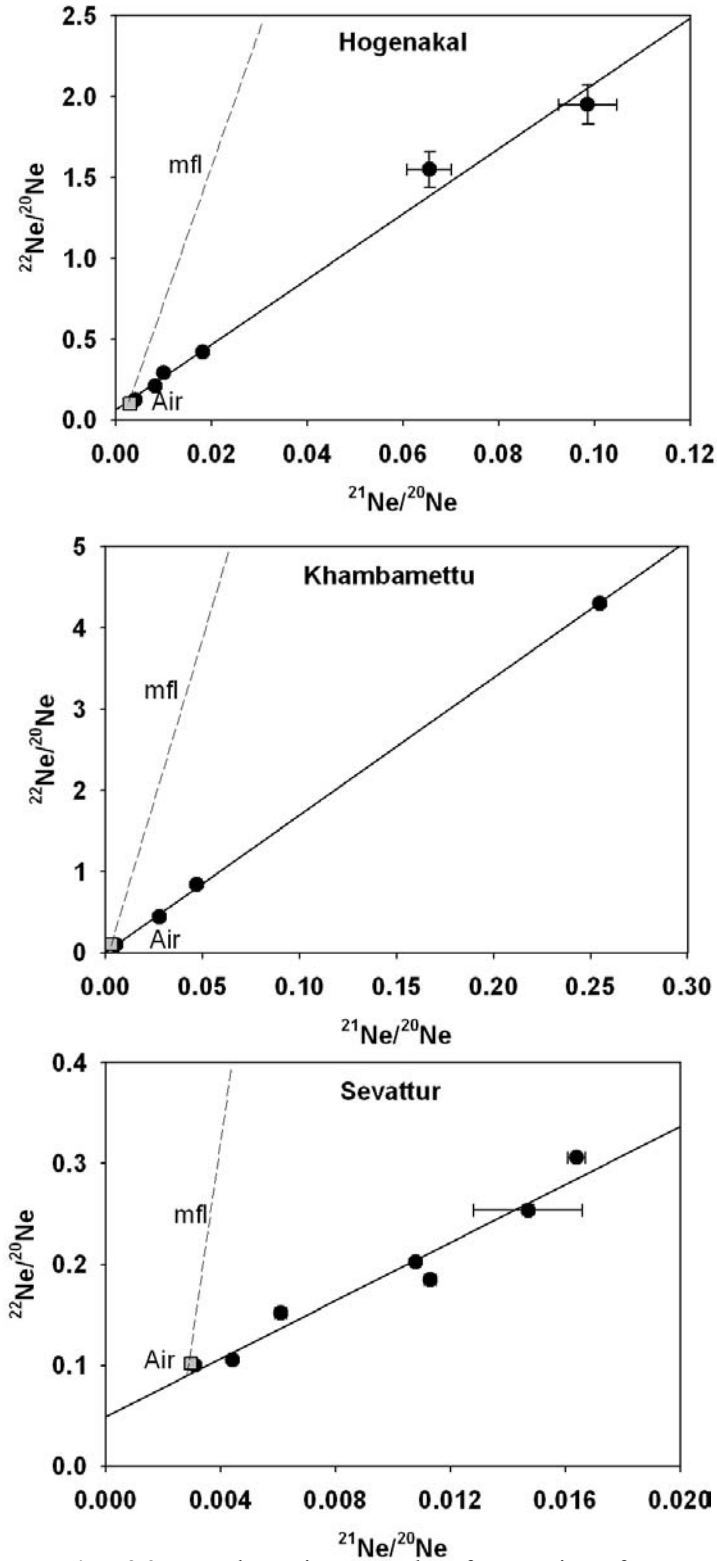

Fig. 3.2 Ne three isotope plot for apatites from Hogenakal, Khambamettu and Sevattur. Clear excesses of ^{21}Ne and ^{22}Ne are seen in all the samples and are unrelated to mass fractionation represented by mass fractionation line (mfl) in the figure

and the neutrons produced in these processes induce various (α,n), (n,α) & (n γ) nuclear reactions with low threshold energies in the samples during their slowing down and interaction with the surrounding atoms (Wetherill, 1954). However, nuclear reactions only on light elements like O, F and Mg have threshold energies low enough for these reactions to occur. In addition, the secondary neutrons produced in alpha-induced reactions have enough energy to induce further nuclear reactions.

3.2 U,Th-^{4}He dating technique

Since the production of α particles from U and Th will be time dependent, several recent studies have evaluated the potential of U-Th/^{4}He dating technique for thermochronometry (Zeitler et al., 1987; Lippolt et al., 1994; Wolf et al., 1996; Warnock et al., 1997; Reiners and Farley, 1999). Since the closure temperature of He for apatite is ~70°C, it is now established that U-Th/He ages of apatite record cooling through lower temperatures

than other dating techniques (Farley, 2000). However, it should be noted that fractional loss of He is also controlled by crystal size and larger crystals should retain a greater fraction of radiogenic He (Reiners and Farley, 2001). The influence of crystal size will be profound in rocks that have been in the range of partial He retention temperature (30-70°C) for long periods of time(>10^7 years). Considering the mean stopping distance of 19.7 μm of α particles in apatites, it has been found that for grains smaller than a few microns in minimum dimension, ejection effects can cause measured He ages to be substantially underestimated (Farley et al., 1996). In that case interpretation of U-Th/He age should incorporate the effect of crystal size. However meaningful He ages can be obtained for larger crystals. If He retentivity is defined as the number of decays which remain confined in the grains divided by the total number of decays, simulated Monte Carlo results for retentivity (F_T) in cylinders with varying length/radius indicate F_T ~ 0.95 for cylinder radius ~ 250 μm (Farley et al., 1996). Thus appropriate sample selection is very crucial for U-Th/He thermometry. In the present study, grains analyzed are much coarser (mm size range) and corrections for α stopping distances are not necessary. Also, the grains selected were cylindrical that retains gases much more than the rounded ones.

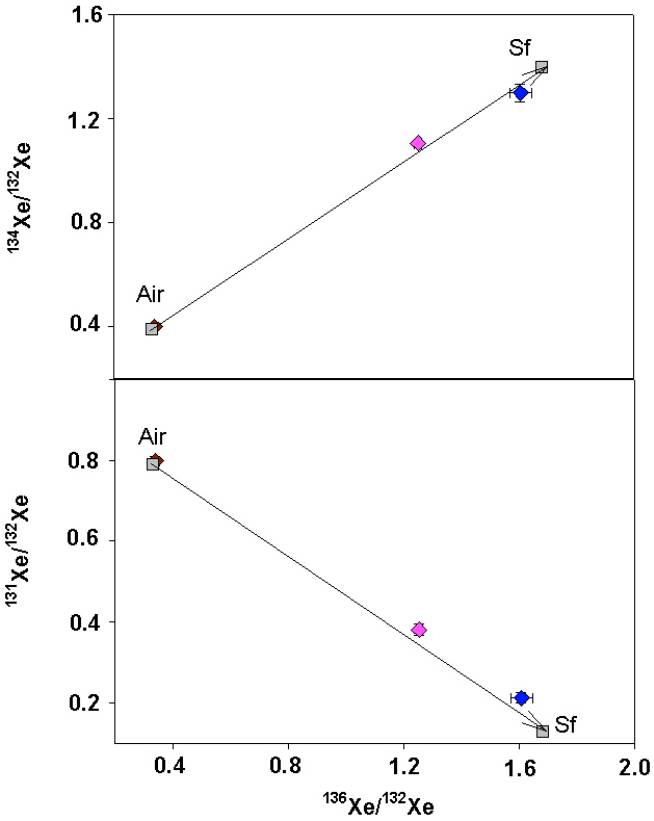

Fig. 3.3 Xe isotopes for apatites from Hogenakal(blue), Sevattur(brown) and Khambamettu(pink) characterized by mixing between air and fission component contributed by ^{238}U

3.3 U-^{136}Xe dating technique

Besides radioactive α decay, U undergoes spontaneous fission, producing among other isotopes, fissiogenic Xe and Kr. The fission gases accumulate in U rich minerals over geological time and can be used for age determinations. The method was first

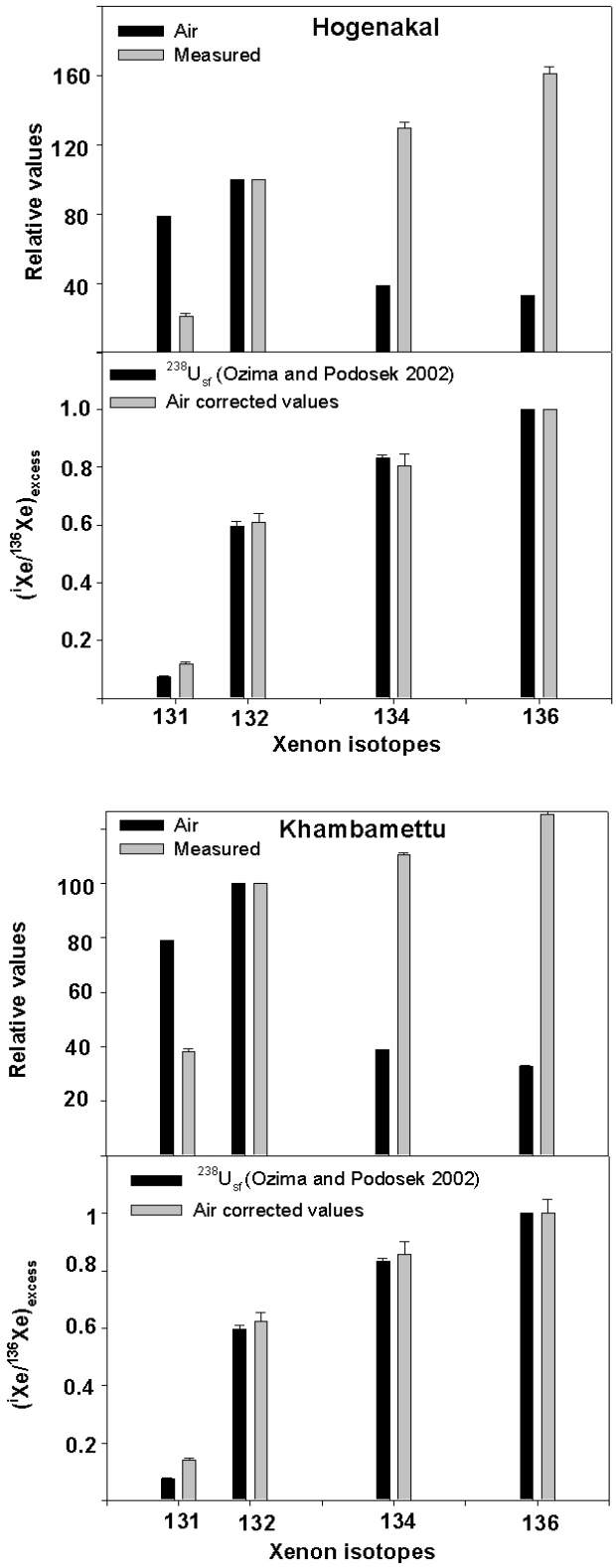

Fig. 3.4 Excess Xe in Hogenakal and Khambamettu apatites for the different isotopes represented by the relative values. When corrected for Air, within errors they are in agreement with that expected from spontaneous fission of ^{238}U

applied to pitchblende where the ages reported were lower than their formation ages and attributed to subsequent geological events (Gerling and Shukolyukov, 1960). However later investigations revealed that fission gases may survive even greenschist facies metamorphic conditions (Eikenberg et al., 1989). In fact unless reset by some high temperature event the systematics has also been found to indicate the formation age of pitchblendes (Meshik et al., 2000a). Thus U-Xe age should either correspond to the formation age of the mineral or indicate resetting by geological event with T>350°C and P>0.4 GPa. Ideally U-Kr systematic should also be equally applicable, but not so commonly used since fissiogenic Kr has been found to be lost more easily than Xe.

3.4 U,Th-^{21}Ne dating technique: Since the production of α particles inducing the nuclear reactions $^{18}O(\alpha,n)^{21}Ne$ and $^{19}F(\alpha,n)^{22}Ne$ depends on the

age of the samples and U,Th concentration in the mineral, the $^{21}Ne(^{21}Ne_n)$ and $^{22}Ne(^{22}Ne_n)$ so produced will also depend on the age of the samples along with target element (F,O) and U,Th concentrations of the mineral. Thus ideally U,Th-$^{21}Ne_n$ and U,Th-$^{22}Ne_n$ systematics can be used as geological clocks. This is the first attempt to check the feasibility of using U,Th-$^{21}Ne_n$ and U,Th-$^{22}Ne_n$ for geochronological purposes, along with the established U,Th-^{4}He and U-Xe dating tools. It is to be mentioned here that the (α,n) reactions account for most of the nucleogenic Ne in minerals with F/Mg > 10^{-4} and > 99% in the Earth's crust (Leya and Weiler, 1999). Since the cross sections for the reactions $^{24}Mg(n, \alpha)^{21}Ne$ and $^{25}Mg(n, \alpha)^{22}Ne$ are low (~ <1-200 and 30-100 millibarns respectively), and Mg concentration measured in these apatites is also very small (0.02-0.10 %), production of $^{21}Ne_n$ and $^{22}Ne_n$ via these reactions can be considered to be negligible. On the other hand, in fluorapatite, (which is the most common form of apatite in carbonatites) the target elements O and F for the reactions $^{18}O(\alpha,n)^{21}Ne$ and $^{19}F(\alpha,n)^{22}Ne$ are more abundant being ~41% and 3% respectively. Also their cross sections are much higher (~300-650 and 75-430 millibarns respectively), and for all practical purposes produces almost all of the $^{21}Ne_n$ and $^{22}Ne_n$ in the samples.

3.5 Calculation of in situ noble gases

For such U,Th rich minerals as apatites, it is not unreasonable to consider the entire $^{4}He_m$ to be radiogenic. However the Ne and Xe should be a mixture of trapped and *in situ* components and it is necessary to decouple the two. In Fig. 3.2 the Ne isotopic ratios are plotted for the apatite from Hogenakal, Khambamettu and Sevattur. Since the normalising isotope (^{20}Ne) is purely of trapped origin, any increase in $^{21}Ne/^{20}Ne$ and $^{22}Ne/^{20}Ne$ over the trapped values have to be either due to mass fractionation or due to the presence of nucleogenic Ne. The Ne data for all these apatites show higher than trapped values and also, they plot far away from the mass fractionation trend.

From two component mixing between trapped and nucleogenic gases, one can obtain the $^{21}Ne_n$ and $^{22}Ne_n$ from the equations

$$^{21}Ne_n = {}^{20}Ne_m[(^{21}Ne/^{20}Ne)_m - (^{21}Ne/^{20}Ne)_t]$$

$$^{22}Ne_n = {}^{20}Ne_m[(^{22}Ne/^{20}Ne)_m - (^{22}Ne/^{20}Ne)_t]$$

where m, t and n stand for measured, trapped and nucleogenic respectively. It is to be noted that all ^{20}Ne present can only be of trapped origin, i.e. no significant contribution of *in situ* ^{20}Ne is expected in the sample.

Fig. 3.3 clearly demonstrates the presence of excess Xe in the pyrolysed apatites from Hogenakal and Khambamettu. Within errors, the Xe present in these two samples indicate mixing between air and contribution of fissiogenic component from ^{238}U. However, the Xe present in Sevattur is more like a pure trapped component without any significant contribution from fission.

The presence of excess Xe above air component is more clearly observed in Fig. 3.4A, where the $^{131\text{-}136}Xe$ isotope composition for Hogenakal apatite is compared with that of air Xe (both normalized to ^{132}Xe). Considering all ^{129}Xe in the apatite to be due to trapped component, (taken to be air Xe; the difference between mantle and air composition for the different Xe isotopes normalized to ^{129}Xe varies within12% and is accommodated in the errors) the excesses at ^{131}Xe, ^{132}Xe, ^{134}Xe with respect to the excess at ^{136}Xe are calculated and compared to those of $^{238}U_{sf}$. Fig. 3.4B is a similar plot for Khambamettu apatite. For both the apatites, the excesses at ^{132}Xe and ^{134}Xe with respect to that at ^{136}Xe agree with the excesses expected at these isotopes due to contribution from $^{238}U_{sf}$. For ^{131}Xe, besides contribution from $^{238}U_{sf}$, additional contribution probably from the reaction $^{130}Ba(n,\gamma\beta)^{131}Xe$ is likely. From the above discussion it is obvious that it will not be unreasonable to assume all excess at ^{136}Xe, (it also has the highest yield for $^{238}U_{sf}$ as compared to the other Xe isotopes) to be due to contribution from $^{238}U_{sf}$.

The trapped component may be air(A) or mantle(M) for ^{22}Ne, air(A) for ^{136}Xe, and air(A), upper or lower mantle (UM or LM) for ^{21}Ne. Table 3.1 gives the concentration of *in situ* gases actually present in the different apatites determined as above.

3.6 U,Th-^{4}He, U,Th-^{21}Ne, U,Th-^{22}Ne, and U-^{136}Xe as dating tools

As mentioned above, the use of noble gases as dating tools is based on their production in the samples after their crystallization as a function of time. Depending on the retention of the various noble gases in different minerals, here for example in apatites, the various clocks will record the timings of the different events that have reset them after the formation of the minerals. The equations that relate the accumulation of the *in situ* noble gases to the relevant age of their retention are discussed below.

Table 3.1 Excess concentrations of ^{4}He, ^{21}Ne, ^{22}Ne and^{136}Xe in apatites (Excess ≈ *in situ*) *Insitu* components calculated considering Air(A), Lower Mantle(LM) or Upper Mantle(UM) to be the trapped components as the case might be for ^{21}Ne, ^{22}Ne and ^{136}Xe. For ^{4}He the measured(Meas) value is assumed to be radiogenic. For all samples, pyrolysis data have been considered except for ^{136}Xe of KA-1 where (P'= Vacuum crushing + subsequent pyrolysis) have been taken into account. U and Th are expressed in ppm. Concentrations of noble gases are in cc STP/g with errors of ± 10%, and ± 15% for ^{136}Xe. *See text for discussion

	^{4}He	^{21}Ne			^{22}Ne		^{136}Xe
	(10^{-6})	(10^{-10})			(10^{-10})		(10^{-12})
	Meas.	A	LM	UM	A	LM/UM	A
H-A	1976	2.7	2.6	1.98	59.7	68.8	20.8
SE-A1	1065	0.9	0.7		80.0	94.2	
K-A1	1360	3.5	3.5	3.4	45.1	47.1	9.1
K-A2	59.3	1.2	1.1	0.5		4.0	
SV-A2	28.2	0.1			2.0	13.1	

$\sum\alpha = U[7.942(e^{\lambda 238t}-1) + 0.0504(e^{\lambda 235t}-1) + 6\{(Th/U) \times (e^{\lambda 232t}-1)\}]$

where $\sum\alpha$ and U are the number of α particles and U atoms / g of the sample

or $0.01063 \times {}^{4}He = U[7.942(e^{\lambda 238t}-1) + 0.0504(e^{\lambda 235t}-1) + 6\{(Th/U) \times (e^{\lambda 232t}-1)\}]$

where ^{4}He is expressed in units of 10^{-6} cc STP/g

For nucleogenic Ne ($^{i}Ne_{n}$) (Leya and Weiler, 1999)

$(^{i}Ne) = [\{W(O, F) \sum\alpha\} \times \{ A + B(Th/U)] / [21.29 + \{4.87(Th/U)\}]$

where

^{i}Ne is the concentration of the nucleogenic isotope of Ne expressed in cc STP/g

W(O,F) is the wt. fraction of oxygen or fluorine or both depending on which is/are the target elements

A and B are coefficients used for calculating nucleogenic production rates in monazite, zircon and apatite

For apatites,

$^{21}Ne_{n} = W(O) \times \sum\alpha \times [X/Y] \times 10^{-26}$

For W(O) = 0.4129

$^{21}Ne_{n}$ (10^{-10} cc STP/g) $= 0.1045 \times \sum\alpha' \times [X/Y]$

$^{22}Ne_{n}$ (10^{-10} cc STP/g) $= 253.1 \times \sum\alpha' \times [(P+Q)/Y]$

where

$X = \{5.62 + 1.91(Th/U)\}$

$Y = \{21.29 + 4.87(Th/U)\}$

$P = W(O)[\{4.59 \times 10^{-6}\} + \{(Th/U) \times 1.30\}]$

$Q = W(F)[\{1.52 \times 10^{-6}\} + \{(Th/U) \times 0.516]$

$\sum\alpha' = U[7.942(e^{\lambda 238t}-1) + 0.0504(e^{\lambda 235t}-1) + 6\{(Th/U) \times (e^{\lambda 232t}-1)\}]$ where U is in ppm.

For fissiogenic ^{136}Xe,

$^{136}Xe_f = [\{(^{238}U \times {}^{i}Y_{sf} \times \lambda_{sf})/ {}^{\lambda 238}\}(e^{\lambda 238t}-1)]$

where

${}^{i}Y_{sf} \times \lambda_{sf} = 5.7 \times 10^{-18}$ /a (Eikenberg et al., 1993)

The values of the different decay constants are

$\lambda 238 = 1.55125 \times 10^{-10}\ y^{-1}$

$\lambda 235 = 9.84850 \times 10^{-10}\ y^{-1}$

$\lambda 232 = 4.94750 \times 10^{-11}\ y^{-1}$

Therefore,

$^{136}Xe_f$(in 10^{-12} cc STP/g units) $= [(e^{\lambda 238t} - 1) \times U(ppm)]/0.2891$

3.7 Estimation of fluorine in apatites from neon three isotope plot

From Fig. 3.2 it is obvious that $^{21}Ne_n$ and $^{22}Ne_n$ have been added to the trapped gases of the samples. The slope of the line is equivalent to $(^{22}Ne/^{21}Ne)_n$ in the sample which will be proportional to the target element concentration of fluorine and oxygen present in the samples.

From the experimental work of Hunemohr (1989) the $^{21}Ne/^{22}Ne$ ratios in U-Th minerals were related to O/F ratio by the given relationship:

$\log(^{21}Ne/^{22}Ne) = (1.038 \pm 0.021)\log(^{18}O/^{19}F) + \log(2.2 \pm 0.3)$

Using the above relation and the $(^{21}Ne/^{22}Ne)_n$ determined from the slope of neon three isotope plots in Fig. 3.2, the fluorine concentration in the apatites have been estimated to be ≈ 3.3%, 2.7% and 2.4% in Hogenakal, Khambamettu and Sevattur respectively for an oxygen concentration of 41%.

3.8 Retentivity of different in situ noble gases in the apatites

The retentivity of a particular noble gas isotope in any sample is defined as the fraction of the gas presently retained in the sample, (and therefore corresponding to the measured concentration), to the amount of that *in situ* isotope that should be

actually present in the sample right from its time of formation had there been no loss of volatiles. The expected concentration of any particular *in situ* isotope in a given sample can be obtained from the equations discussed earlier (section 3.5), and the measured U, Th concentration in the samples. The O content for an ideal apatites is ~41%, while the F content as obtained from section 3.6 has been used. The expected concentrations as well as the retentivity of the different isotope of noble gases for the various apatites are given in Table 3.2. As expected the retention of the lightest isotope ^{4}He is the least, followed by ^{21}Ne and the ^{136}Xe is retained the maximum. For example in Hogenakal apatite the retention of in situ ^{4}He, ^{21}Ne and ^{136}Xe (in %) are 8.5, 30, and 52.5 respectively. For the Sevattur apatite the retention for *in situ* ^{4}He and ^{21}Ne are 41% and 78% respectively. For Sung Valley the retentivity of the different isotopes have not been calculated since the U and Th have not been measured on the same aliquot that has been analyzed for noble gases. For the Khambamettu apatites, retentivity (in %) for ^{4}He and ^{136}Xe in K-A1 are 32 and 69 respectively. ^{4}He retentivity of K-A2 is 41%. However it is to be mentioned that both these Khambamettu apatites behave anomalously where the measured ^{21}Ne is greater than the expected value (see Section 3.10).

Table 3.2 Expected in situ concentrations and retentivity of ^{4}He, ^{21}Ne, ^{22}Ne and ^{136}Xe in apatites

The U and Th (expressed in ppm) concentrations have been determined by ICPMS and have an error of 2%. The noble gas concentrations are with 10% errors. Concentrations of noble gases are in cc STP/g. *Ages are taken from (Kumar et al., 1998; Ray et al., 1999 and Ray and Pande., 1999). Khambamettu ages are from Kumar (unpublished data).

	Age* (Ma)	U	Th	^{4}He (10^{-6})	^{21}Ne (10^{-10})	^{22}Ne (10^{-10})	^{136}Xe (10^{-12})	Retentivity(%)		
					Expected			^{4}He	^{21}Ne	^{136}Xe
H-A	2400	25.4	189	23168	8.9	4485	39.6	8.5	30	52.5
SE-A1	770	7.11	84.6	2567	1.02	570	3.1	41	78	
K-A1	523	44.9	83	4201	1.4	378	3.1	32	69	
K-A2	523	0.78	6.2	143	0.06	28.1	0.2	41		
SV-A2	107	0.81	20.9	73.2	0.03	19.2	0.05			

The difference in retentivity of the same isotope produced *in situ* among different samples may reflect different geological processes that the samples might have

undergone with time resulting in differential loss of gases. Some variation may also be due to differences in physical parameters like grain size and shape that greatly influence gas loss from a sample. For example, the maximum retentivity of gases is found in the Sevattur apatite that is relatively much coarser (length ≈2.6cm,diameter ≈0.80 cm) than either Hogenakal (length ≈0.25 cm, diameter ≈0.15 cm) or Khambamettu (length ≈0.55 cm, diameter ≈0.2 cm). For Hogenakal, the low retentivity may be influenced by the age of the sample and therefore the complex geological history that is likely to be associated with it.

The low retentivity of ^{22}Ne as compared to ^{21}Ne is probably related to the enhanced O/F ratio in the 10-40 μm range of the 4-9 MeV α particles produced by U, Th decay in the apatites. In other words, within the reaction sphere of 10-40 μm range of the α particles the O/F ratio is not that of an average apatite. Such a discrepancy has also been observed from the study of crustal fluid samples from broad geographical distributions where the crustal O/F ratio of 110 calculated from $^{21}Ne/^{22}Ne$ is 4-10 times lower than the average crustal ratio, the discrepancy being accounted for by an enhanced O/F ratio within the range of the U,Th generated α particles (Kennedy et al., 1990). Similarly in the case of the apatites analysed in the present study, the lower production of nucleogenic ^{22}Ne is probably due to reduced interaction of α particles with fluorine within their range.

3.9 Age estimation in Hogenakal, and Sevattur apatites from in situ ^{4}He, ^{21}Ne, and ^{136}Xe

In a given sample the retentivity of the different noble gases will be related to its closure temperature. The closure temperature for ^{4}He in apatites have been estimated to be 75 ±5°C. which is insensitive to grain size or chemical composition as inferred from the study of various igneous samples (Wolf et al., 1996). The U,Th-^{4}He, U,Th-^{21}Ne and U-^{136}Xe ages obtained both from the different apatites are given in Table 3.3. The ages show variation with the youngest age being represented by U,Th-^{4}He and the oldest age being obtained from the U-^{136}Xe systematics. The three different ages are likely to be related to the closure temperature of ^{4}He, ^{21}Ne and ^{136}Xe. ^{4}He must have the lowest closure temperature and therefore the least retentivity, indicating a low temperature geological event, while the highest closure temperature and therefore a higher temperature event is obtained from the U-^{136}Xe systematic.

Both Hogenakal and Sevattur are associated with the Eastern Ghat mobile belt (EGMB) and are only 70 km apart. They occur within a narrow transition zone where the low metamorphic grade peninsular gneisses to the north grades into granulite facies in the south (Condie et al., 1982). As seen in Table. 3, the U,Th-^{4}He, U,Th-^{21}Ne and U-^{136}Xe ages of Hogenakal are 234±35, 607±91 and 1370±205 Ma respectively. The U,Th-^{4}He, and U,Th-^{21}Ne ages for Sevattur are 326±82 and 609±152 respectively.

Table 3.3. Ages (in Ma) obtained from U,Th and different noble gas systematics of apatites from Hogenakal and Sevattur

	U,Th-^{4}He	U,Th-^{21}Ne	U-^{136}Xe
Hogenakal	234	607	1370
	±35	±91	±205
Sevattur	326	609	N.D*
	82	152	

N.D* not determined

In peninsular India, besides the peak granulite metamorphism before the formation of these carbonatites at 2.5 Ga, there are reports of further events of granulite metamorphism at ≈ 1.6 ± 0.2 Ga and 0.9 ± 0.1 Ga related to Indo-Antarctic collision, followed by a younger event at 0.55 ± 0.1 Ga corresponding to Pan African orogeny (Kale., 1998). Considering the P-T conditions of ≈13 Kbar and 1000°C for granulite metamorphism, it is not unlikely that the different events might reset the various geological clocks that will be recorded by the different geochronological systematics. Among the different events of granulite metamorphism, the last event should leave its imprint which is indeed the case. For both Hogenakal and Sevattur, the U,Th-^{21}Ne ages are in agreement with the last granulite event observed in the terrain. However, it is obvious from our studies that the U-^{136}Xe systematic is much more retentive than the other systematics. In fact, earlier works have revealed that xenon can be very retentive and the closure times of the U-Xe systematics correspond to formation ages of pitchblendes from vein type epi-and-hydrothermal deposits of Schwarzwald (Meshik et al., 2000a). In fact, in Hogenakal the U-^{136}Xe age is not reset, at least completely by granulite metamorphism of the last episode. Rather the U-^{136}Xe ages

from both Hogenakal is probably a partial reset ages of the last event of granulite metamorphism, while the U,Th-^{21}Ne ages are indicative of the final episode of granulite metamorphism in this terrain.

The general agreement between the U,Th-^{4}He ages of Hogenakal and Sevattur of 234±35Ma and 326±82 Ma respectively correspond to the age when the rocks were cooled to the closure temperature of 75±5°C of U,Th-^{4}He systematic. This corresponds roughly to the upper 2-4 km of the earth's crust and represents the ages when these rocks were exhumed to this level.

The large errors involved in the measurements are because of the errors associated with U and Th measurements and mainly the noble gas concentrations. Also the error accommodates the difference in ages that would be obtained by assuming different trapped components namely air or the mantle. It is more likely that samples have a mixture of both air and mantle as trapped components (see Chapter 4 and Chapter 5). Since the ages from the three systematics U,Th-^{4}He, U,Th-^{21}Ne and U-^{136}Xe vary progressively from younger to older, it clearly indicates that the closure temperature for these three isotopes are different in apatites. Constraining their closure temperature can be very useful to understand the cooling history of any terrain. Since this is the first attempt to check the feasibility of U,Th-^{21}Ne as a dating tool, it should be noted that it records events that may otherwise go undetected, and hence may be applied in U, Th rich minerals (like monazites and zircons) from other terrains as well Basu et al., 2001).

3.10 Age estimation of Khambamettu apatite: indication of crustal contamination

For the two Khambamettu apatites analyzed the U,Th-^{4}He ages of 175$\pm$26 Ma and 220$\pm$33 Ma are in agreement within errors and may represent the exhumation ages of these samples. However, it was already seen that for both the apatites the measured $^{21}Ne_n$ are greater than that expected for the samples. For one of the apatites (K-A1), the U,Th-^{21}Ne age (1223±183 Ma) is greater than the U-^{136}Xe age (367±55 Ma). Any event that resets the U-^{136}Xe systematic should also reset the U,Th-^{21}Ne system as well since the closure temperature for ^{21}Ne is expected to be much lower than that of ^{136}Xe in any mineral. Although there was no fissiogenic ^{136}Xe in the other apatite from Khambamettu (K-A2), it gives an anomalously high U,Th-^{21}Ne age greater than that of the Earth. This implied presence of additional ^{21}Ne that is not accountable by

the U and Th concentrations in the mineral. Crustal contribution may be one source for the additional ^{21}Ne. Hence, using the noble gas dating tools discussed above may throw additional light as to the presence of any crustal component in a given sample.

3.11 Summary

The present work demonstrates the feasibility of using U,Th-^{21}Ne as a dating systematics in U,Th rich samples like apatites. In conjunction with the already existing dating tools like U,Th-^{4}He and U-^{136}Xe, valuable information regarding the geological history of a terrain may be obtained. It is clearly seen that the retentivity and therefore the closure temperature of ^{4}He, ^{21}Ne and ^{136}Xe in apatites are variable and increases from the lighter to the heavier isotopes. Therefore they are expected to record different geological events that might reset them. Also it is possible that an event unrecorded by U,Th-^{4}He systematics (since it might be subsequently reset by a lower temperature event) and which only partially resets the U-^{136}Xe dating tool is recorded by the U,Th-^{21}Ne clock that is reset completely.

For Hogenakal and Sevattur, two carbonatites 70 km away from each other, the general agreement between their U,Th-^{4}He ages of 234±35Ma and 326±82 Ma respectively represents the ages when these rocks were exhumed to 2-4 km in the earth's crust. The U-^{136}Xe age of 1370±205 Ma for Hogenakal indicates that it was not reset completely by granulite metamorphism whose youngest episode from the terrain is recorded to be 0.55 ± 0.1 Ga corresponding to Pan African orogeny. Rather, the U,Th-^{21}Ne ages of 607±91 and 609±152 for Hogenakal and Sevattur are in agreement to each other and corresponds to this youngest granulite metamorphic event. For the Khambamettu apatites, presence of ^{21}Ne in excess of expected values indicates crustal component in the samples.

Chapter 4

Noble gases in carbonatites - Trapped components

4.1 Introduction

Noble gas signatures, both isotopic ratios and abundance patterns characterize magmatic sources and processes. Their usefulness lie in their chemical inertness as a result of which sometimes they may even reveal isotopic differences in the mantle sources not apparent from the study of other trace elements like Sr. For e.g. $^{87}Sr/^{86}Sr$ ratios reported from the Reunion and Grande hotspots which are two overlying hotspots are in agreement, whereas their $^{3}He/^{4}He$ and $^{40}Ar/^{36}Ar$ ratios are different (Kaneoka et al., 1986). While the Reunion basalts have a high $^{3}He/^{4}He$ ratio (13-15R_A) with $^{40}Ar/^{36}Ar$ values ranging from 430-1900, the Grand Comore samples show a $^{3}He/^{4}He$ value slightly below MORBs with a relatively low $^{40}Ar/^{36}Ar$~380, implying that Reunion and Grand Comore magmas originate from hot spot mantle sources with different noble gas compositions.

Noble gas isotopic ratios like $^{22}Ne/^{20}Ne$ and $^{129}Xe/^{132}Xe$ are very distinct for mantle and air (Chapter 1) and can be used to identify the presence of mantle gases in the samples. $^{3}He/^{4}He$, $^{21}Ne/^{20}Ne$ and $^{40}Ar/^{36}Ar$ are different between air, UM and LM and reflect the source region of the magma in the mantle. The original isotopic composition of the mantle source may alter by processes of addition of radiogenic isotopes, mixing between different magmatic sources and assimilation of crustal components. The absolute abundances and relative patterns of noble gases in mantle are controlled by magmatic processes such as partial melting, fractional crystallization, transportation and degassing.

In this chapter, the trapped noble gas components from the carbonatites of Hogenakal, Khambamettu, Sevattur, Sung Valley and Ambadongar will be assessed from both vacuum crushing (VC) and pyrolysis (P) studies and their implications to understanding the magma sources will be discussed.

From the above carbonatites 25 carbonates(4 from Hogenakal,7 from Sevattur,3 from Khambamettu, 5 from Sung Valley and 6 from Ambadongar), five apatites(1 each from Hogenakal, Sevattur and Sung Valley, 2 from Khambamettu) and 3 magnetites(all from Sung Valley) have been analysed by sequential crushing. In addition, apatites have been analysed by pyrolysis as well.

All the noble gases (except Kr), and N have been studied for both isotopic composition and abundances. Kr isotopic composition had been studied initially for five samples but ratios are atmospheric. Since Kr ratios are generally air like for trapped gases in mantle samples, it was only studied for its abundance in the subsequent analyses. Gas release pattern, elemental ratios and isotopic ratios are discussed in sequence and the inferences drawn. The abundances and isotopic ratios for the light noble gases (He and Ne) are given in Table 4.3 and that for Xe and Kr in Table 4.4. The Ar concentrations and isotopic ratios are given in chapter 5 (Table 5.1) along with N.

4.2 Release pattern of noble gases by vacuum crushing

In the present study VC of apatites, carbonates and magnetites essentially liberated gases trapped in their vesicles. In order to study in a more systematic way the possible change of composition of the released gases with sequential crushing, gases were liberated by 15, 300/500 and again 300/500 strokes and separately analyzed. VC has been done essentially to release the trapped gases present in the vesicles under the assumption that they have remained intact since trapping and have not exchanged any fluid component. However the $^{21}Ne/^{20}Ne$ as well as the $^{22}Ne/^{20}Ne$ ratios above the trapped values of mantle and air clearly indicates that some contribution from *in situ* gases during VC cannot be ruled out entirely. The ratios $^{21}Ne/^{20}Ne$ and $^{22}Ne/^{20}Ne$ can be used as indices for nucleogenic contribution during VC. In general, progressive crushing releases more *in situ* gases as revealed by the $^{21}Ne/^{20}Ne$ and $^{22}Ne/^{20}Ne$ signatures. This may indicate either of the following:

- Progressive release of lattice component during sequential crushing. Progressive crushing should gradually increase the damage to the lattice structure of the mineral with more release of *in situ* gases
- Significant contribution of *in situ* gases (through diffusion into the vesicles) in the smaller fluid inclusions because of their larger surface area/volume ratio. Such diffusion-in of radiogenic He in the smaller fluid inclusions resulting in lower $^{3}He/^{4}He$ ratios has been reported from other mantle samples (Stuart et al., 1994).

For U, Th rich samples the ^{4}He released during VC can be essentially considered to be radiogenic and should be sited in the lattice. However contribution of dominantly lattice sited ^{4}He during VC should show a trend of increasing ^{4}He with progressive crushing contrary to observation. This reflects that part of the ^{4}He may be of trapped origin. Another likely possibility is the faster loss of He from smaller vesicles. Since

the K concentration in the samples is generally low, the $^{40}Ar/^{36}Ar$ ratio reflects the trapped value only. The $^{40}Ar/^{36}Ar$ ratio can be considered as index for atmospheric contamination since higher atmospheric contamination should result in lower $^{40}Ar/^{36}Ar$ ratios as compared to mantle values. The general trend of increasing $^{40}Ar/^{36}Ar$ ratios, during VC as crushing progresses, implies either of the following:

- The influence of atmospheric Ar decreases with progressive crushing. Atmospheric noble gases released in the initial crushing step may be owing to the noble gases adsorbed on mineral surfaces.
- More mantle gases in smaller sized vesicles. Similar trends of different sized vesicles reflecting variable mixing between mantle and atmospheric gases have also been observed earlier in MORB samples (Marty et al., 1983).

4.3 Release pattern of noble gases by pyrolysis (apatites)

Pyrolysis of apatites by stepwise heating till their melting at 1800°C was done to release all the gases, both in the vesicles and matrix present in them. In Fig. 4.1, the release pattern of He, Ne and Ar for the apatites analysed are shown. For the five apatites analyzed, stepwise pyrolysis indicate that most of the ^{4}He is released at 600°C-950°C interval. A large fraction of ^{20}Ne is released at the initial combustion step of 400°C. However the $^{21}Ne/^{20}Ne$ and the $^{22}Ne/^{20}Ne$ ratios suggest that the nucleogenic component is mostly released at higher temperature of 1200°C-1400°C. Analysis of apatites from spinel-lherzolite xenoliths also show that the nucleogenic/spallogenic Ne is released at higher temperature steps of 1450°C-1600°C (Matsumoto et al., 1997). For the Ar release pattern, typically a large fraction of ^{40}Ar (as high as 94% for Sung Valley apatite) is released at 600-950°C, with another peak release at melting temperature step of 1800°C. For the Hogenakal apatite, as much as 72% of ^{40}Ar is released in the final melting step. The dual release pattern is probably related to Ar being released from two different sites in the minerals- probably from decrepitated vesicles and the dissolved Ar fraction from the matrix. A similar release pattern of Ar observed in MORBs from Mid-Atlantic had also been advocated to release from vesicles and matrix in the different temperature steps (Marty et al., 1983). For ^{132}Xe and ^{84}Kr almost all the gas is released during the melting of the apatites. The difference in the release pattern for the different noble gases in the apatites reflects the diffusion rate for each gas species in apatite as well as their siting in the mineral. For example, release at the initial 400°C combustion step

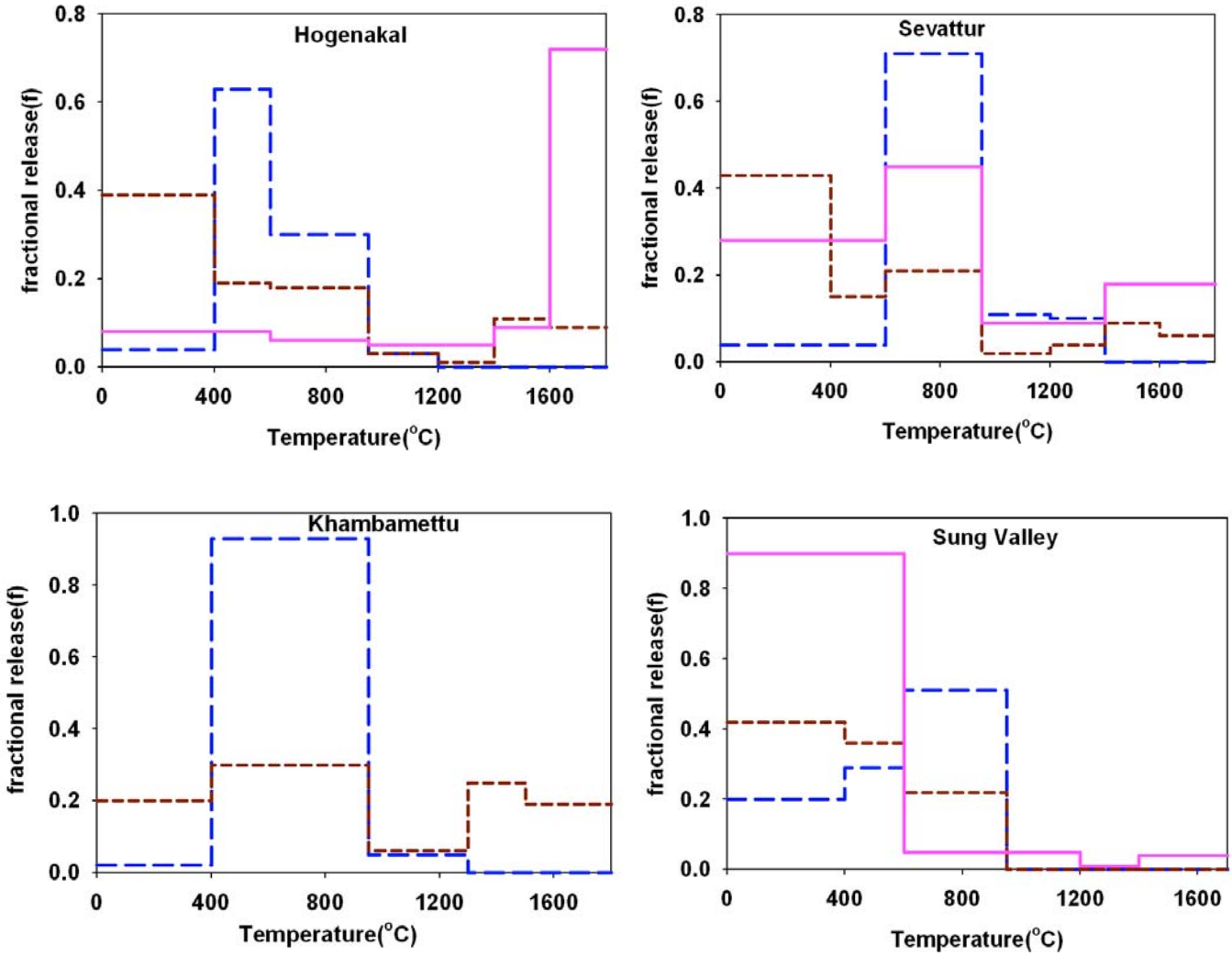

Fig. 4.1 Stepwise release pattern of different noble gases during pyrolysis of apatites from Hogenakal, Sevattur, Khambamettu and Sung Valley. Release pattern of ^{4}He(blue, long-dashed), ^{20}Ne(brown, short-dashed) and ^{40}Ar(pink, solid) are shown. Essentially the release is controlled by their diffusion coefficients, i.e. lighter noble gases are released at lower temperature while the heavier noble gases are released at higher temperature.

corresponds mostly to release of adsorbed gases from the surface of the mineral. Gases trapped in the fluid inclusions are released on their decrepitation. On the other hand release of all *in situ* produced gases and those residing in the matrix will be controlled by their diffusion. Thus in U,Th rich samples where most of the ^{4}He can be considered to be radiogenic, ^{4}He is released at an early step while the ^{132}Xe that should be dominantly fissiogenic is released only at melting temperature.

4.4 Comparison of gas released during VC and P for apatites

Comparison of gas released during VC with that of P can provide with an estimation of the fraction of each trapped gas (only ^{20}Ne and ^{36}Ar have been considered for which no *in situ* contribution is expected) residing in the vesicles and that in the

matrix. Since VC should predominantly release the trapped gases in the vesicles, comparison of (VC), and (P - VC) should indicate approximately the fraction of gases trapped in the vesicles and that dissolved in the lattice respectively. Considering H-A, K-A1 and K-A2 it is apparent that <5% of ^{20}Ne resides in the vesicles. In case of ^{36}Ar ≥ 30% resides in the vesicles (fluid inclusions). Since the solubility of Ne in a silicate melt should be systematically higher than that of Ar, Ne can be enriched in the melt phase relative to Ar after exsolution of a separate bubble phase. Earlier workers have noted He enrichment in MORB glasses with respect to Ne and Ar that had been attributed to outgassing of MORB magmas (Jambon et al., 1986). A good index of such gas fractionation process would have been the ^{4}He/^{40}Ar* ratio (where the ^{40}Ar* is the non atmospheric component of ^{40}Ar in the samples) which for the mantle is ~ 1.7 (Honda and Patterson. 1999). However, in the present case ^{4}He is dominated by *in situ* contribution and thus the ^{4}He/^{40}Ar* would not reflect the trapped value.

Since the comparison between VC and P might be affected by sample heterogeneity in terms of fluid inclusion distribution, crushed samples had been subsequently pyrolyzed so that VC may be compared with P'. However, powdered samples can be highly prone to loss of gas as well as atmospheric contamination due to surface adsorption. As seen from earlier studies on MORBs, about 4% of the total ^{4}He in the basalt powder had been released during 15 hours at the room temperature (Marty et al., 1983). In the present study the samples had been exposed to atmosphere after removal from the crusher and considerable time had elapsed before they were pyrolysed. Loss of ^{4}He and ^{21}Ne from the crushed samples are apparent. For example, in case of H-A comparison of P'+VC and P indicate that only ~ 34% of ^{4}He and ~ 55% of ^{21}Ne are retained in the powdered samples. Although the ^{40}Ar in both case are approximately in agreement with slight enrichment in case of VC+P', the ^{129}Xe/^{132}Xe ratio and the concentration of ^{132}Xe indicate a strong enrichment of atmospheric Xe in case of the powdered sample which resulted from surface adsorption of atmospheric gases. Thus the results from P' should be used with caution and the data of P' and P-VC is not in agreement because of the following reasons:

- Adsorption of heavy noble gases (Ar, Kr and Xe) on powdered samples when they are exposed to air (prior to pyrolysis experiment).

- Loss of light noble gases like He and Ne from the finely crushed samples during the time elapsed between VC and P', most likely due to facilitation by micro-channels that result from radiation damage.

4.5 Variation of concentration of magmatic gases in different mineral phases

In an attempt to investigate if concentration of magmatic gases follows the crystallisation order, carbonates, apatites and magnetites were separated and analysed from the same rock samples of Sung Valley. Since noble gases are incompatible, they should be enriched in the melt with progressive crystallisation. Thus late crystallising phases like magnetites should have a higher concentration of magmatic gases as compared to the other earlier crystallising phases if volatiles are retained in the course of crystallisation. This has been observed for magnetites in Kola carbonatites, as compared to the olivines and pyroxenes from the same rock suites (Tolstikhin et al., 2002). Here we have compared the ^{3}He concentration (since He should not have any air contaminant), ^{20}Ne and ^{36}Ar in carbonate(SV-C1), and magnetite(SV-M1B) derived from the same rock sample, and in another set of carbonate(SV-C3) and magnetite(SV-M3). For none of these three isotopes any *in situ* contribution in the samples is expected. The concentration of each gas (in cc STP/g) in the different samples is tabulated in Table 4.1 below.

Table 4.1 Concentrations (in cc STP/g) for carbonates and magnetites separated from the same rock piece for two samples

Samples	^{3}He (10^{-4})	^{20}Ne (10^{-10})	^{36}Ar (10^{-10})
SV-C1	0.5	13.4	22.1
SV-A1	n.d*	5.2	18.4
SV-M1(B)	0.5	5.1	8.6
SV-C3	3.8	12.3	25.3
SV-M3	8.7	4.6	7.7

n.d* not determined

The concentration trend for ^{3}He, and ^{20}Ne and ^{36}Ar are in opposite direction for the carbonates and magnetites. While the ^{3}He concentration is higher in SV-M3 and comparable in SV-M1B with SV-C3 and SV-C1 respectively, the ^{20}Ne and ^{36}Ar concentration are almost three times in the carbonates as compared to the magnetites. The controlling parameters may be both vesciculariy and the relative solubility of He,

Table 4.2. Elemental ratios normalised to ^{36}Ar.Column 1 gives the concentration of ^{36}Ar in cc STP/g

	^{36}Ar (10^{-10})	$^{4}He/^{36}Ar$ (10^{4})	$^{20}Ne/^{36}Ar$ (10^{1})	$^{84}Kr/^{36}Ar$ (10^{-2})	$^{132}Xe/^{36}Ar$ (10^{-2})
		Hogenakal			
H-C1A(VC)	27.4	1.10	0.40	2.31	0.17
H-C2(VC)	22.9	3.20	0.69	2.94	0.20
H-C1B(VC)	21.3	1.03	0.35	1.88	0.87
H-C4(VC)	33.3	0.12	0.40	1.65	0.31
H-A(VC)	8.4	18.06	0.74	2.12	0.55
H-A(P')	20.5	23.42	25.25		1.00
H-A(P)	24.8	79.58	20.07	0.29	0.63
		Sevattur			
SE-C1(VC)	31.9	0.06	0.22	1.42	0.08
SE-C2(VC)	15.9	0.16	0.34	0.87	0.09
SE-C5(VC)	7.2	2.56	1.24	5.07	0.49
SE-C3A(VC)	17.9	0.25	0.32		
SE-C3B(VC)	16.5	0.43	0.66	2.34	0.11
SE-C6(VC)	21.1	14.25	1.04	3.84	0.76
SE-C7(VC)	29.9	1.20	0.55	1.67	0.27
SE-A1(VC)	25.9	2.09	0.48	0.69	0.23
SE-A2(P)	6.5	57.75	11.27		
		Khambamettu			
K-C1A(VC)	13.7	1.96	0.39	2.34	0.12
K-C1B(VC)	7.9	5.37	0.46		0.31
K-C3(VC)	23.5	10.99	0.29	2.35	0.07
K-A1 (VC)	4.5	2.66	0.34		
K-A2(VC)	4.0	5.44	0.45		
K-A2(P)	1.7	37.04	237.4		
		Sung Valley			
SV-C3(VC)	25.3	3.22	0.49	0.56	0.33
SV-M3(VC)	7.7	9.52	0.60	2.83	0.48
SV-C4(VC)	24.5	0.20	0.78		

SV-C5(VC)	13.8	0.33	4.64	4.52	0.25
SV-C1(VC)	22.1	0.63	0.61		0.51
SVM1A(VC)	16.4	0.42	0.51		
SV-M1B(VC)	8.6	0.58	0.59		
SV-A1(VC)	18.4	0.26	0.29		
SV-A2(P)	19.7	1.43	0.26		
		Ambadongar			
A-C1(VC)	172.8	0.06	0.78		0.13
A-C2(VC)	148.2	0.05	0.76		0.11
A-C3(VC)	150.6	0.05	0.62	1.68	0.06
A-C5(VC)	33.1	0.04	0.87		0.16
A-C4(VC)	289.1	0.01	0.79		0.06
A-C6(VC)	24.4	1.06	0.70	6.39	0.13
Air	208.3	1.7E-5	0.52	2.1	0.01

Ne and Ar. Vesicles may be formed in the magma due to pressure release as it rises to the surface. During outgassing of bubble phases or formation of vesicles the Ar and Ne partition into the vesicles much more than He. Since carbonates are generally rich in fluid inclusions (William-Jones and Palmer, 2002), is likely to have a higher density of fluid inclusions than magnetites. Thus the ^{36}Ar and ^{20}Ne concentration is likely to be higher in the carbonates than the magnetites. During outgassing of the bubble phases, the melt should be enriched in He owing to its higher solubility. The He in the melt gets progressively enriched as crystallization progresses owing to its incompatibility and thus its concentration is higher in the late crystallizing phase like magnetite. This also highlights the totally decoupled behaviour of He with other noble gases during magmatic processes. However it should be borne in mind that He is highly prone to diffusive loss, even at post eruptive stages and may show large variation in concentration among different samples. Also if the apatite(SV-A1) is compared with the corresponding carbonate(SV-C1) and magnetite(SV-M1), it is to be noted that while the ^{20}Ne concentration in the sample is in agreement with that of the magnetite, its ^{36}Ar concentration is similar to the carbonate. Thus simple solubility vescicularity and time of formation may not be the only controlling factors.

Crystallisation of SV-A1 is at an intermediate stage as indicated by La/Yb ratio (see Chapter 1). In that case the comparable ^{36}Ar of the apatite with that of the early crystallising carbonate may be a simple coincidence. It is possible that enrichment of ^{36}Ar in the sample is due to the presence of a fractionated component, enriched in Ar relative to Ne (Harrison et al., 2003), and is either adsorbed on the surface of the mineral or incorporated in the sample via subduction

4.6 Noble gas elemental pattern:

The noble gas elemental ratios $^{m}X/^{36}Ar$ for all the samples analysed are listed in Table 4.2. For N, the same is listed in chapter 5, Table 5.1. The rare gas abundance data are plotted in Fig. 4.2 by using a fractionation factor F^m where $F^m = (^{m}X/^{36}Ar)_s/(^{m}X/^{36}Ar)_{air}$. Here S is the sample and X is a noble gas isotope of mass m. In the present study, since the samples are U, Th rich, the $^{4}He/^{36}Ar$, $^{84}Kr/^{36}Ar$ and $^{132}Xe/^{36}Ar$ may be affected by radiogenic ^{4}He and fissiogenic ^{84}Kr and ^{132}Xe. However the $^{20}Ne/^{36}Ar$ will be free from any *in situ* contribution. Within errors the $^{132}Xe/^{36}Ar$ does not change appreciably even after fission correction for ^{132}Xe assuming that all ^{136}Xe excess is fissiogenic. But because of the higher diffusivity of ^{4}He, a considerable amount of matrix sited ^{4}He should be released during VC of the samples which is difficult to distinguish from any trapped He that will also be released. The $^{20}Ne/^{36}Ar$ and $^{84}Kr/^{36}Ar$ ratios are atmospheric within errors. Some enrichment for F^{132} is observed for the samples in the present study. Such enrichment of ^{132}Xe with respect to ^{36}Ar coupled with enriched Ne is typical of mantle samples and has been reported from quenched rims of submarine basalts, a sub aerial basalt and an olivine xenolith from Hawaii and a CO_2 well gas from Harding County, New Mexico. Such elemental pattern has been attributed to high temperature solubility and diffusion and bulk melting in the mantle (Ozima and Alexander, 1976). In the present study the coupled enrichment of Ne along with Xe is only pronounced during pyrolysis of the apatites from Hogenakal, Sevattur and Khambamettu and some carbonates of Sung valley and Ambadongar. This may be owing to the higher solubility of Ne that is retained in the melt during vesicle formation and therefore released only during pyrolysis. In certain holocrystalline submarine basalts, elemental pattern characterized by Ne depletion and an enrichment of Kr and Xe has been observed attributed to low temperature adsorption of noble gases (Ozima and Alexander,1976). The elemental pattern for the VC samples in the present case may simply indicate a noble gas pattern observed in most mantle samples affected by

adsorbed noble gases on its surface i.e. a hybrid of the two patterns discussed by Ozima and Alexander (1976). While the type 1 pattern is typical of that of mantle samples characterised by enriched ^{20}Ne, slightly depleted ^{84}Kr and enriched ^{132}Xe, type 3 pattern is observed in samples with adsorbed surficial atmospheric gases resulting in ^{20}Ne depletion and enrichment of the heavier noble gases.

Elemental fractionation for noble gases may be brought about by magmatic processes like crystal-melt partitioning during partial melting and fractional crystallisation, solubility controlled partitioning between melt and gas phases during bubble formation and magma outgassing, and diffusion related differences in the mobility of noble gases in crystals and melts. Some important mantle elemental ratios that have been well constrained so that elemental fractionation can be estimated are $^{4}He/^{21}Ne^{*}\sim(2.2\pm0.1)*10^{7}$ (Yatsevich and Honda, 1997), $^{3}He/^{22}Ne$ ratio of 7.7±2.6 (Honda and Mcdougall, 1998) and $^{4}He/^{40}Ar$ ~1.7. However in this study ^{4}He, ^{21}Ne and even sometimes ^{22}Ne in the samples may be dominated by *in situ* production and may not reflect the true mantle value. Also meaningful ^{3}He values could only be obtained for some Sung Valley samples. The production ratio of $^{4}He/^{21}Ne^{*}\sim(2.2\pm0.1)*10^{7}$ (Yatsevich and Honda,

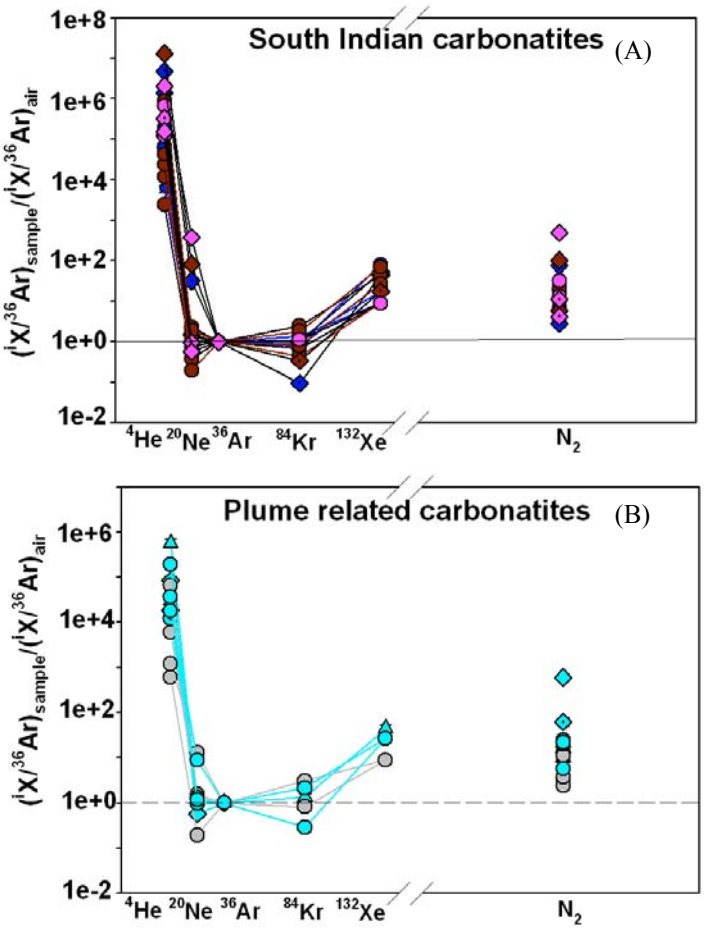

Fig. 4.2 Elemental plot for noble gases and nitrogen in A) South Indian carbonatites of Hogenakal(blue), Sevattur(brown), Khambamettu(pink) B) Plume related carbonatites of Sung Valley(cyan) and Ambadongar(grey). Patterns indicate presence of mantle gases as well as some adsorbed component

1997) also holds good for U,Th rich minerals as in the present case and deviations can be indicators of He loss by diffusion.

The $^{4}He/^{21}Ne^{*}$ ratio (where $^{21}Ne_{m}\equiv$measured has been corrected for trapped component by assuming air to be the trapped gas and all $^{20}Ne_{m}$ to be trapped. If instead trapped Ne is considered to be of mantle origin, the $^{21}Ne^{*}$ calculated will not be too different and the conclusions reached will remain valid) for Hogenakal, Sevattur and Khambamettu ranges from $(0.1\text{-}3.3)*10^{7}$ indicating variable loss of He from the samples by diffusion probably controlled by individual grain sizes. However nominally high $^{4}He/^{21}Ne$ ratios in some samples also indicate the presence of trapped He of mantle origin. Diffusional loss of ^{4}He is also indicated from the youngest 65 Ma Ambadongar carbonates where the $^{4}He/^{21}Ne^{*}$ ranges from $(0.1\text{-}0.7)*10^{7}$ as well as from the 107 Ma Sung Valley carbonates and magnetites with $^{4}He/^{21}Ne^{*}$ ratio similar to that of Ambadongar.

For SV-C3 and SV-M3 both $^{3}He/^{22}Ne$ as well as $^{4}He/^{21}Ne^{*}$ ratios are available for consideration. The $^{3}He/^{22}Ne$ for SV-C3 and SV-M3 are 0.04 and 0.19 respectively both indicating diffusional loss of He from the samples, or the consequence of differential solubility of He and Ne between melt and vesicles. However the corresponding $^{4}He/^{21}Ne^{*}$ in the samples are $8.1*10^{7}$ and $7.3*10^{7}$ respectively. This can have the following implications:

- A part of the ^{4}He is trapped i.e. $^{4}He_{m} > {}^{4}He$ radiogenic
- Additional source of ^{4}H e(crustal fluids?)

Both $^{4}He/^{21}Ne$ and $^{4}He/^{40}Ar$ ratios for a closed system reservoir depend on the U,Th and K content of the mantle. In the present study, the $^{4}He/^{21}Ne^{*}$ ratio is not only higher than the typical production ratio for SV-C3 and SV-M3, even SV-A2(P) for which $^{4}He/^{21}Ne^{*}$ is ~ $23.5*10^{7}$show the presence of excess ^{4}He. An estimation of trapped ^{4}He in these samples was obtained considering the $^{4}He/^{40}Ar$ production ratio of the mantle to be ~1.7 (Honda and Patterson, 1999). The $^{4}He/^{21}Ne^{*}$ corrected for any trapped He will be given by

$$^{4}He/^{21}Ne^{*} = [^{4}He_{m}-(^{40}Ar_{m}*1.7)]/^{21}Ne^{*}$$

The $^{4}He/^{21}Ne^{*}(10^{7})$ ratios determined after correction for any trapped ^{4}He for SV-C3, SV-M3 and SV-A2(P) are~ 6.7, 7.1 and 19.2 i.e. still higher than the typical production ratio. It is to be noted that this ratio should be a lower limit since He must have undergone greater diffusional loss as compared to Ne that is also seen from the

$^{3}He/^{22}Ne$ values. Even if the $^{4}He/^{40}Ar$ production ratio of the mantle is considered to be ~5 which is the present day instantaneous production ratio that is the highest value

Table 4.3 He, Ne abundances and isotopic ratios of all samples

No of strokes(VC) Or °C(P)	^{4}He (10^{-6})	^{20}Ne (10^{-10})	$^{21}Ne/^{20}Ne$	$^{22}Ne/^{20}Ne$	$^{3}He/^{4}He$ (R/R_a)
		Hogenakal			
		H-C1A(VC)(1.0128g)			
50	12.0	7.2	0.0042	0.1032	
			±.0002	±.0003	
300	11.6	3.2	0.0056	0.1182	
			.0002	.0014	
800*	6.5	1.1	0.0055	0.1544	
			.0001	.0020	
total	30.1	11.5	0.0047	0.1123	
			.0002	.0008	
		H-C2(VC)(1.6637g)			
25	4.5	5.00	0.0039	0.1084	
			.0001	.0038	
500	64.5	9.8	0.0042	0.0799	
			.0002	.0073	
500	2.2	1.0	0.0077	0.1503	
			.0002	.0159	
500	2.1	0.6	0.0051	0.1600	
			.0002	.0094	
total	73.3	16.4	0.0043	0.0935	
			0.0002	0.0068	
		H-C1B(VC)(1.7386g)			
15	3.2	2.4	0.0056	0.1020	
			.0001	.0007	
300	18.8	5.0	0.0051	0.1028	
			.0002	.0005	
total	22.0	7.4	0.0052	0.1026	
			.0001	.0006	
		H-C4(VC)(1.9537g)			
15	0.8	3.5	0.0058	0.1046	
			.0001	.0005	
300	2.7	8.5	0.0049	0.1033	
			.0001	.0016	
300	0.5	1.5	0.0067	0.1107	
			.0007	.0022	
total	4.0	13.5	0.0053	0.1045	
			.0003	.0014	
		H-A(VC)(0.8246g)			
15	14.8	0.9	0.0228	0.3136	
			.0015	.0178	
300	57.8	1.0	0.0625	0.9540	
			.0053	.0717	
300	40.4	0.7	0.0718	1.035	
			.0070	.0973	
800	79.9	4.3	0.0262	0.4112	
			.0016	.0212	
total	192.9	6.9	0.0319	0.4881	
			.0017	.0216	
		H-A(P')(0.1818g)			
400	472.5	47.4	0.0076	0.2111	

			.0001	.0007
1200	4.1	69.9	0.0137	0.3950
			.0018	.0522
1400	3.1	317.0	0.0036	0.1074
			.0001	.0003
1800	1.4	84.5	0.0038	0.1413
			.0001	.0002
Total	481.1	518.8	0.0054	0.1611
			.0001	.0004
		H-A(P)(0.1752g)		
400	69.5	159.9	0.0032	0.1005
			.0001	.0002
600	1247	76.3	0.0041	0.1264
			.0001	.0014
950	600.4	74.1	0.0100	0.2896
			.0001	.0025
1200	56.7	10.9	0.0655	1.549
			.0047	.1113
1400	0.6	5.9	0.0986	1.951
			.0061	.1202
1600	0.7	46.3	0.0083	0.2116
			.0001	.0017
1800	0.8	38.8	0.0181	0.4196
			.0002	.0023
total	1976	412.2	0.0096	0.2469
			.0001	.0021
		Sevattur		
		SE-A1(VC)(1.9554g)		
15	3.9	7.5	0.0039	0.1013
			±.0001	±.0016
500	32.8	4.1	0.0076	0.1261
			.0002	.0013
500	17.4	0.9	0.0132	0.1199
			.0010	.0076
total	54.1	12.5	0.0058	0.1108
			.0002	.0019
		SE-A1(P')(0.1479g)		
400	417.3	54.7	0.0029	0.1021
			.00001	.0006
950	550.4	111.8	0.0070	0.9194
			.0005	.0224
1500	43.7	462.4	0.0038	0.0771
			.0001	.0009
Total	1011	628.9	0.0043	0.2291
			.0001	.0032
		SE-C1(VC)(1.62g)		
25	0.4	4.9	0.0039	0.1025
			.0001	.0046
500	1.1	1.8	0.0088	0.1261
			.0008	.0193
total	1.5	6.7	0.0052	0.1089
			.0003	.0086
		SE-C2(VC)(1.63g)		
25	0.4	2.8	0.0053	0.1050
			.0002	.0054
500	1.4	1.9	0.0063	0.0886
			.0004	.0057
500	0.8	0.7	0.0086	0.0731
			.0005	.0153
total	2.6	5.4	0.0061	0.0952

			.0003	.0068
		SE-C3A(VC)(1.93g)		
25	1.3	3.3	0.0045	0.1041
			.0002	.0016
500	3.2	2.4	0.0072	0.1336
			.0002	.0031
total	4.5	5.7	0.0056	0.1164
			.0002	.0022
		SE-C3B(VC)(1.7591g)		
15	1.1	5.0	0.0044	0.1045
			.0003	.0020
300	5.0	5.9	0.0052	0.1073
			.0002	.0011
total	7.1	10.9	0.0048	0.1060
			.0002	.0015
		SE-C5(VC)(1.7747g)		
15	3.7	3.4	0.0067	0.1205
			.0002	.0024
300	14.7	5.5	0.0089	0.1372
			.0003	.0028
total	18.4	8.9	0.0082	0.1307
			.0002	.0026
		SE-C6(VC)(1.7372g)		
15	73.4	9.3	0.0043	0.0982
			.0002	.0009
300	196.1	11.4	0.0048	0.1025
			.0004	.0066
300	31.2	1.4	0.0093	0.1132
			.0011	.0118
total	300.7	22.1	0.0049	0.1014
			.0003	.0044
		SE-C7(VC)(1.4293g)		
15	12.6	9.4	0.0085	0.1408
			.0003	.0011
300	20.4	5.9	0.0163	0.2148
			.0003	.0031
300	3.00	1.3	0.0151	0.1497
			.0011	.0089
total	36.0	16.6	0.0118	0.1678
			.0003	.0024
		SE-A2(P)(0.4554g)		
400	53.5	119.5	0.0031	0.1003
			.0001	.0001
600	54.8	41.2	0.0044	0.1054
			.0001	.0010
950	1012	58.4	0.0061	0.1522
			.0002	.0023
1200	155.8	6.8	0.0147	0.2538
			.0019	.0056
1400	104.9	11.6	0.0164	0.3060
			.0003	.0019
1600	43.2	24.2	0.0113	0.1851
			.0002	.0007
1800	10.3	18.2	0.0108	0.2021
			.0001	.0010
total	1435	279.9	0.0060	0.1380
			.0001	.0008

		Khambamettu		
		KC-1A(VC)(2.09g)		
15	9.5	3.5	0.0044	0.1191
			±.0001	±.0029
500	17.4	1.9	0.0042	0.0761
			.0001	.0012
total	26.9	5.4	0.0044	0.1039
			.0001	.0021
		KC-1B(VC)(1.5130g)		
15	11.7	2.5	0.0047	0.1047
			.0003	.0010
300	30.7	1.1	0.0106	0.1044
			.0005	.0026
total	42.4	3.6	0.0066	0.1046
			.0004	.0015
		KC-3(VC)(1.43g)		
15	71.4	4.4	0.0059	0.1189
			.0005	.0090
300	146.7	2.2	0.0100	0.1234
			.0020	.0238
300	40.2	0.3		
total	258.3	6.6		
		K-A2 (VC)(0.6984g)		
15	8.8	1.5	0.0074	0.0916
			.0007	.0015
500	13.0	0.3	0.0340	0.2114
			.0035	.0103
total	21.8	1.8	0.0119	0.1120
			.0011	.0025
		K-A2 (P')(0.1216g)		
400	3.0	112.1	0.0035	0.1019
			.0001	.0008
950	9.8	112.6	0.0062	0.2347
			.0008	.0231
1200	1.9	108.2	0.0047	0.0981
			.0001	.0006
1600	1.2	153.7	0.0038	0.1289
			.0001	.0038
total	15.9	486.6	0.0045	0.1403
			.0002	.0049
		K-A2 (P) (0.3096g)		
400	4.0	221.9	0.0076	0.1024
			.0001	.0003
950	39.2	BL		
1400	13.6	BL		
1800	2.5	105.5	0.0046	0.0783
			.0001	.0001
total	59.3	337.4	0.0064	0.0918
			.0001	.0002
		K-A1 (VC)(1.7015g)		
15	1.8	0.8	0.0094	0.1090
			.0003	.0013
500	10.1	0.7	0.0273	0.4105
			.0009	.0112
total	11.9	1.5	0.0178	0.2497

			.0006	.0059	
		K-A1 (P')(0.1616g)			
400	426.1	52.8	0.0044	0.1100	
			.0001	.0023	
400	103.4	45.6	0.0032	0.1112	
			.0001	.0006	
950	346.8	110.0	0.0192	0.6493	
			.0008	.0127	
1200	0.5	17.4	0.0447	0.7830	
			.0146	.2389	
1500	-	63.6	0.0092	.2794	
			.0012	.0377	
1800	-	85.4	0.0079	0.3632	
			.0007	.0309	
Total	876.8	374.8	0.0121	0.3861	
			.0009	.0254	
		K-A1 (P) (0.3625g)			
400	20.8	18.1	0.0053	0.0941	
			.0001	.0010	
950	1265	27.6	0.0275	0.4389	
			.0001	.0142	
1300	74.0	5.0	0.2546	4.3056	
			.0008	.0120	
1500	0.2	22.3	0.0470	0.8430	
			.0002	.0054	
1800	-	17.6	0.0351	-	
			.0002		
total	1360	90.6	0.0420	0.6001	
			.0002	.0065	
		Sung Valley			
		SV-C3(VC)(1.738g)			
50	17.3	3.3	0.0045	0.0828	3.95
			±.0002	±.0002	±.35
300	52.4	6.8	0.0041	0.0859	3.31
			0002	.0024	.29
300	11.6	2.2	0.0028	0.0895	2.46
			.0009	.0105	.43
total	81.3	12.3	0.0040	0.0857	3.32
			.0003	.0032	.32
		SV-M3(VC) (1.501g)			
15	17.7	2.4	0.0049	0.0995	9.01
			.0003	.0013	.85
500	44.2	2.2	0.0064	0.0974	8.25
			.0004	.0037	.70
500	11.4	BL			8.41
					.71
total	73.4	4.6	0.0056	0.0985	8.46
			.0003	.0025	.77
		SV-C1(VC)(1.9933g)			
15	3.4	4.4	0.0044	0.0901	3.74
			.0001	.0013	.32
300	9.3	7.3	0.0043	0.0868	2.57
			.0001	.0021	.25
300	1.2	1.7	0.0043	0.0879	1.04
			.0003	.0030	.48
total	13.9	13.4	0.0043	0.0880	2.69
			.0001	.0019	.28
		SV-M1A(VC)(1.2562g)			
15	1.1	4.3	0.0039	0.1009	7.60

			.0001	.0022	.84
500	4.2	2.7	0.0060	0.0958	6.95
			.0003	.0030	.61
500	1.5	1.4	0.0069	0.2257	-
			.0005	.0068	
total	6.8	8.4	0.0051	0.1202	
			.0002	.0032	
		SV-M1B(VC)(1.5113g)			
15	0.9	2.8	0.0048	0.0980	8.49
			.0002	.0009	.91
500	3.3	2.3	0.0069	0.1000	7.86
			.0002	.0014	.66
total	4.2	5.1	0.0057	0.0989	
			.0002	.0011	
		SV-C4(VC)(1.9g)			
15	1.5	14.4	0.0037	0.0906	
			.0001	.0042	
300	3.4	4.8	0.0040	0.0942	
			.0002	.0051	
total	4.9	19.2	0.0038	0.0915	
			.0001	.0044	
		SV-C5(VC)(1.4505g)			
15	1.2	58.6	0.0030	0.0971	
			.0001	0.0003	
300	2.9	5.3	0.0043	0.1030	
			.0002	0.001	
total	4.1	63.9	0.0031	0.0976	
			.0001	0.004	
		SV-A1(VC)(0.4707g)			
15	0.5	3.1	0.0050	0.1042	
			.0004	.0024	
500	4.3	2.1	0.0094	0.1728	
			.0008	.0093	
total	4.8	5.2	0.0068	0.1320	
			.0006	.0052	
		SV-A2(P)(0.1130g)			
400	5.7	2.1	0.0032	0.1022	
			.0001	.0001	
600	8.1	1.8	0.0031	0.1035	
			.0010	.0002	
950	14.4	1.1	0.0034	0.1143	
			.0001	.0014	
total	28.2	5.0	0.0032	0.1060	
			.0001	.0004	
		Ambadongar			
		A-C1(VC)(0.7558g)			
15	3.9	64.8	0.0033	0.0991	
			±.0001	±.0003	
300	5.9	62.5	0.0036	0.0981	
			.0001	.0008	
300	0.8	6.7	0.0054	0.0993	
			.0002	.0013	
total	10.6	134.0	0.0035	0.0986	
			.0001	.0006	
		A-C2 (VC)(1.7147g)			
15	2.2	44.5	0.0032	0.0996	
			.0001	.0003	
300	4.9	62.1	0.0034	0.0989	
			.0001	.0005	
300	0.7	6.7	0.0041	0.1016	

			.0001	.0010	
total	7.8	113.3	0.0033	0.0994	
			.0001	.0004	
		A-C3(VC) (1.5902g)			
15	1.2	35.6	0.0031	0.1025	
			.0001	.0003	
300	3.1	53.9	0.0032	0.1012	
			.0001	.0002	
300	3.7	4.6	0.0050	0.1040	
			.0002	.0027	
total	8.0	94.1	0.0032	0.1019	
			.0001	.0004	
		A-C4(VC)(0.7235g)			
15	0.2	6.4	0.0047	0.0974	
			.0002	.0008	
300	0.9	17.6	0.0037	0.0999	
			.0002	.0018	
300	0.3	4.8	0.0028	0.0810	
			.0007	.0025	
total	1.4	28.8	0.0038	0.0963	
			.0003	.0017	
		A-C5 (VC)(0.6591g)			
15	0.6	122.7	0.0030	0.1020	
			.0001	.0006	
300	1.3	97.9	0.0030	0.1000	
			.0001	.0004	
300	0.2	8.5	0.0045	0.0790	
			.0002	.0026	
total	2.1	229.1	0.0030	0.1003	
			.0001	.0006	
		A-C6(VC)(1.5709g)			
15	0.9	11.5	0.0040	0.1169	9.19
			.0001	.0026	.78
300	17.3	4.4	0.0072	0.1596	
			.0009	.0196	
300	7.6	1.2	0.0071	0.0906	
			.0010	.0117	
total	25.8	17.1	0.0051	0.1258	
			.0003	.0070	

VC stands for vacuum crushing, P for pyrolysis and P' for pyrolysis subsequent to VCThe first column indicates the number of strokes for VC or temperature in (°C) for P.H stands for Hogenakal, SE for Sevattur, K for Khambamettu, SV for Sung Valley and A for Ambadongar. C stands for carbonates, A for apatites and M for magnetites. For example, a carbonate from Hogenakal will be represented as H-C1 where the index no.1 is used for identification of the particular sample. All repeat samples have the same index no, followed by the alphabets A and B denoting the first and the second analyses of the same sample respectively. The weight of each sample analysed is also indicated. All concentrations for noble gases are in cc STP/g,
*Combination of two steps since gas amount is low
BL gas in blank level

due to shorter integration time (Honda and Patterson, 1999), the $^{4}He/^{21}Ne^{*}(10^{7})$ ratios for SV-C3, SV-M3 and SV-A2(P) are ~ 3.8, 6.7, and 10.7 respectively i.e. still higher than the typical production value. This indicates the presence of additional source of ^{4}He in the samples. A likely candidate would be the crustal fluids that may be incorporated as the magma ascends through the crust or may be introduced by the

down going slab during subduction of terrigeneous sediments derived from ancient continental areas. Carbonatite melts are presumed to remain unaffected by crustal contamination because of their low temperatures of 600-770°C (Secher and Larsen, 1980) Contribution from ancient subducted oceanic crust for the Sung Valley magma has already been suggested based on C isotopes (Ray et al., 1999). Such old oceanic crust can introduce ^{4}He, ^{40}Ar and $^{21}Ne_n$ during its dehydration and partial melting which should be complete by 30 km to incorporate the crustal noble gases in the ascending carbonatite magma. Evidences for the presence of such subducted crust left stranded at shallow levels in the mantle comes from Nd, Hf and Pb isotopes from studies on basalts from the Kerguelen Province (Ingle et al., 2003).

4.7 Isotopic ratios

While elemental ratios can be subjected to fractionation during magma ascent and post eruptive diffusive loss from the sample, an isotopic ratio is expected to indicate the composition of the magma and should not be much affected by fractionation. But the isotopic ratios are likely to reflect the presence of different components that have contributed to the magma as well as a late stage addition of atmospheric noble gases that may obscure the mantle isotopic signatures. Such late stage atmospheric gases may be related to the process of eruption when magma interacts with surface equilibrated fluids or atmospheric gases may be adsorbed on the sample surface. In certain cases, the atmospheric component could be due to experimental procedures. There are even reports of micro fractures being created during sample collection and preparation being filled with air (Ballentine & Barfod, 2000). It is to be mentioned that it is not always possible to get rid of this late stage atmospheric contaminant simply by baking the sample at 150°C even for several hours prior to analysis. Thus it becomes important to decouple all the components to infer about the source composition.

4.7A Lighter noble gases:

Helium: Most of $^{4}He_m$ should be of radiogenic origin especially for the Hogenakal (2400 Ma) and Sevattur (770Ma) carbonatites. It has already been seen that part of the ^{4}He may be trapped from the mantle or incorporated from crustal sources as in case of Sung Valley carbonatites. Thus the observed $^{3}He/^{4}He$ values of $(3.32\pm0.32)R_A$ and $(8.46\pm0.77)R_A$ for SV-C3 and SV-M3 respectively might be lower than the true trapped values. Corrected for ^{4}He radiogenic derived from $^{4}He/^{21}Ne^{*}$ production ratio of $(2.2\pm0.1)x10^{7}$ the $^{3}He/^{4}He$ values for SV-C3 and SV-M3 can be scaled up to

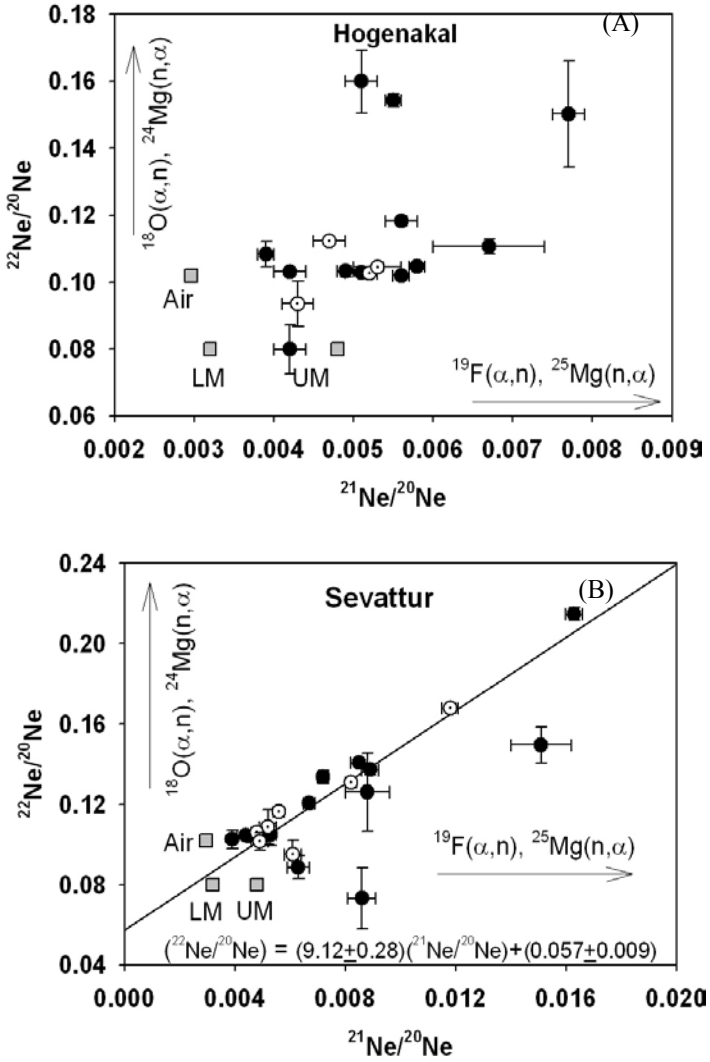

Fig. 4.3 Neon three isotope plot for carbonates of a)Hogenakal b)Sevattur during VC. Ratios greater than trapped values indicate partial release of in situ component during crushing

~ $5R_A$ and $19R_A$. However these values should also be under estimate as part of the ^4He may be from crustal derived fluids as well. This tends to suggest a plume origin for the Sung Valley carbonatites, as $^3He/^4He$ is higher than the typical MORB value of $8R_A$. Some previous studies have already postulated that the Sung Valley carbonatites closely associated with the Rajmahal-Sylhet-Bengal (RSB) flood basalts are related to the early Cretaceous Kerguelen plume (Kumar and Mamallan, 1996; Kent et al., 1992). This is the first direct evidence of a plume origin for the Sung Valley carbonatites. Although ^3He could not be determined from the Ambadongar carbonatites, it is spatially and temporally associated with the Deccan flood basalts (DFB) (Ray et al., 1999). Since a plume origin has been postulated for the DFB (Basu et al, 1993) based on high $^3He/^4He$ signatures, the Sung valley carbonatites are also believed to be related to the Reunion plume. In fact direct evidences of plume origin of carbonatites from $^3He/^4He$ and Ne isotopic ratios have been obtained from Devonian Kola carbonatites also associated with alkaline rocks (Marty, 1998)

Neon: Contribution for ^{21}Ne and ^{22}Ne from *in situ* nucleogenic component cannot be ruled out during VC. Therefore in the present study ^{20}Ne has been used as the

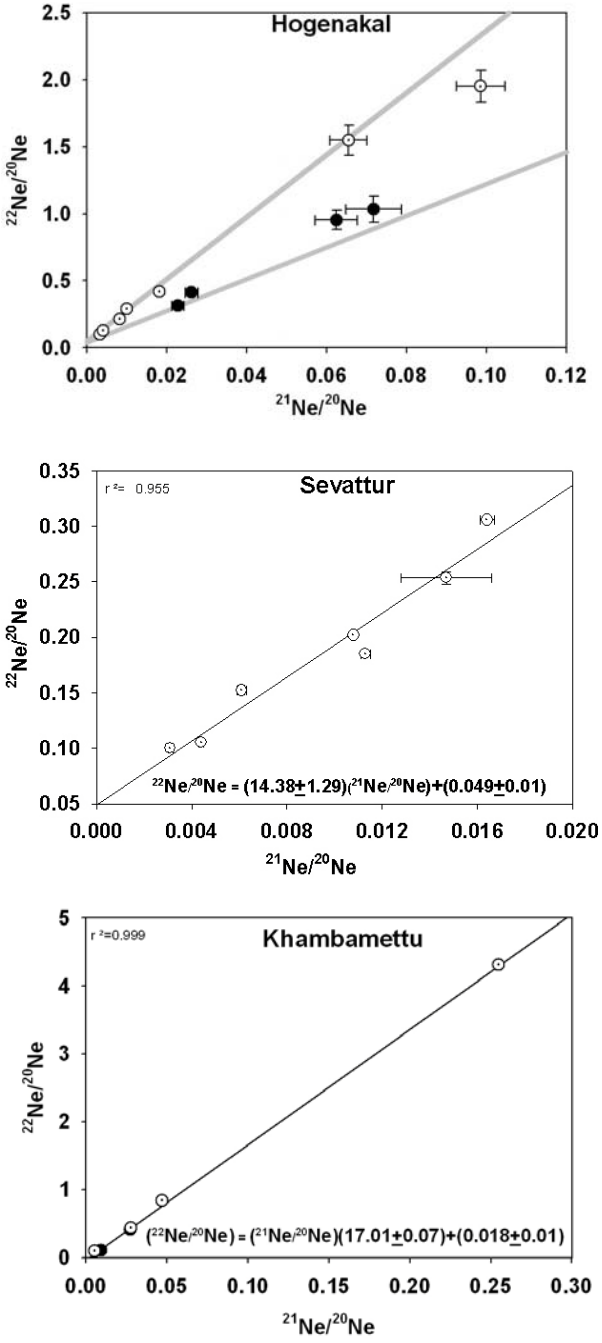

Fig. 4.4 Neon three isotope plot for apatites from Hogenakal, Sevattur and Khambamettu for VC(filled circles) and P(open dotted circles).The slope corresponds to the $(^{22}Ne/^{21}Ne)_n$ and therefore is correlatable to the F/O ratio in the sample

normalising isotope as it is purely of trapped origin and any *in situ* ^{21}Ne and ^{22}Ne can be visualised easily. In a three isotope plot for Ne where $^{21}Ne/^{20}Ne$ vs. $^{22}Ne/^{20}Ne$ are plotted (Fig. 4.3), we clearly see the release of excess ^{21}Ne and ^{22}Ne for both Hogenakal and Sevattur carbonates as both the ratios are above trapped values. From the correlation in the plot, the $^{21}Ne/^{20}Ne$ ratio can be estimated to be 0.0025 ± 0.0009 for Sevattur (taking mantle value of ~0.08 for $^{22}Ne/^{20}Ne$) indicating presence of LM volatiles in the samples. For the Hogenakal carbonates, no such estimate can be obtained owing to the poor correlation coefficient of the plot. It is difficult to assess the cause of this poor correlation, but one possibility may be the inhomogenisation between the different trapped components in Hogenakal. Thus instead of being a two component mixture of trapped and *in situ* gases, the samples behave as multicomponent systems with *in situ* gases and more than one trapped components that retain their discrete signatures. However ideally, carbonates should not contribute $^{22}Ne_n \equiv$nucleogenic as their F content is low and the cross section for the production of $^{22}Ne_n$ via the nucleogenic reaction by $^{25}Mg(n,\alpha)^{22}Ne$ is rather low. Significant ^{22}Ne can be produced by $^{19}F(\alpha,n)^{22}Ne$ but concentration of F in carbonates should be negligible unless it is contaminated with apatites or fluorite during mineral separation. However for all the South Indian carbonatites the

($^{22}Ne/^{20}Ne)_m$ are above the trapped values. Mineralogical and petrology study from Hogenakal and Sevattur does not report the presence of any fluorite (Pandit et al., 2002). But presence of apatites in the carbonatites cannot be ruled out. For example, for H-C1A, the ^{22}Ne excess (taking air as the trapped component) is ~$0.12X10^{-10}$ cc STP/g, if all the ^{20}Ne present is also trapped. In the apatite measured the $^{22}Ne_n$ ~$2.7X10^{-10}$ cc STP/g. If all the ^{22}Ne excess in the carbonate is to be accounted for by the presence of apatite, about 4% of the carbonate should be contaminated with apatite, and XRD analysis should be able to detect that level of apatite. However XRD analysis, performed on the vacuum crushed powder does not indicate the presence of apatite in H-C1A. The ^{22}Ne excess observed in most of the south Indian carbonatites must be from an alternative source. A likely source would be the crustal fluids that can carry the radiogenic and nucleogenic ^{22}Ne, ^{4}He, ^{21}Ne and ^{40}Ar. The crustal production rate for the three Ne isotopes has been calculated by Leya and Weiler (1999). Since carbonatites are unlikely to be affected by crustal contamination, the most likely means by which crustal fluids may be introduced into the magma could be by recycling.

Excess ^{22}Ne in the South Indian carbonatites is clear evidence of the presence of crustal fluids in the samples since average F concentration in the mantle is ~ 25 times lower than in the crust (Mason and Moore, 1982.). Such an enrichment of ^{22}Ne along with ^{4}He, ^{21}Ne, ^{136}Xe and ^{40}Ar has been identified from polycrystalline diamonds in Jwaneng kimberlite, Botswana, and has been advocated to be due to the presence of crustal fluids related to subduction processes in the mantle (Honda et al., 2004). Besides ^{22}Ne, the other isotopes must also be present from crustal fluids in these carbonatites, but their identification may not be straight forward like ^{22}Ne as part of the excess of ^{4}He may be radiogenic and ^{21}Ne and ^{136}Xe may be nucleogenic and fissiogenic respectively in such U, Th rich samples.

Vacuum crushing of apatites also shows the presence of excess Ne above the trapped value for all the apatites studied. For example for Hogenakal apatite the $^{21}Ne/^{20}Ne$ and $^{22}Ne/^{20}Ne$ ratios are ~ 0.032 and 0.49 respectively. As seen earlier the $(^{4}He/^{21}Ne)_n$ production ratio of $2.2X10^{7}$ for Hogenakal apatite yields values of 0.0074 and 0.02 for VC and P respectively clearly indicating under corrected $^{21}Ne_n$ and loss of He from the sample. Fig 4.4 is a three isotope plot for Ne for Hogenakal, Sevattur and Khambamettu apatites for P and VC. Assuming a two component mixture for Ne

between trapped and nucleogenic gases, from the plot it is obvious that the sample is dominated only by excess gases that can be from the following sources:

- In situ and/or
- Crustal

The slope of the plot in Fig. 4.4 is an index of $(^{22}Ne/^{21}Ne)_n$ in the samples. Within errors this is in agreement for all the samples for VC and P. The $(^{22}Ne/^{21}Ne)_n$ is also an index of the $F/^{18}O$ in the sample which can be estimated from the experimental work of Hunemohr, 1989. For the Hogenakal, Sevattur and Khambamettu apatites the $(^{22}Ne/^{21}Ne)_n$ ratios of ~18, 14 and 17 that corresponds almost to that of an ideal fluorapatite(~15). Accordingly, the $F/^{18}O$ in the samples are ~35, 27 and 33 respectively in agreement within errors with that of an ideal apatite value of ~29. Also the uniformity of $(^{22}Ne/^{21}Ne)_n$ within errors during VC and P in the Hogenakal and Khambamettu samples imply isotopic equilibrium between the melt and vesicles for Ne. From the correlation in the plot, for mantle $^{22}Ne/^{20}Ne$ ratio of ~0.08, the $^{21}Ne/^{20}Ne$ ratio is estimated to be 0.0036±0.0006 and 0.0022±0.0007 for Khambamettu and Sevattur respectively that are much lower than the UM ratio implying the likely presence of LM volatiles in the samples. However because of the large errors involved in the slope(m) and intercept(c) for Hogenakal no inference can be drawn on its trapped $^{21}Ne/^{20}Ne$ value.

Presence of mantle gases is seen in both Sung Valley and Ambadongar during sequential crushing from $^{22}Ne/^{20}Ne$ ratio that indicates mixing between air and mantle value. Fig. 4.5A and 4.5B is a plot of $^{22}Ne/^{20}Ne$ vs. cumulative fractional release of ^{20}Ne in sequential crushing for different samples of magnetites and carbonates in Sung Valley. It is observed that $^{22}Ne/^{20}Ne$ for both carbonates and magnetites are uniform during crushing and are a mixture of air and mantle components. However, in the magnetites a larger proportion of air like gases are indicated probably related to late stage crystallisation of magnetites and consequent interaction with hydrothermal fluids containing air like gases. Fig. 4.5C for Ambadongar also indicates mixing between air and mantle gases. Only for the ferrocarbonatite the trapped gas is mostly air like. This is due to the late stage low temperature hydrothermal activity involving large scale participation of ^{18}O depleted groundwater (Viladkar and Schidlowski, 2000) bearing air like noble gases. It is noteworthy that in the two ferrocarbonatites A-C4 and A-C5, in the final crushing steps $^{22}Ne/^{20}Ne$ ratios are very close to mantle

value. This may be related to decreasing air contamination in the later crushing steps, but such a trend is not observed in the $^{40}Ar/^{36}Ar$ ratios. Probably this is due to the presence of fractionated air component that affects the Ar ratios without affecting the

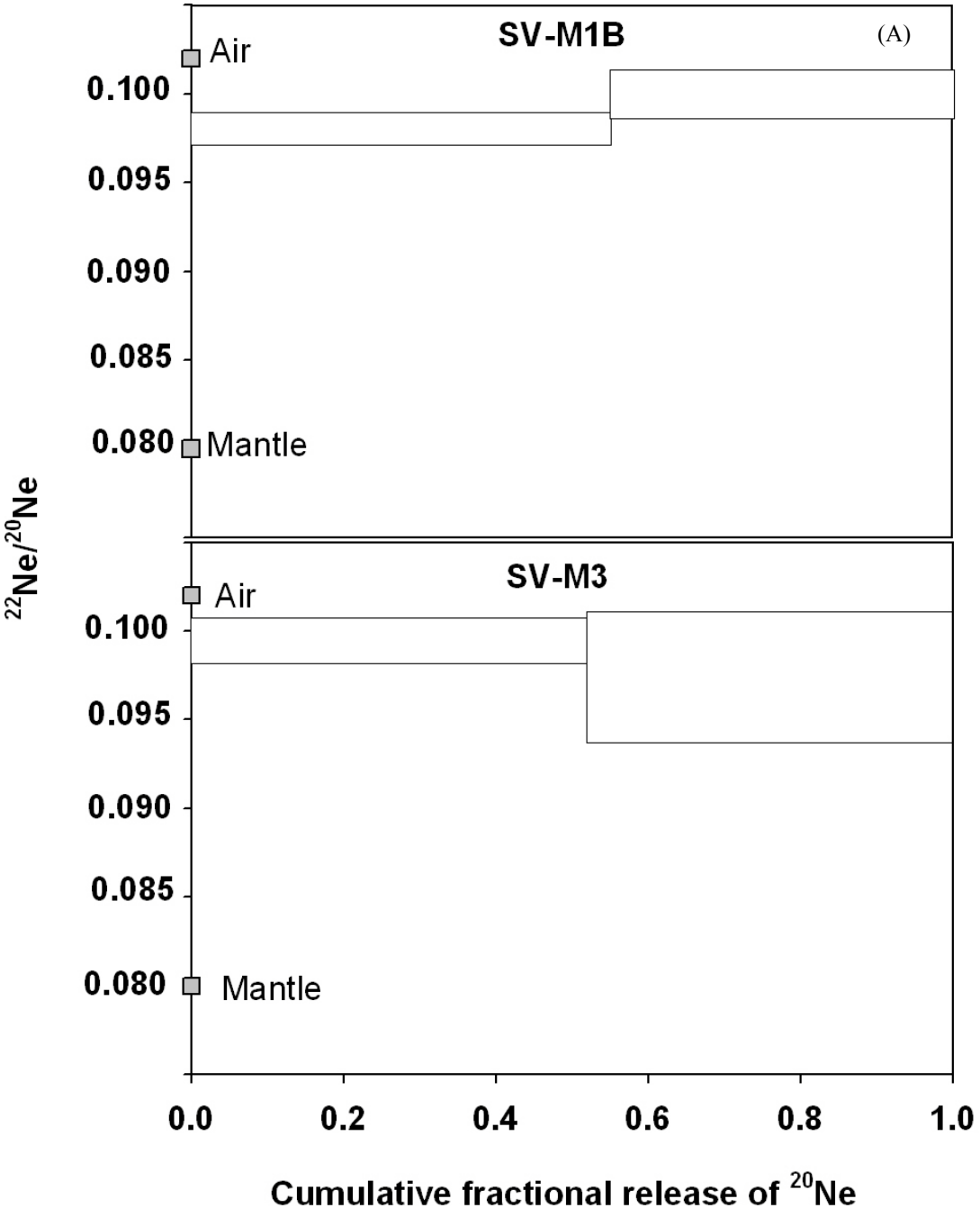

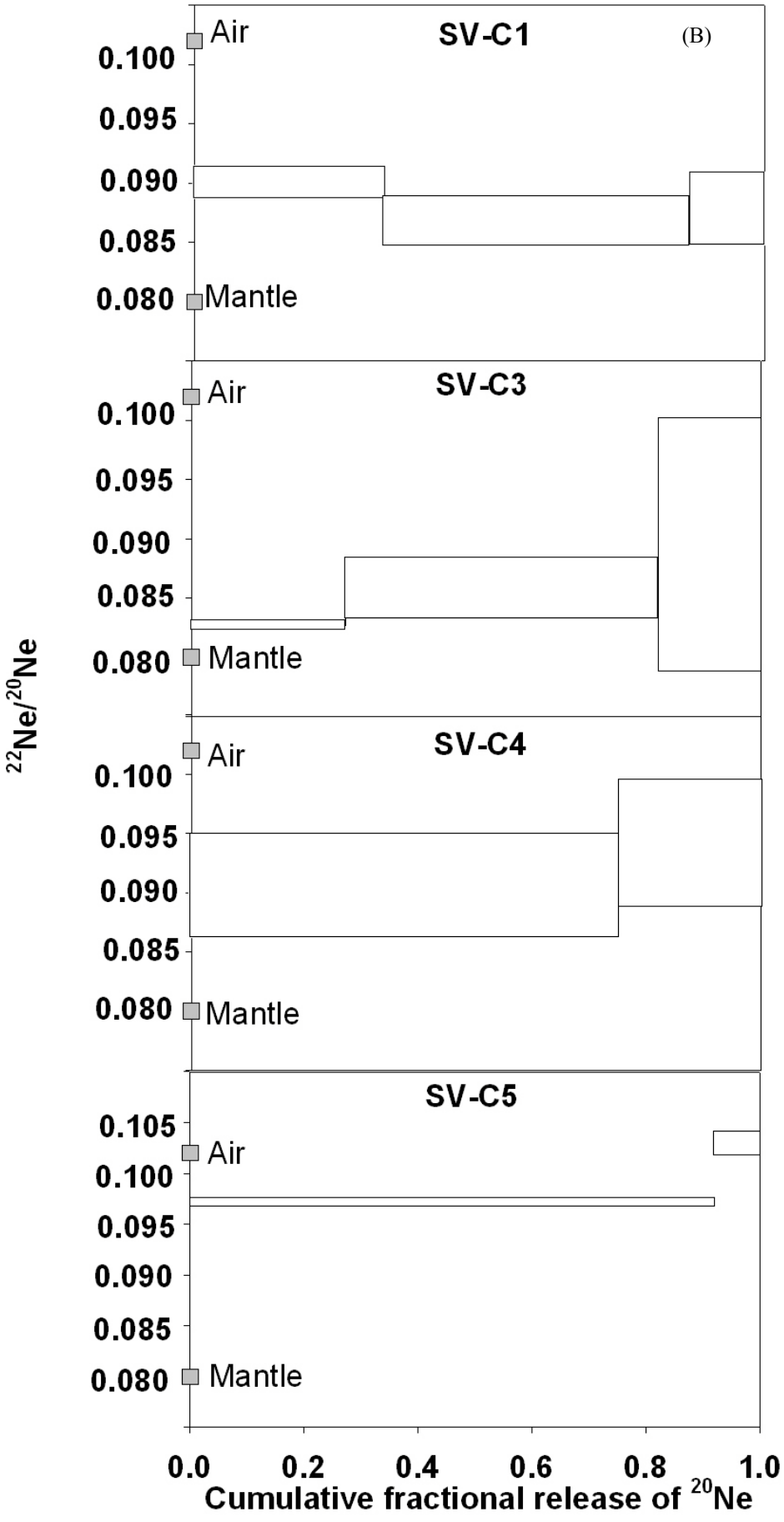
SV-C1
(B)
Air
Mantle
SV-C3
Air
Mantle
SV-C4
Air
Mantle
SV-C5
Air
Mantle
0.105
0.100
0.095
0.090
0.085
0.080
0.0
0.2
0.4
0.6
0.8
1.0
$^{22}Ne/^{20}Ne$
Cumulative fractional release of ^{20}Ne

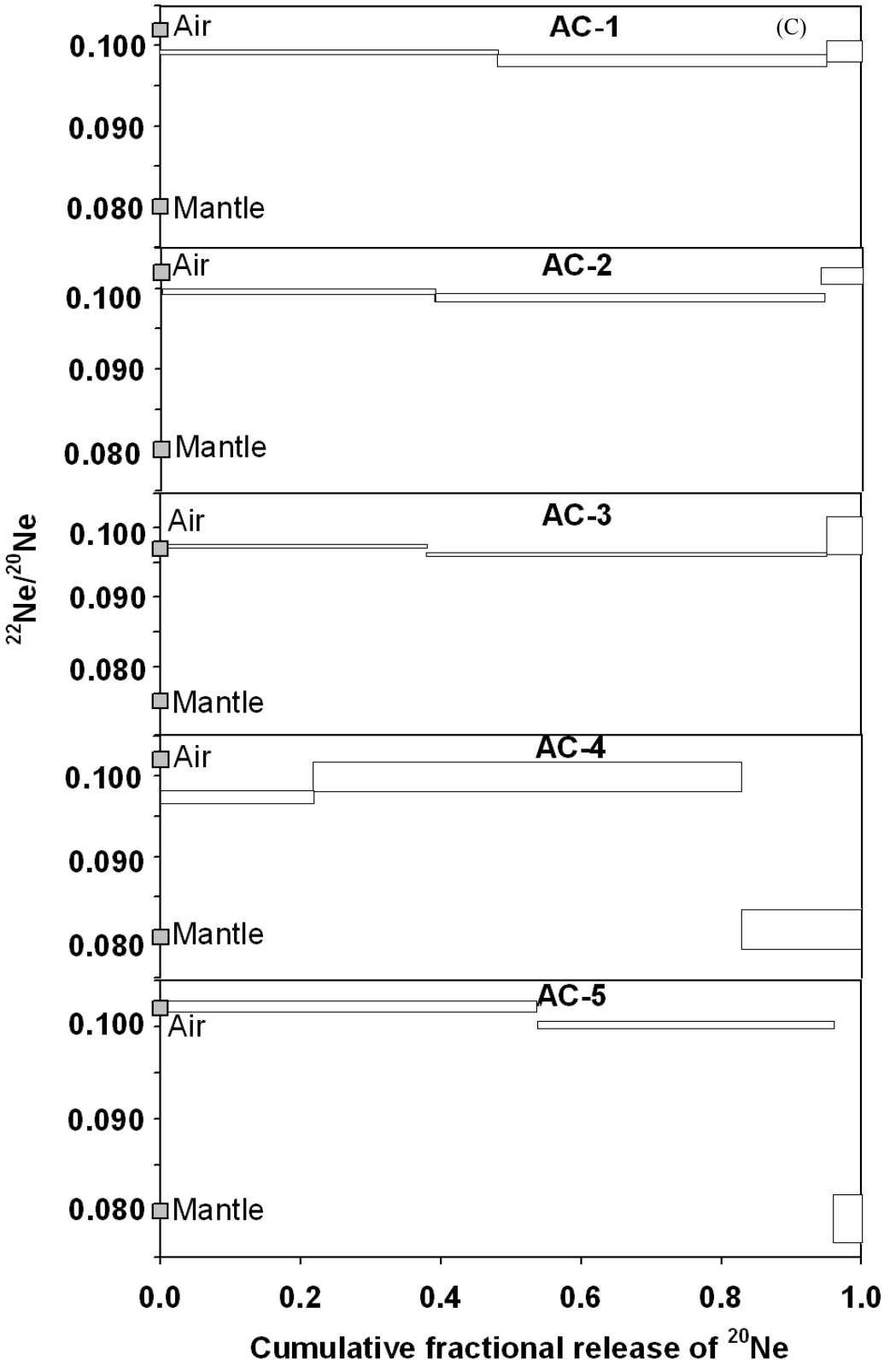

Fig. 4.5 Plot of $^{22}Ne/^{20}Ne$ vs. cumulative release of ^{20}Ne during sequential crushing of Sung Valley magnetites (SV-M1(B) and SV-M3), carbonates (SV-C1, SV-C3, SV-C4 and SV-C5), and Ambadongar calcio carbonatites (A-C1 and A-C2) and ferro carbonatites(A-C3, A-C4 and A-C5). Presence of mantle gases and air in samples are indicated.

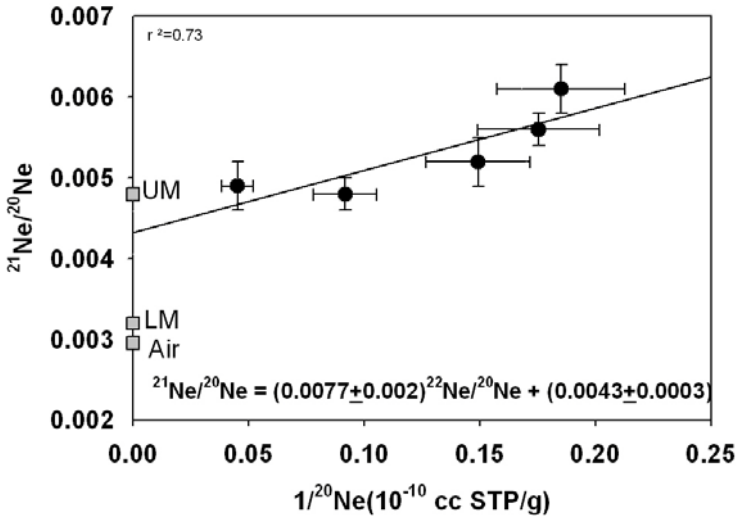

Fig. 4.6 Plot of $1/^{20}Ne$ vs. $^{21}Ne/^{20}Ne$ for Sevattur carbonates. Assuming a two component mixing, the trapped $^{21}Ne/^{20}Ne$ can be obtained from the intercept (assuming that the in situ component has been added to the trapped gases). The trapped value reflects presence of UM volatiles in the samples.

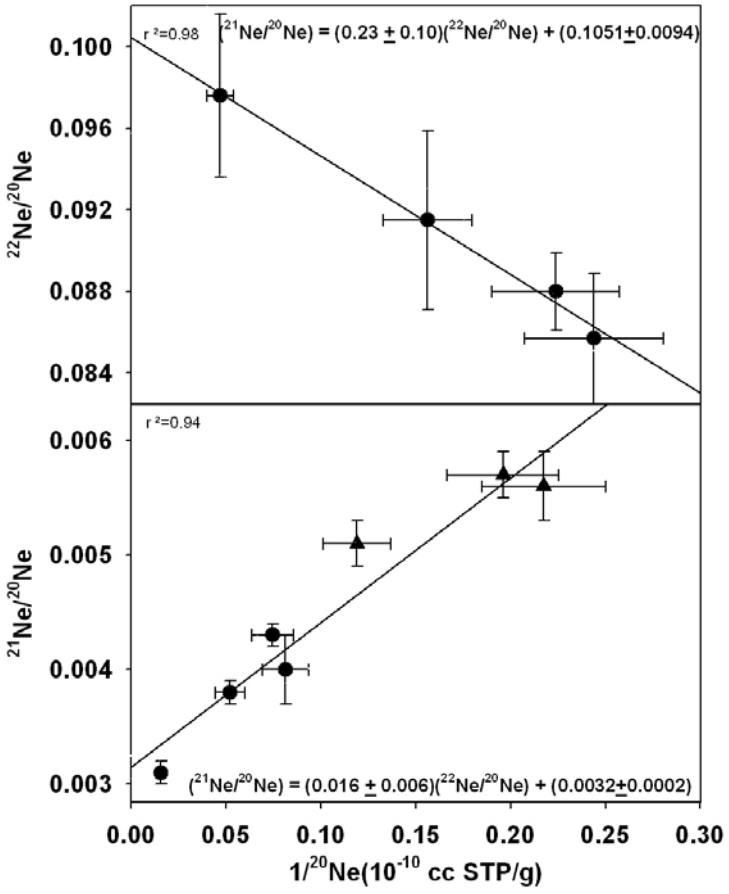

Fig. 4.7 Plot of $1/^{20}Ne$ vs. $^{22}Ne/^{20}Ne$ suggests two component mixing between air and mantle gases in Sung valley carbonates. Intercept from the plot $1/^{20}Ne$ vs. $^{21}Ne/^{20}Ne$ suggests that the mantle component is likely to be the LM

Ne isotopic values and is only discernible when the proportion of normal air component is low.

Trapped Ne component can be estimated from a linear trend in a plot of $^{21}Ne/^{20}Ne$ vs. $1/^{20}Ne$ for a suite of samples of a given province where variable amounts of the second component are added to a component with known $^{21}Ne/^{20}Ne$ ratio. Such a plot for Sevattur carbonates (Fig. 4.6) indicates presence of UM volatiles in the samples. It is to be mentioned that the Sevattur carbonates SE-C5 and SE-C6 have not been included in the plot because of their high $^{22}Ne/^{20}Ne$ and $^{21}Ne/^{20}Ne$ ratios indicating dominance of excess component over any trapped gases that may be present. For Sung Valley, a similar plot has been constructed for $^{22}Ne/^{20}Ne$ vs. $1/^{20}Ne$ (Fig. 4.7) which indicates mixing between air and a mantle component. Fig 7B indicates that the trapped $^{21}Ne/^{20}Ne$ ratio is likely to be air or LM. Since $^{3}He/^{4}He$ value as seen earlier implies presence of a deep plume component, it is likely that the

$^{21}Ne/^{20}Ne$ trapped ratio also correspond to LM component. It is to be noted that the $^{21}Ne/^{20}Ne$ trapped value so derived is unlikely to be the result of mixing between air and UM, as the maximum air present in some of the samples (SV-C3,SV-C1) as estimated from $^{22}Ne/^{20}Ne$ ratio is ~50%, that fails to pull down the UM $^{21}Ne/^{20}Ne$ ratio of ~0.0048 to ~0.0032. In fact from similar plot of Sung Valley apatite, from Fig. 4.8, mixing between air and mantle component to which excess ^{22}Ne has been added is observed. The $(^{21}Ne/^{20}Ne)_m$ in the three heating steps during P of apatite is in agreement indicating the presence of a single component in the sample. The $(^{21}Ne/^{20}Ne)_m$ is in agreement with the $^{21}Ne/^{20}Ne$ trapped value derived for the carbonates. Thus the $^{21}Ne/^{20}Ne$ ratio of ~0.0032 for both the carbonates and the apatite reflects the trapped $^{21}Ne/^{20}Ne$ ratio for the Sung Valley source and indicates that it is derived from the LM. Presence of mantle gases has been seen in the calcitic carbonatites of Ambadongar from Fig. 4.5C. However, both for A-C1 as well as A-C2 the $^{21}Ne/^{20}Ne$ can be explained by mixing between UM and an air/LM component where the fraction of mantle and air components can be estimated from the $^{22}Ne/^{20}Ne$ ratio. In fact earlier works from Nd, Pb and Sr isotopic systematics have already identified

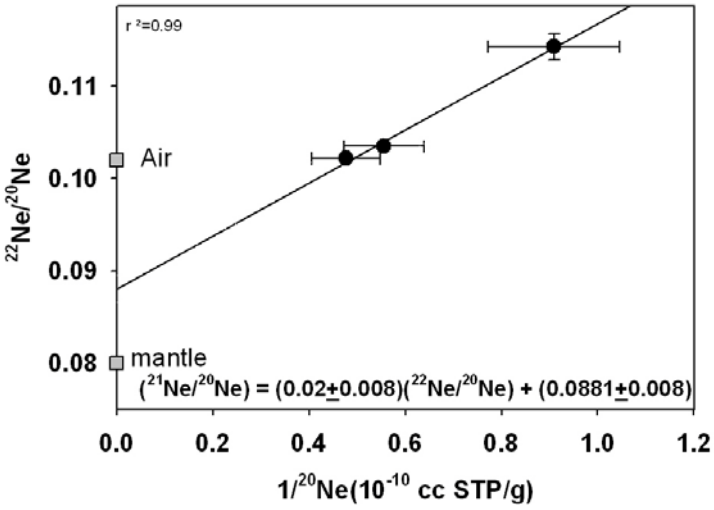

Fig. 4.8 Plot of $1/^{20}Ne$ vs. $^{22}Ne/^{20}Ne$ suggests two component mixing between air and mantle gases in Sung Valley apatite

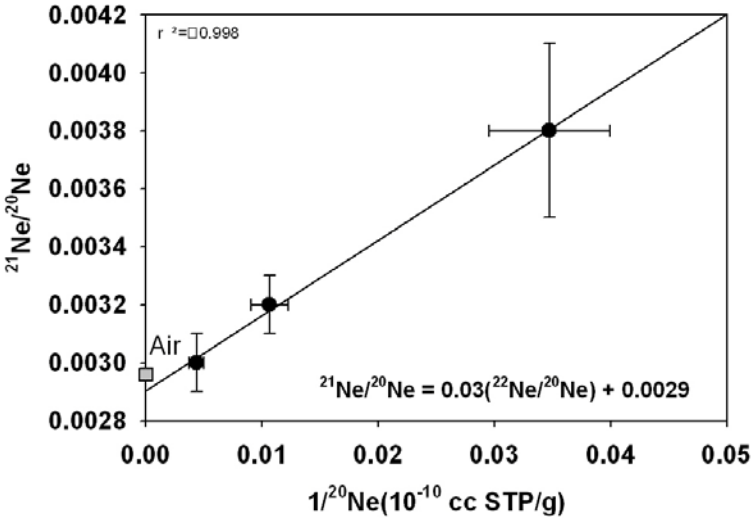

Fig. 4.9 In ferro carbonatites from Ambadongar, plot of $1/^{20}Ne$ vs. $^{21}Ne/^{20}Ne$ suggests that the trapped component is dominantly air like in the samples

presence of asthenosphere (Indian MORB like) mantle component along with Reunion Plume component in the Ambadongar carbonatite (Simonetti et al., 1998). Ne data from the present study also imply the probable presence of UM volatiles. From Fig. 4.9, the trapped $^{21}Ne/^{20}Ne$ value derived from the ferrocarbonatites is almost air like.

Table 4.4 Xe, Kr abundances and isotopic ratios of Xe for all samples Abbreviations as in Table 4.3. Concentrations in cc STP/g units

No of strokes(VC) Or °C(P)	^{132}Xe ($x10^{-12}$)	^{84}Kr ($x10^{-12}$)	$^{129}Xe/^{132}Xe$	$^{131}Xe/^{132}Xe$	$^{134}Xe/^{132}Xe$	$^{136}Xe/^{132}Xe$
			Hogenakal			
			H-C2(VC)			
25	1.1	22.6	0.99 ±.02	0.83 ±.07	0.45 ±..09	0.35 ±.07
500	2.2	44.8	0.98 .09	0.77 .05	0.40 .04	0.35 .04
total	3.3	67.4	0.99 .01	0.79 .06	0.42 .05	0.35 .05
			HC1A(VC)			
50	2.5	36.8	1.11 .01	0.84 .01	0.46 .01	0.37 .01
300	2.0	26.5	1.03 .01	0.84 .01	0.43 .01	0.37 0.02
total	4.5	63.3	1.07 .01	0.84 .01	0.45 .01	0.37 .01
			H-C4(VC)			
15	2.8	11.6	1.14 .02	0.83 .01	0.38 .01	0.35 .01
300	6.6	37.6	1.14 .01	0.80 .01	0.39 .01	0.33 .01
300	1.0	5.7	1.18 .02	0.84 .02	0.38 .01	0.33 .01
total	10.4	54.9	1.14 .01	0.81 .01	0.39 .01	0.34 .01
			H-C1B(VC)			
15	5.1	12.4	1.18 .01	0.83 .02	0.37 .01	0.33 .01
300	13.5	27.8	1.15 .01	0.80 .02	0.39 .01	0.33 .01
total	18.6	40.2	1.16 .01	0.81 .02	0.38 .01	0.33 .01
			H-A(VC)			
15	1.3	3.8				
500	3.4	7.5	1.11 .01	0.78 .01	0.46 .01	0.42 .01
500	-	6.7				

total	4.7	17.9				
			H-A(P')			
1200	2.7	17.8	0.81	0.80	0.77	0.88
			.01	.01	.04	.08
1400	2.6	0.1	0.51	0.67	1.04	1.17
			.02	.03	.04	.04
1800	15.2	14.6	0.29	0.34	1.20	1.42
			.01	.03	.02	.01
Total	20.5	32.5	0.38	0.44	1.13	1.32
			.01	.03	.02	.02
			H-A(P)			
1800	13.0	5.9	0.03	0.21	1.30	1.61
			.002	.01	.04	.04
			Sevattur			
			SE-C2(VC)			
25	0.8	11.8	1.00	0.80	0.41	0.37
			.01	.01	.01	.01
500	0.6	2.1	1.04	0.84	0.38	0.35
			.02	.01	.02	.02
total	1.4	13.9	1.01	0.81	0.40	0.36
			.02	.01	.02	.01
			SE-C1(VC)			
25	1.8	31.4	1.04	0.78	0.40	0.34
			.01	.01	.01	.01
300	0.9	14.0	1.02	0.86	0.41	0.38
			..01	.01	.01	.01
total	2.7	45.4	1.04	0.81	0.40	0.36
			.01	.01	.01	.01
			SE-C5(VC)			
15	0.9	11.5	1.03	0.84	0.37	0.32
			.01	.01	.01	.01
300	2.6	25.0	1.04	0.83	0.38	0.31
			.01	.01	.01	.01
total	3.5	36.5	1.04	0.83	0.38	0.31
			.01	.01	.01	.01
			SE-C3B(VC)			
15	0.7	16.9	1.05	0.82	0.39	0.32
			.01	.01	.01	.01
300	1.1	21.8	1.04	0.82	0.38	0.32
			.01	.01	.01	.01
total	1.8	38.7	1.04	0.82	0.39	0.32
			.01	.01	.01	.01
			SE-C6(VC)			
15	6.1	31.9	1.04	82.97	37.98	31.69
			.01	.30	.15	.27
300	10.1	49.2	1.05	82.65	37.83	31.74
			.01	.18	.25	.24
total	16.2	81.1	1.04	82.77	37.89	31.72
			.01	.23	.21	.25
			SE-C7(VC)			
15	3.8	31.3	0.99	0.79	0.40	0.35
			.01	.01	.01	.01
300	4.3	18.8	1.12	0.79	0.38	0.36
			.01	.01	.01	.01
total	8.1	50.1	1.06	0.79	0.39	0.36
			.01	.01	.01	.01

			SE-A1(VC)			
15	2.8	3.8	0.98	0.78	0.40	0.34
			.01	.01	.01	.01
500	3.2	14.2	1.09	0.82	0.40	0.34
			.01	.01	.01	.01
total	6.0	18.0	1.04	0.80	0.40	0.34
			.01	.01	.01	.01
			SE-A1(P')			
1500	22.4		1.01	0.82	0.40	0.34
			.01	.01	.01	.01
1800	143.4		1.04	0.79	0.40	0.34
			.01	.01	.01	.01
Total	165.8		1.05	0.80	0.40	0.34
			.01	.01	.01	.01
			Khambamettu			
			K-C1A(VC)			
15	0.9		0.98	0.82	0.43	0.37
			.01	.03	.01	.01
300	0.7		0.97	0.77	0.48	0.41
			.01	.01	.02	.01
total	1.6		0.98	0.80	0.45	0.39
			.01	.02	.01	.04
			K-C2(VC)			
15	1.4		1.16	0.78	0.39	0.35
			.01	.03	.01	.01
300	1.0		1.06	0.75	0.40	0.36
			.03	.01	.01	.01
total	2.4		1.12	0.77	0.40	0.35
			.02	.01	.01	.01
			K-A1 (P')			
1800	7.8		0.27	0.38	1.10	1.25
			.01	.01	.01	.01
total	7.8		0.27	0.38	1.10	1.25
			.01	.01	.01	.01
			Sung valley			
			SV-C3(VC)			
15	1.8	3.5	1.05	0.81	0.38	0.35
			.01	.01	.01	.01
300	5.0	8.6	1.01	0.81	0.41	0.35
			.01	.01	.01	.02
300	1.4	2.00	1.03	0.81	0.38	0.31
			.02	.01	.01	.01
total	8.3	14.1	1.02	0.81	0.40	0.34
			.01	.01	.01	.01
			SV-M3(VC)			
15	1.4	7.9	1.00	0.79	0.38	0.31
			.01	.01	.01	.01
500	2.3	13.9	1.13	0.81	0.37	0.32
			.02	.01	.01	.01
total	3.7	21.8	1.08	0.80	0.38	0.32
			.02	.01	.01	.01
			SV-C1(VC)			
15	2.8		1.03	0.77	0.40	0.33
			.01	.01	.01	.01
300	8.5		1.05	0.78	0.39	0.34
			.01	.01	.01	.01
total	11.3					
			SV-C5(VC)			

15	1.5	27.7	0.98	0.81	0.38	0.30
			.01	.01	.01	.01
300	2.0	34.5	0.99	0.81	0.38	0.31
			.01	.01	.02	.01
total	3.5	62.2	0.99	0.81	0.38	0.31
			.01	.01	.02	.01
			SV-C2(VC)			
25	1.6	23.8	1.06	0.84	0.40	0.34
			.01	.01	.01	.01
500	2.5	24.8	0.99	0.78	0.40	0.34
			.01	.01	.01	.01
500	0.6	6.4	1.00	0.77	0.42	0.37
			.01	.01	.02	.01
total	4.7	55.0	1.02	0.80	0.40	0.35
			.01	.01	.01	.01
			Ambadongar			
			A-C6(VC)			
15	1.1	75.6	1.04	0.80	0.40	0.37
			.02	.01	.01	.01
300	2.0	80.4	1.01	0.81	0.41	0.36
			.01	.01	.01	.01
total	3.1	156.0	1.02	0.80	0.40	0.36
			.02	.01	.01	.01
			A-C5(VC)			
300	5.4		1.05	0.80	0.40	0.34
			.01	.01	.01	.01
total	5.4		1.05	0.80	0.40	0.34
			.01	.01	.01	.01
			A-C4(VC)			
15	8.1		0.99	0.82	0.41	0.34
			.01	.01	.01	.01
300	7.9		1.00	0.79	0.39	0.34
			.01	.01	.01	.01
total	16.0		1.00	0.80	0.40	0.34
			.01	.01	.01	.01
			A-C1(VC)			
15	9.5		1.05	0.78	0.40	0.34
			.01	.01	.01	.01
300	12.4		1.05	0.78	0.39	0.33
			.02	.01	.01	.01
total	21.9		1.05	0.78	0.39	0.33
			.02	.01	.02	.01
			A-C2(VC)			
15	5.3		1.04	0.81	0.39	0.33
			.01	.01	.01	.01
300	10.3		1.06	0.81	0.40	0.34
			.5	.01	.01	.01
300	1.2		1.05	0.77	0.41	0.34
			.01	.01	.01	.01
total	16.8		1.05	0.81	0.40	0.34
			.01	.01	.01	.01
			A-C3(VC)			
15	2.8	91.4	0.99	0.80	0.41	0.34
			.01	.01	.01	.01
300	5.6	162.1	0.98	0.78	0.40	0.34
			.01	.01	.01	.01
total	8.4	253.5	0.98	0.79	0.40	0.34
			.01	.01	.01	.01

4.7B Heavier noble gases:

Lighter noble gases indicate the presence of LM volatiles in Sung Valley and UM volatiles in the Sevattur carbonatite. For the other carbonatites it is difficult to conclude anything definite regarding the source of the trapped volatiles (UM and/or LM) solely on the basis of lighter noble gases. All the carbonatites show the presence of crustal fluids added probably during subduction at a shallow level so as to still retain the light noble gases. Better constraint of LM and UM volatiles can be obtained from $^{40}Ar/^{36}Ar$ ratios that are very distinct for air, UM and LM. The $^{40}Ar/^{36}Ar$ ratio also indicate the presence of UM volatiles in the south Indian carbonatites with the maximum $^{40}Ar/^{36}Ar$ being ~ 29000 (Hogenakal), 16000 (Sevattur) and 16000 (Khambamettu). But the possibility that the carbonates trap gases from the air and LM, and excess ^{40}Ar is introduced from crustal fluids cannot also be ruled out. In such U,Th rich samples, ^{40}Ar contribution from the crust in terms of excess ^{21}Ne and ^{136}Xe cannot be obtained from crustal $^{40}Ar/^{21}Ne$ and $^{40}Ar/^{136}Xe$ ratios. This is because part of the excess ^{21}Ne and ^{136}Xe may be nucleogenic/fissiogenic in origin. However we can qualitatively rule out the possibility of all ^{40}Ar excess from crustal sources to have been added to volatiles from LM/air. If we consider the two samples H-C2 and H-C1B with $^{40}Ar/^{36}Ar$ ratios of ~14311 and 11392 respectively, approximately 44% and 30% of Ar in the two samples must come from crustal sources if LM (with $^{40}Ar/^{36}Ar$ ~ 8000) is the trapped component. However, assuming all ^{22}Ne excess in the carbonates to be crustal (trapped component being mantle), the crustal contribution for ^{22}Ne is only 14% and 22% in the two samples. If we assume all ^{136}Xe excess to be crustal, it would require 6% and 1% crustal contribution in the above two samples respectively. Therefore even solubility fractionation during incorporation of crustal fluids into the magma cannot account for the trend observed if all ^{40}Ar excess is crustal. Had all excess ^{21}Ne, ^{40}Ar and ^{136}Xe been from crustal fluids and the variable contribution is related to fractionation, then trend for the three isotopes should be unidirectional which is not the case. Thus Ar has been entrapped from the UM, without any substantial contribution from crustal material. However, Sevattur carbonates show a range of $^{40}Ar/^{36}Ar$ varying from as low as 415±4 that may indicate mixing between air and mantle components in varying proportions. Also another interesting observation is that while the carbonates from these south Indian

carbonatites seem to trap UM volatiles, the $^{40}Ar/^{36}Ar$ ratios for their apatites are in the LM range. The following two implications are possible:

- UM volatiles with an air component can lower the $^{40}Ar/^{36}Ar$ ratio in the apatites as well as account for the range observed in Sevattur carbonates.
- Different generations of melts from different sources are responsible for the formation of the apatites and the carbonates. This finding is similar to the study of noble gases in apatite grains in spinel/lherzolite xenoliths from the Australian lithospheric mantle where while apatite has a Ne isotope signature similar to that of plume related volcanism, associated mineral phases like olivine and amphibolites have isotopic signatures typical of mid-ocean-ridge basalts (Matsumoto et al., 1997).

If Ar in the sample is a mixture of magmatic Ar and atmospheric derived Ar, data points should show a linear trend in the $^{40}Ar/^{36}Ar$ vs. $1/^{36}Ar$ plot lying on a line expressed as $(^{40}Ar/^{36}Ar)_{sample} = (^{40}Ar/^{36}Ar)_{air} + {}^{40}Ar_{excess} \times (1/^{36}Ar)_{sample}$

However neither the Sevattur carbonates, nor the apatites show such a trend. It would thus not be unreasonable to assume that the apatites are derived from the LM rather than being a mixture of air+UM, and the observed variation in the Sevattur carbonates may be due to one or a combination of the following reasons:

- Mixing of two magmas with different$^{40}Ar/^{36}Ar$ ratios.
- Variable $^{40}Ar/^{36}Ar$ due to addition of atmospheric derived Ar as seen in case of Unzen Volcano Japan (Haneya and Kaneoka, 1997). It was observed that the $^{40}Ar/^{36}Ar$ decreased sequentially from plagioclase, hornblende and then biotite that are also in order of crystallization of these minerals. Since carbonate crystallization can persist from early to late stages, the range of $^{40}Ar/^{36}Ar$ ratio in Sevattur can reflect progressive addition of air to the magma.

These Sevattur carbonates also show a decreasing trend of $^{40}Ar/^{36}Ar$ in many cases with increasing degree of crushing implying that the $^{40}Ar/^{36}Ar$ ratios in smaller vesicles to be lower than in the bigger ones (SE-Cl, SE-C3B, SE-C6). This is also observed for the Hogenakal carbonate H-C2. Since bubbles in a magma grow due to a combination of decompression and diffusion, the largest vesicle can be assumed to be nucleated earlier than the smaller ones (Sparks., 1978; Sparks et al., 1994; Proussevitch et al., 1993). Progressive contamination of the magma prior to eruption would result in the smallest and therefore the last formed to have trapped the most

contaminated volatiles. However this is not the general trend for most of the Sevattur samples as well as that seen from the analyses of carbonates from other regions.

Isotopic disequilibrium observed for vesicles from Atlantic MORB glasses (Jambon et al., 1985) have been explained by the involvement of two generations of magma. For the South Indian carbonatites it is possible that a magma chamber containing LM volatiles existed that provided the source for the apatites and may be some carbonates with lower $^{40}Ar/^{36}Ar$ ratios as in Sevattur. Interaction with crustal fluid bearing subducted component can further lower the $^{40}Ar/^{36}Ar$ ratios depending on the duration of the melt-vesicle interaction. This was followed by a new batch of magma, which because of rapid temperature and pressure drop is strongly super cooled resulting in the formation of larger vesicles bearing volatiles from the UM that may be variably affected by crustal fluid bearing subducted melt. The carbonates crystallised from the second batch of magma thus host UM volatiles, but in some cases may also trap some smaller vesicles formed from the previous generation of magma. This is reflected in the $^{40}Ar/^{36}Ar$ ratios in smaller vesicles to be lower than the bigger ones (SE-Cl, SE-C3B, SE-C6). Thus the lower $^{40}Ar/^{36}Ar$ ratios in the final crushing steps are because they host LM gases, and also because they have a longer resident time in the magma and therefore equilibrate more with the atmospheric component that is added to the melt by subducted component. The $^{40}Ar/^{36}Ar$ for the Sung Valley carbonates and Ambadongar are similar to that expected for LM. Only the magnetites for Sung Valley and the ferro-carbonates for Ambadongar have a lower $^{40}Ar/^{36}Ar$ owing to the interaction with air saturated hydrothermal fluids, which had also affected the $^{22}Ne/^{20}Ne$ signature.

Xe isotopic ratios like $^{129}Xe/^{132}Xe$ can be lowered due to ^{132}Xe by spontaneous fission. However for apatites fission component is only released at the melting temperature of 1800°C and not much fission contribution is expected during VC. Thus the $^{129}Xe/^{132}Xe$ value of ~ 1.1 for Hogenakal apatite and ~ 1.04 for Sevatur apatite signifies the presence of mantle gases in these samples. In both cases assuming all excess ^{136}Xe to be related to spontaneous fission and then deriving the $^{132}Xe_f$, corresponding correction still does not affect the $^{129}Xe/^{132}Xe$ ratios much. Thus if these apatites were derived from the UM, a highly fractionated air component enriched in Ar with respect to Xe is required. However such a fractionated component is not possible (generally Xe is enriched due to fractionation) again indicating that the

apatites are derived from the LM. It is to be mentioned that for the other apatites trapped $^{129}Xe/^{132}Xe$ ratios during VC could not be determined because of low gas amounts.

The $^{129}Xe/^{132}Xe$ ratio is above trapped value (air or mantle), in many of the South Indian carbonatites (for example H-C4, H-C1B, K-C2). Besides excess ^{22}Ne, this also indicates that an additional component is present in the carbonatites. A likely candidate would be the crustal fluids. Crustal fluids are likely to carry radiogenic and nucleogenic components, either leached out from the country rocks or recoiled and/or diffused out of the surrounding rocks (Andrews et al., 1989). The above processes of incorporating fission Xe into crustal fluids might lead to chemically fractionated fission Xe (CFF Xe) being taken up (Shukolyukov et al., 1994). CFF can lead to excesses at certain isotopes compared to the normal ^{238}U fission found in crustal rocks. Assuming all ^{136}Xe excess to be fissiogenic, since it has the highest yield from fission of ^{238}U, an estimate of fission contribution to ^{131}Xe, ^{132}Xe and ^{134}Xe can be made and corrected for. The corrected $^{131}Xe/^{132}Xe$, $^{134}Xe/^{132}Xe$ and $^{136}Xe/^{132}Xe$ for the various samples are tabulated in Table 4.5. The nominal fission corrected ratios are still above the air Xe values for the $^{131}Xe/^{132}Xe$ and $^{134}Xe/^{132}Xe$ ratios, and in some cases the $^{129}Xe/^{132}Xe$ ratio is higher than mantle values. The corresponding $(^{129}Xe/^{131}Xe)_{excess}$ ratios, corrected for trapped mantle gases assuming all ^{132}Xe to be of trapped origin are also mentioned for those samples whose $^{129}Xe/^{132}Xe$ ratio is above mantle value and $^{131}Xe/^{132}Xe$ ratio is above atmospheric after correcting for spontaneous fission.

Table 4.5 $^{129}Xe/^{132}Xe$, $^{131}Xe/^{132}Xe$ and $^{134}Xe/^{132}Xe$ ratios in samples from South Indian carbonatites after correcting for spontaneous fission contribution, assuming all ^{136}Xe excess to be fissiogenic. The $(^{129}Xe/^{131}Xe)_{excess}$ is obtained by further correcting the fission corrected ratios for trapped mantle/air gases

Sample	$^{129}Xe/^{132}Xe$	$^{131}Xe/^{132}Xe$	$^{134}Xe/^{132}Xe$	$(^{129}Xe/^{131}Xe)_{excess}$
H-C2	1.00	0.80	0.42	
	±.01	.01	.01	
H-C1A	1.10	0.86	0.38	
	.01	.01	.01	
H-C4	1.15	0.81	0.34	1.4
	.01	.01	.01	.1

H-C1B	1.16	0.81	0.38	2.4
	.01	.01	.01	.2
H-A(VC)	1.13	0.82	0.48	0.6
	0.02	.02	.01	.1
SE-C2	1.03	0.83	0.41	
	.02	.01	.02	
SE-C1	1.05	0.82	0.41	
	.01	.01	.01	
SE-C7	1.08	0.81	0.40	
	.01	.01	.01	
SE-A1(VC)	1.05	0.81	0.40	
	.01	.01	.01	
SE-A1(P')	1.05	0.80	0.40	
	.01	.01	.01	
K-C1A	1.01	0.83	0.47	
	.02	.02	.01	
K-C2	1.13	0.78	0.40	
	.02	.01	.01	
SV-C3	1.03	0.81	0.40	
	.01	.01	.01	
SV-C1	1.06	0.79	0.39	
	.01	.01	.01	
SV-C2	1.03	0.81	0.41	
	.01	.01	.01	
A-C6	1.04	0.82	0.41	
	.02	.01	.01	
A-C5	1.06	0.81	0.40	
	.01	.01	.01	
A-C4	1.00	0.81	0.40	
	.01	.01	.01	
A-C1	1.05	0.79	0.40	
	.01	.01	.01	
A-C2	1.06	0.81	0.40	
	.01	.01	.01	
A-C3	0.99	0.79	0.40	
	.01	.01	.01	

Excess ^{132}Xe unexplainable by contributions from $^{238}U_{sf}$ and $^{235}U_{nf}$, is clearly seen from Fig. 4.10 for Hogenakal, Sevattur and Sung Valley. This pulls down the

measured $^{136}Xe/^{132}Xe$ as well as the $^{134}Xe/^{132}Xe$ ratios in the samples. It is difficult to identify the excess^{132}Xe from $^{131}Xe/^{132}Xe$ ratios, as it could be masked by the ^{131}Xe produced by the reaction $^{130}Ba(n,\gamma\beta^-)^{131}Xe$ in these carbonates that are likely to be rich in Ba. ^{129}Xe excess is also seen in carbonates from Hogenakal but not distinguishable from other locations. It may not always be possible to distinguish anomalous ^{129}Xe in the samples from mantle contributions even if present. However caution should be exercised before advocating all excess ^{129}Xe to mantle contribution as they may simply reflect xenon with anomalous composition.

Besides crustal fluids, CFF-Xe may be indigenous to the samples themselves. Anomalous xenon (CFF-Xe) has been reported earlier from different geological environments like that of the MORBs, natural gases, diamonds and ancient continental rocks. As in other cases CFF-Xe might have been formed by the migration of intermediate fission products from U rich to comparatively U depleted carbonates in the vicinity. The complimentary counterpart should be present in the various U-rich minerals in the carbonatites provided it is not already lost due to U-radiation damages. Some possible candidates might be pyrochlore, perovskite, the REE minerals and thorite. The isotopic compositions however are different from that of Okelobondo nuclear reactor reported by Meshik et al., 2000b. This may be because of the fact that the CFF-Xe in these cases had been identified and measured in totally U free phases mainly consisting of alumophosphates, while in the present study carbonates may consist of reasonable concentration of U(average 7.2 to 13 ppm) and Th(average 52 to 276 ppm). Also the U-phase in the reactor were U-oxides like U_3O_8 and UO_2, while in carbonatites the U-phases would be much poorer in U as compared to the oxides.

While it is possible that excesses at ^{131}Xe and ^{134}Xe could be due to CFF-Xe, excess at ^{129}Xe is unlikely even in CFF-Xe, due to poor fission yield at mass 129. Another possibility could be that some specific (n,γ) reactions on specific targets have produced excesses at specific Xe isotopes. A case in point could be (n,γ) reactions on Te that produce both ^{129}Xe and ^{131}Xe. One can assess this possibility by looking at the ratio of the excesses $(^{129}Xe/^{131}Xe)_{excess}$ over the trapped values of mantle composition.

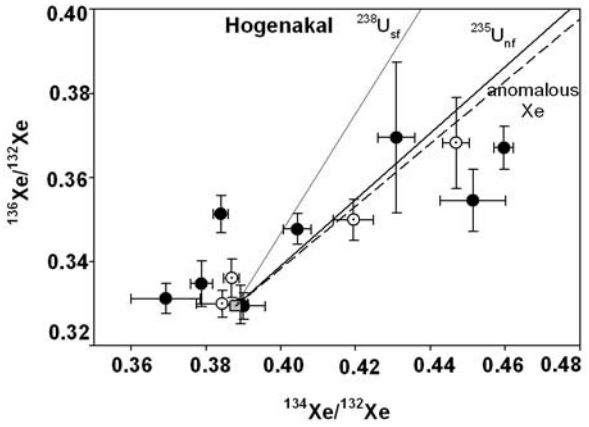
Hogenakal
$^{238}U_{sf}$
$^{235}U_{nf}$
anomalous Xe
$^{136}Xe/^{132}Xe$
$^{134}Xe/^{132}Xe$

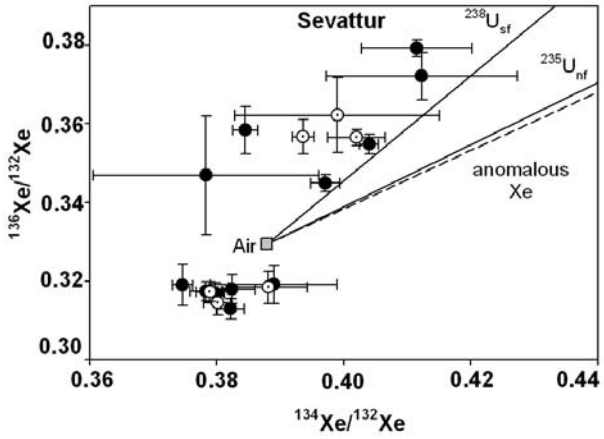
Sevattur
$^{238}U_{sf}$
$^{235}U_{nf}$
anomalous Xe
Air
$^{136}Xe/^{132}Xe$
$^{134}Xe/^{132}Xe$

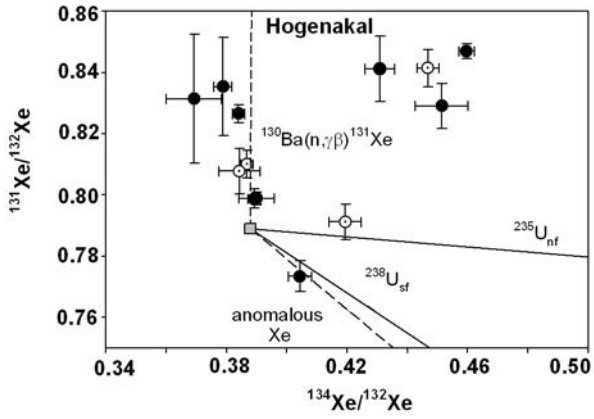
Hogenakal
$^{130}Ba(n,\gamma\beta)^{131}Xe$
$^{235}U_{nf}$
$^{238}U_{sf}$
anomalous Xe
$^{131}Xe/^{132}Xe$
$^{134}Xe/^{132}Xe$

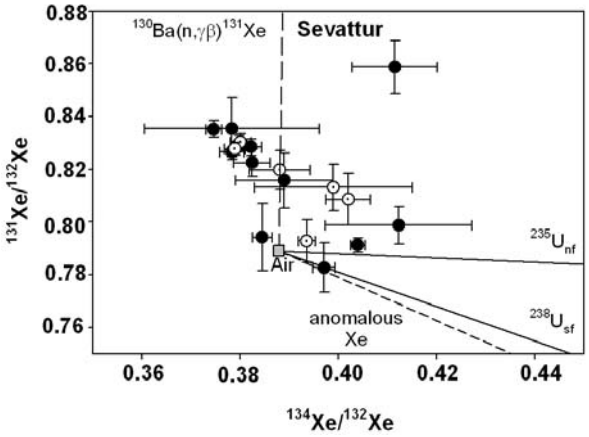
$^{130}Ba(n,\gamma\beta)^{131}Xe$
Sevattur
$^{235}U_{nf}$
Air
anomalous Xe
$^{238}U_{sf}$
$^{131}Xe/^{132}Xe$
$^{134}Xe/^{132}Xe$

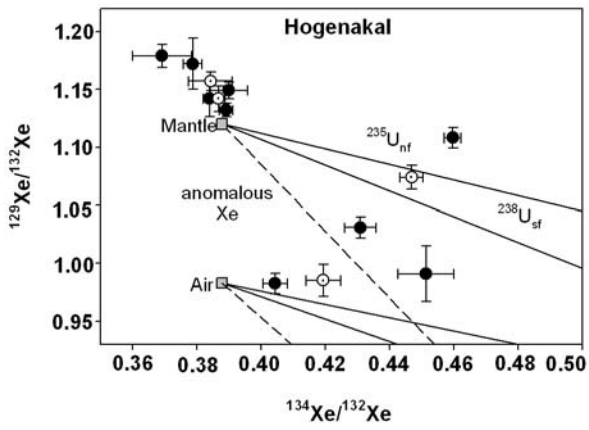
Hogenakal
Mantle
$^{235}U_{nf}$
$^{238}U_{sf}$
anomalous Xe
Air
$^{129}Xe/^{132}Xe$
$^{134}Xe/^{132}Xe$

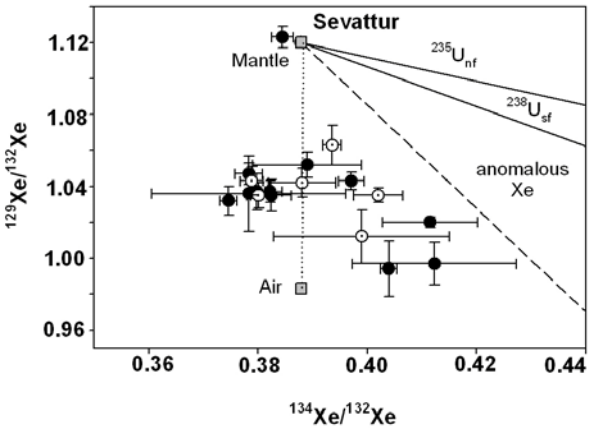
Sevattur
Mantle
$^{235}U_{nf}$
$^{238}U_{sf}$
anomalous Xe
Air
$^{129}Xe/^{132}Xe$
$^{134}Xe/^{132}Xe$

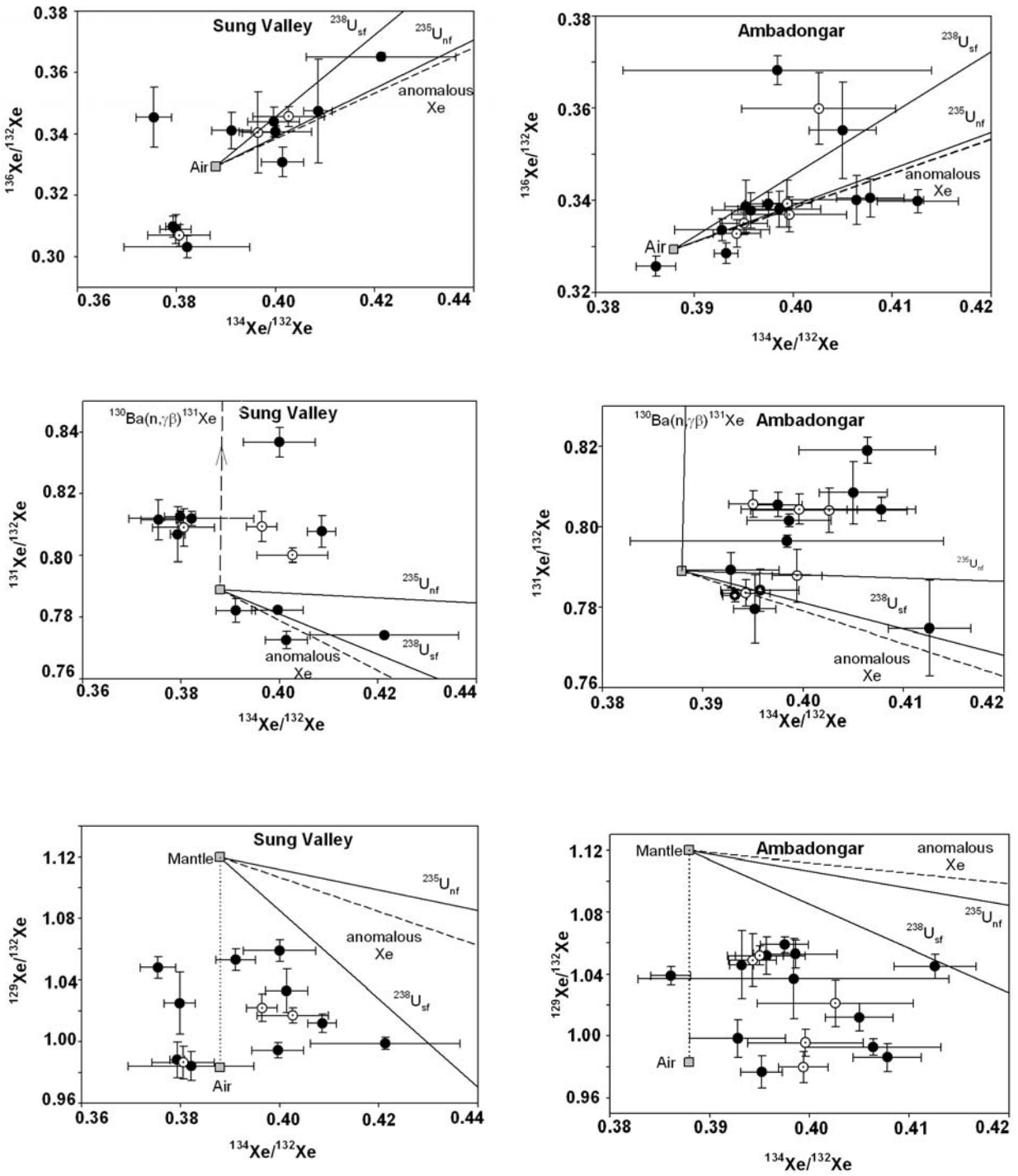

Fig. 4.10 Xenon isotope plots for carbonates from Hogenakal , Sevattur, Sung Valley and Ambadongar. Excess component, in addition to air, mantle and contribution from spontaneous fission ($^{238}U_{sf}$) is clearly seen. Trends for $^{235}U_{nf}$ and anomalous Xe also indicated. Closed circles refer to isotopic ratios in individual crushing steps, open circles correspond to totals of VC.

The ratio of the excesses for the three samples is within errors in the range of (0.7-4.0) expected for (n,γ) reactions on Te (Brown and Berman, 1973). Signatures of crustal fluids have also been inferred through noble gas isotopes in diamonds from Jwaneng kimberlite (Honda et al., 2004). For the apatites H-A and SE-A1, it is to be mentioned here that even after correction for spontaneous fission no significant $^{131}Xe_{excess}$ is observed from the $^{131}Xe/^{132}Xe$ ratios. Thus the $^{129}Xe/^{132}Xe$ value after correction for spontaneous fission reflects the trapped value itself.

4.8 Disequilibrium between vesicles and matrix in apatites

The samples H-A, K-A2 and SV-A all have higher $^{21}Ne/^{20}Ne$ and $^{22}Ne/^{20}Ne$ during VC as compared to P (Table 4.3). This is contrary to expectation as $^{21}Ne_n$ and $^{22}Ne_n$ should reside in the matrix leading to higher $^{21}Ne/^{20}Ne$ and $^{22}Ne/^{20}Ne$ ratios during P. The $^{40}Ar/^{36}Ar$ ratios are also lower during P when compared with VC. Similar isotopic disequilibrium of Ar had been observed in mid-Atlantic ridge basalts attributed to contamination effect (Marty et al., 1983). Such disequilibrium may arise if contamination of the melt is more than for the vesicles. Such a possibility arises if the melt is contaminated with air like gases but the duration of contact between the vesicles and the contaminated melt was very short. This is again evidence that the contaminant was added at a very late stage. Surface equilibrated fluids (groundwater, hydrothermal fluids) are plausible candidates as well as recycled component. Crustal fluids introduced by subduction have been seen from lighter noble gases. This probably acted as the late stage contaminant resulting in disequilibrium between the vesicle and melt.

4.9 Mixing plots

Noble gas isotopic systematics have indicated a multi-component system for the carbonatites. Better understanding can be obtained from the following mixing plots:

a) $^{22}Ne/^{20}Ne$ vs. $^{40}Ar/^{36}Ar$

b) $^{129}Xe/^{132}Xe$ vs. $^{40}Ar/^{36}Ar$

Mixing curves in a plot between different isotopic systems are in general hyperbolic, their curvature depending on the ratio of the elements in the two end members involved. This ratio is conventionally denoted by r.

In a plot of $^{22}Ne/^{20}Ne$ vs. $^{40}Ar/^{36}Ar$, where r is defined as $[(^{20}Ne/^{36}Ar)_{mantle}/(^{20}Ne/^{36}Ar)_{air}]$ a good correlation is obtained for both Sung Valley and Ambadongar

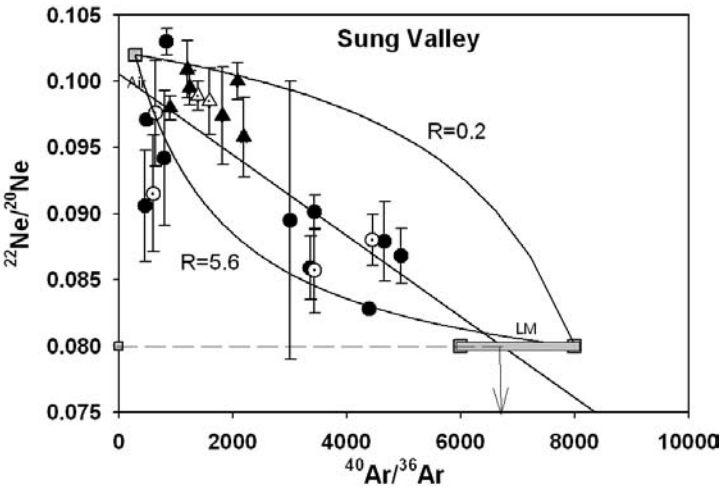

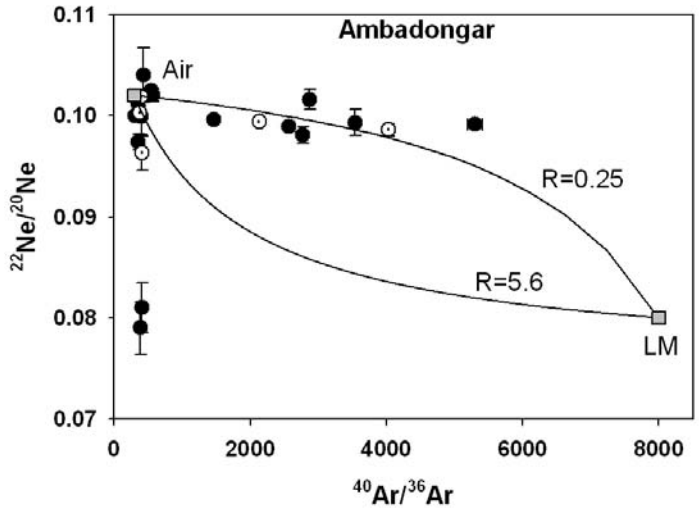

Fig. 4.11 Plot of $^{40}Ar/^{36}Ar$ vs. $^{22}Ne/^{20}Ne$ for Sung Valley carbonates (circle) and magnetites (triangle) and Ambadongar carbonates. Filled symbols represent individual crushing steps, totals are represented by open symbols. Values of R indicated against each trend and discussed in text. In both cases the data are explainable by R = 0.2 to 5.6. The $^{40}Ar/^{36}Ar$ ratio corresponding to mantle $^{22}Ne/^{20}Ne$ value of 0.08 is 7000-8000 in both cases in the range of LM.

carbonate separates(Fig. 4.11).Similar trends have been observed earlier in various mantle samples for e.g. deformed xenoliths (Farley et al., 1994) in plots of $^{40}Ar/^{36}Ar$ vs. $^{22}Ne/^{20}Ne$. Most of the magnetites anchor at the air like pole for Sung Valley. A plausible question is whether the air like component is a contaminant or it originated by some other sources like subduction. Since it has already been seen earlier that magnetites derive air like gases from hydrothermal fluids, in the present case also such a source seems probable. The crustal fluids introduced by subduction may also be a likely contribution of air like gases. Presence of mantle $^{22}Ne/^{20}Ne$ has been observed earlier. $^{22}Ne/^{20}Ne$ value being the same for both UM and LM, this ratio cannot be used to distinguish between the two sources. But the value of $^{40}Ar/^{36}Ar$ is very different for the two reservoirs. For a mantle ratio of ~ 0.08, the $^{40}Ar/^{36}Ar$ can be inferred to be ~ 7000, that matches with LM value which suggest the presence of LM gases. All data points within errors can be explained with R varying between ~ 0.2 to 5.6. The value of $^{40}Ar/^{36}Ar$ inferred from either of the trend still lies in the LM range. In a similar plot for Ambadongar the data points can also be explained by R lying

between 5.6 and 0.3. From the trends, for mantle value of ~ 0.08, the $^{40}Ar/^{36}Ar$ value is ~ 8000 implying the presence of LM volatiles.

However typical value of R for OIB mantle, believed to be the LM source is 5.6 whereas in the present cases it varies up to 0.2. Such an enrichment of Ar cannot be simply accounted for by vesicle formation and melt related solubility. Such component can be explained if the air in the source is fractionated with enriched Ar/Ne ratio. A fractionated component should have atmospheric isotopic ratios and is probably derived from surface equilibrated aqueous fluids or from adsorbed atmospheric component. In the presence of such a fractionated air component the value of R would be raised. Therefore it may be inferred that the few samples lying on the trend corresponding to R=5.6 is the effect of a dominant fractionated air component that probably adsorbs such contaminant on its surface. These samples are characterized by low $^{40}Ar/^{36}Ar$ for high values of $^{22}Ne/^{20}Ne$ as expected for such contaminated samples (Harrison et al., 2003).

In a plot of $^{129}Xe/^{132}Xe$ vs. $^{40}Ar/^{36}Ar$, MORBs and Brazilian carbonatites plot on distinct trends of R (Sasada et al., 1997). The value of R corresponds to $(^{132}Xe/^{36}Ar)_{mantle}/(^{132}Xe/^{36}Ar)_{air.}$ The MORBs lie on R=0.6 and characterise the UM source, whereas the Brazilian carbonatites lie on R=0.06 characterizing the LM source. The Sung Valley samples can be explained by mixing of Air+LM and contribution from a third component with R=4 (Fig. 4.12B). Addition of such an enriched Xe component via subduction is not improbable. Similar trend has been observed in Xe-Ar plot for other terrestrial samples where old oceanic sediments have been recycled and added to a plume source (Kaneoka., 1998).The Ambadongar carbonates, like the Brazilian carbonatites plot on the trend defined by R=0.06 (Fig. 4.12A) and is thus derived from the LM. UM volatiles even if present must be very insignificant. Sevattur carbonatites can be explained by taking into account Air+UM +LM in a plot of $^{129}Xe/^{132}Xe$ vs. $^{40}Ar/^{36}Ar$ (Fig. 4.12C) which is in agreement to our conclusions from $^{40}Ar/^{36}Ar$ isotopes.

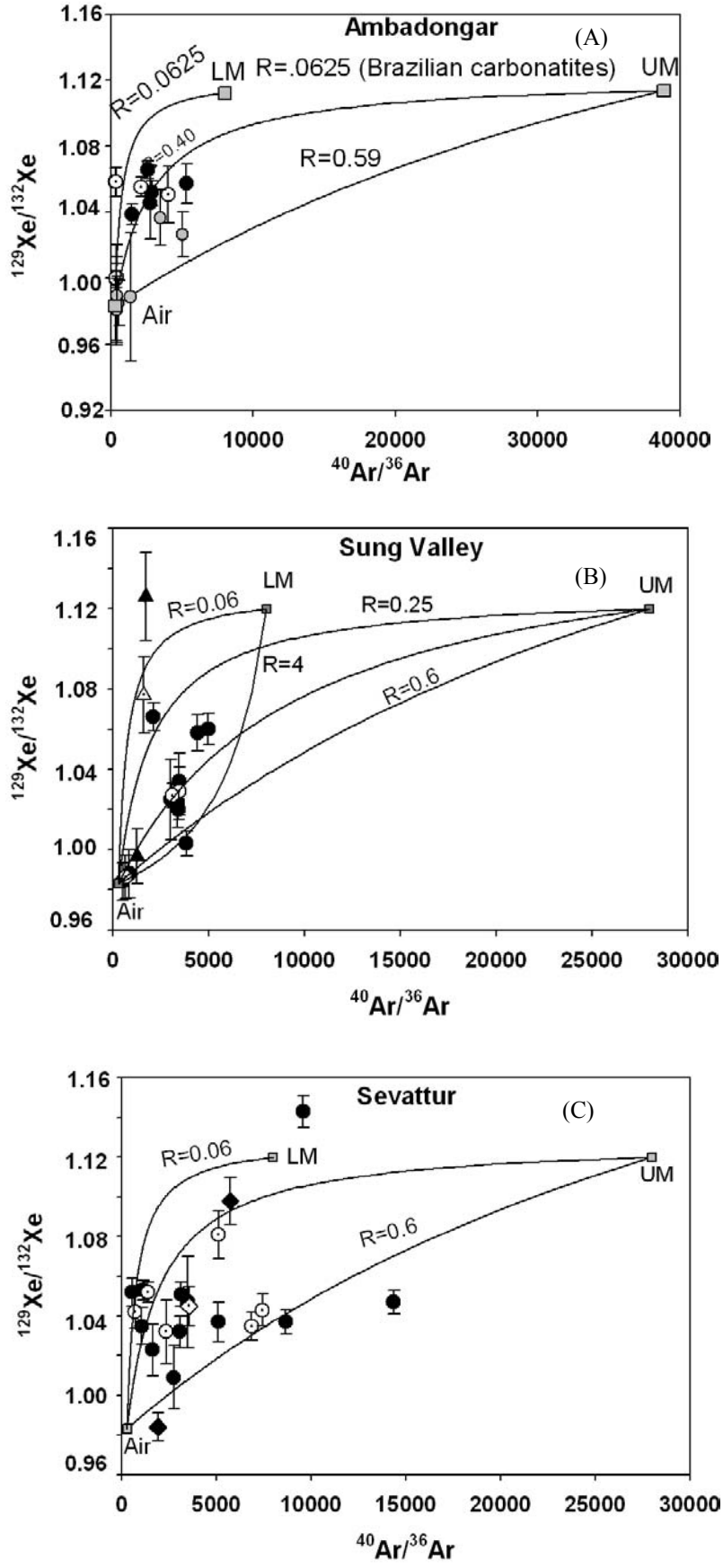

Fig. 4.12 Plot of $^{40}Ar/^{36}Ar$ vs. $^{129}Xe/^{132}Xe$ for Ambadongar, Sung Valley and Sevattur. Symbols as in Fig. 4.11. Apatites, represented by diamonds also plotted. In all cases the $^{129}Xe/^{132}Xe$ ratios have been corrected for spontaneous fission contribution to ^{132}Xe. The corresponding value of R is indicated against each trend and defined in text. From the plots, Ambadongar is dominated by LM volatiles, while Sung Valley indicates mixing between Air, LM and recycled components. For Sevattur, presence of Air, LM and UM volatiles is indicated.

4.10 Summary

The carbonatites studied have trapped volatiles from various sources as implied from their trapped noble gas components. While Sung Valley and Ambadongar acquire their noble gases from the LM mainly with minimum input from UM volatiles, all the South Indian carbonatites show significant contribution from the UM volatiles. But the apatites in the South Indian carbonatites seem to have derived their volatiles from the LM, and it is probable that more than one generations of magma were responsible for the formation of the carbonates and apatites. In fact in Sevattur, it has been shown that two generations of magma, the early generation derived from the LM led to the formation of the apatites and some carbonates, whereas the late generation melt carried the UM volatiles. Presence of excess ^{4}He, ^{22}Ne (as well as ^{21}Ne and ^{40}Ar) unaccountable by radiogenic processes have been attributed to subduction at shallow level for crustal fluids in all the carbonatites. Such air loaded recycled component may have probably led to isotopic disequilibrium between the vesicles and melt in the apatites. From the noble gas studies the carbonatites may be broadly grouped into the plume dominated Sung Valley and Ambadongar, and the South Indian carbonatites dominated by UM volatiles.

Chapter 5

Nitrogen and argon in carbonatites: A coupled study

5.1 Introduction

The nitrogen isotopic composition is different among the different reservoirs of the earth. While the $\delta^{15}N$ is zero for the atmosphere and positive for the crustal samples, it is negative for the mantle reservoir. Within each reservoir, there is some variability in $\delta^{15}N$, brought about by biological and geological processes. For example, the $\delta^{15}N$ value is between +2 to +10‰ in organic N from marine sediments (Peters et al., 1978) and +2 to +15‰ for ammoniacal N in metasediments (Haendel et al., 1986; Bebout and Fogel, 1992; Boyd et al., 1993). During subduction the $\delta^{15}N$ of the subducting rocks and basalts increase further with increasing metamorphic grade (Bebout and Fogel, 1992). On the other hand the $\delta^{15}N$ value of the UM is highly depleted and is between -5 to -15‰ (Marty and Humbert, 1997; Mohapatra and Murty, 2004). This nitrogen isotopic disequilibrium between different reservoirs of the earth can be very useful to identify the various components that may be present in any mantle sample and to some extent learn more about the incorporation of these different components in any sample. For recycled component it is particularly useful as noble gas signatures are identical for air and subducted components and their differentiation is not be very straightforward (Mohapatra and Murty, 2002).

The N disequilibrium between the various terrestrial reservoirs can be accounted for by the evolution of N in the Earth. Based on O isotopic match, E-chondrites are considered to be the principle building blocks of Earth. (Javoy and Pineau, 1983; Javoy, 1999). Accordingly the initial $\delta^{15}N$ of the Earth should be ~-35‰ with N content of 300±100 ppm (Mohapatra, 1998). However, since N is a siderophile element, under reducing conditions a part of the N may be partitioned into the metallic core when it segregates from the silicate mantle (Mohapatra, 1998; Hashizume et al., 1997). But core formation should not result in any isotopic fractionation as it is an equilibrium process occurring at high temperature. Isotopic modification of the mantle N along with changes in its N budget must have occurred subsequently during magma degassing of the mantle. The layered structure of the mantle as evident from noble gases must have also been established at this stage due to differential degassing

between the shallow UM, and the undegassed/less degassed LM. Since the present atmosphere and the crust can only account for 1 ppm of N, it will be interesting to know if a part of the N is still locked up in the mantle or if it is lost from atmospheric reservoir by hydrodynamic escape in the early stages.

The available N estimate for the mantle is very variable. It is estimated to be around 1-3 ppm for the UM assuming it behaves as an incompatible element (Marty B, 1995), while it was estimated to be about 36 ppm assuming that it behaves as a compatible element (Javoy, 1998). However N is generally believed to be an incompatible element in the mantle similar to Ar, as no fractionation between the two is observed for variable degree of fractional crystallization, partial melting or magma degassing (Marty and Humbert, 1997). In this context it will be interesting to know if a part of N is still locked up in the LM and if its $\delta^{15}N$ is still pristine and close to that of the E-chondritic value of -20 to -45‰ (Javoy and Pineau, 1983). Since carbonatites have been found to trap volatiles from LM (Chapter 4), they may be ideal samples to constrain the $\delta^{15}N$ of LM and assess the amount of N locked up in the LM.

The N concentration in most of the mantle samples are a few ppm with diamonds being an exception often containing about two orders of more N than other mantle materials. The study of N is challenging due to its low abundance making it very sensitive to contamination from atmospheric and surface derived organic N. However trace element geochemistry and petrology of various carbonatite complexes and the associated alkaline rocks indicate that they are derived from a volatile enriched mantle (Anderson, 1987; Hawkesworth et al., 1990; Kramm and Kogarko, 1994). Thus, they are likely to contain a lot of N as well as noble gases in them. Atmospheric gases, especially Xe and N, may be largely adsorbed on the grain surfaces and should be reflected in their accompanying isotopic ratios. The $^{40}Ar/^{36}Ar$ ratio that is distinctly different between mantle and air can be used as an index of atmospheric contamination. Thus a coupled discussion of N and Ar would be very useful. The N and Ar data are given in Table 5.1.

As explained in the experimental chapter, the vacuum crushing (VC) technique has been especially developed to facilitate gas analyses in carbonates which would have been otherwise impossible. We have analysed carbonates, magnetites and apatites by sequential crushing, while apatites have been also analysed by stepwise pyrolysis. The sequential crushing is carried out in three steps. An initial step of 15 strokes (mainly

to get rid of surficial gases), a main step of 300-500 strokes where most of the sample gases are expected and a final step of 500 strokes to ensure complete gas release.

Unlike He and Ne, N and Ar due to low K contents in the samples do not have any *in situ* components. While Ar could be either present as a component trapped in vesicles or as a component dissolved in the matrix, N in addition to the above two, can be present in a solid speciation. This later component will not be released during VC and will be exclusively released during P.

In this chapter we will initially concentrate on the N release pattern, abundance and isotopic ratios separately for the carbonates, and magnetites during VC, and for both VC and P for the apatites. The $^{40}Ar/^{36}Ar$ ratios would be discussed simultaneously as index for contamination and presence of mantle gases in the samples. The $N_2/^{36}Ar$ ratio in the different samples and the implications would be considered next. Finally taking into account the results and the observations we would try to identify the various N components in the samples.

5.2 Release pattern of nitrogen during vacuum crushing

5.2A Carbonates: The N concentration between the various carbonates from the different carbonatites studied varies between 51-2837 ppb while the $\delta^{15}N$ among most carbonates is positive ranging from 3.51 to 11.74‰. However, some carbonates of Ambadongar have negative $\delta^{15}N$ values up to -13.72‰. Also, variations of $\delta^{15}N$ and $^{40}Ar/^{36}Ar$ are observed during sequential crushing for a given sample, mostly as a result of preferential release of contaminants in earlier stages. Thus progressive increase in $\delta^{15}N$ accompanied by increasing $^{40}Ar/^{36}Ar$ (H-C1A and K-C3) reflects decreasing atmospheric contamination with increasing crushing. However some samples also show decreasing $\delta^{15}N$ with increasing crushing steps along with higher $^{40}Ar/^{36}Ar$ ratio (H-C1B, SE-C7, SV-C1, A-C1). In fact a lighter nitrogen component is observed in the final crushing step for many of the carbonates(H-C4, SE-C2, SE-C3B,SE-C5,SE-C6,SV-C3,SV-C5) often accompanied by $^{40}Ar/^{36}Ar$ ratio typically in the mantle range. This indicates presence of more than one component of N in the samples, a light N (mantle component?) and a second component of N with heavier isotopic ratio. Presence of vesicles in the same sample that host gases from two magmas, one deep seated Ar and the other atmospheric Ar where the two components are distinctly preserved without homogenisation have been reported from Atlantic MORB glasses (Jambon et al., 1985).

Table 5.1. Elemental and isotopic ratios of N and Ar in the carbonates(C), apaties(A) and magnetites(M) from Hogenakal(H), Sevattur(SE), Khambamettu(K), Sung Valley(SV) and Ambadongar(A) for vacuum crushing(VC) and subsequent pyrolysis(P'), and total pyrolysis(P). Errors in concentrations of N (ppb) and Ar (cc STP/g) are ±10%, while errors in isotopic ratios represent 95% confidence limits.

No of Strokes(VC) or °C(P)	N	$\delta^{15}N$(‰)	^{36}Ar (10^{-10})	$^{40}Ar/^{36}Ar$	$^{N_2}/^{36}Ar$ (10^6)	$^{N_2}/^{40}Ar$
			Hogenakal			
H-C1A(VC)						
50	420.6	3.51 .59	22.7	6415 ±63		
300	510.0	4.56 .52	1.6	14641 127		
300	207.6	4.80 .30	1.9	16440 146		
500	249.6	6.08 .40	0.9	22297 179		
500	117.5	6.47 .32	0.3	29216 162		
total	1505	4.70 .44	27.4	8367 78	0.44	53
H-C2(VC)						
25	n a	n a	7.7	8806 84		
500	n a	n a	12.3	17927 17		
500	n a	n a	1.8	19886 18		
500	n a	n a	1.1	3037 26		
total			22.9	14311 40		
H-C1B(VC)						
15	85.77	8.83 .29	7.7	5879 54		
300	312.3	4.53 .27	12.2	14063 131		
300	53.12	1.51 .30	1.4	18597 148		
total	451.2	4.99 .28	21.3	11392 104	0.17	15
H-C4(VC)						
15	78.01	0.41 .26	6.3	6609 61		
300	248.6	10.06 .16	23.1	8183 77		
300	46.34	1.22 .48	3.9	10700 94		
total	372.9	6.94 .22	33.3	8095 75	0.09	11
H-A(VC)						
300	38.58	-18.86 ±.51	1.6	3359 25		

1000*	35.26	-26.31 .19	6.8	4986 41		
Total	73.84	-22.42 .36	8.4	4679 38	0.07	15
H-A(P')						
950	5191	3.02 .44	4.7	1234 6		
1400	178.0	11.38 1.04	1.8	2121 2		
1800	519.6	6.97 .70	14.0	2252 19		
Total	5889	3.62 .48	20.5	2007 15	2.30	1145
H-A(P)						
600	1879	5.68 ±.16	1.4	4015 15		
950	1888	12.55 .18	0.9	4322 36		
1400	1702	10.30 .13	2.5	1373 6		
1600	53.04	-3.65 1.47	9.1	664 1		
1800	394	-3.03 .16	10.9	4595 7		
total	5916	8.54 .17	24.8	2787 6	1.91	685
		Sevattur				
SE-A1(VC)						
15	163.6	1.83 .63	15.4	1913 ±18		
500	278.1	9.29 .26	9.6	5719 53		
500	35.79	1.88 .14	0.9	8463 64		
total	477.5	6.18 .38	25.9	3549 33	0.15	42
SE-A1(P')						
400	194.0	-3.18 .66	10.8	2643 19		
1200	2702	7.40 .21	5.6	828 3		
1800	1722	-15.36 .43	56.3	506 5		
Total	4618	-1.54 .31	72.7	849 7	0.51	599
SE-C1(VC)						
25	n a	n a	18.1	1116 11		
500	n a	n a	6.5	3125 30		
500	n a	n a	7.3	413 4		
total			31.9	1363 13		
SE-C2(VC)						
25	n a	n a	9.4	1631 16		
500	n a	n a	5.3	3484 34		

500	n a	n a	1.2	3114 29		
total			15.9	2357 23		
SE-C3A(VC)						
25	n a	n a	9.5	946 9		
500	n a	n a	7.6	2249 22		
500	n a	n a	0.8	3197 26		
total			17.9	1598 15		
SE-C3B(VC)						
15	49.48	-0.35 .12	6.0	549 5		
300	94.77	7.79 .27	6.3	1048 10		
300	29.37	-3.80 .18	4.2	451 4		
total	173.6	3.51 .21	16.5	715 7	0.08	118
SE-C5(VC)						
15	80.02	-0.62 .66	2.8	3081 28		
300	311.1	8.29 .14	4.1	8667 81		
300	46.88	-3.36 .60	0.3	16678 115		
total	438.0	5.41 .28	7.2	6859 62	0.49	71
SE-C6(VC)						
15	402.8	9.15 .57	9.1	5093 49		
300	867.9	12.75 1.08	6.9	14366 136		
300	129.3	7.01 .36	5.1	2135 20		
total	1400	11.18 .86	21.1	7428 70	0.53	71
SE-C7(VC)						
15	324.9	12.37 .67	20.3	2750 26		
300	571.3	6.63 .40	8.9	9584 88		
300	82.79	-2.26 .58	0.7	16064 111		
total	978.9	7.81 .48	29.9	5115 46	0.26	51
SE-A2(P)						
600	230.5	6.38 .48	1.2	5121 82		
950	594.7	11.40 .38	1.4	7051 9		
1400	908.2	3.60 .39	2.9	671 2		
1800	345.3	6.95 .57	1.0	3967 11		
total	2079	6.70	6.5	3350	2.56	764

		.43		6		
		Khambamettu				
K-C1A(VC)						
15	n a	n a	8.6	3045 ±29		
500	n a	n a	4.5	10051 96		
500	n a	n a	0.6	10456 86		
total			13.7	5686 54		
K-C1B(VC)						
15	265.4	11.82 1.07	5.2	3516 32		
300	425.1	8.53 .19	2.6	12806 109		
300	81.88	4.44 .09				
total	772.4	9.23 .48	7.9	6613 58	0.78	118
K-C3(VC)						
15	258.4	3.78 .77	7.3	3334 32		
300	439.0	7.59 .30	15.7	2858 27		
300	259.9	14.15 .14	0.5	16000 116		
total	957.3	8.34 .39	23.5	3304 31	0.33	99
K-A2(VC)						
15	42.81	-0.04 .46	2.6	2545 20		
500	96.87	-15.88 .31	1.4	7967 55		
total	139.7		4.0	4468 32	0.28	63
K-A2(P')						
1200	3630	4.76 .28	n a	n a		
1600	384.3	7.36 .06	n a	n a		
1800	699.3	5.14 .16	n a	n a		
total	4714	5.03 .25				
K-A2(P)						
950	566.3	5.11 .37	0.6	3512 27		
Melting step	2059	6.55 .37	1.1	1748 11		
Total	2626	6.24 .40	1.7	2347 16	12.36	5265
K-A1 (VC)						
15	15.38	-22.51 .10	1.7	673 6		
1000*	43.21	-5.13 .24	2.8	1235 9		
total	58.59	-9.69 .20	4.5	1021 8	0.10	102
K-A1 (P')						

950	1727	7.18	n a	n a		
		.69				
1200	348.4	7.83	n a	n a		
		.29				
1500	184.5	8.44	n a	n a		
		.13				
1800	40.32	11.12	n a	n a		
		.48				
total	2300	7.68				
		.54				
KA1(P)						
400	174.6	-0.61	n a	n a		
		.19				
950	374.2	7.40	n a	n a		
		.35				
1300	381.5	10.10	n a	n a		
		.71				
1500	516.9	8.58	n a	n a		
		.38				
1800	319.4	11.52	n a	n a		
		.11				
Total	1767	8.28	n a	n a		
		.38				
		Sung Valley				
SV-C3(VC)						
15	392.7	9.55	2.6	4395		
		.18		40		
300	1073	13.60	20.2	3364		
		.13		32		
300	268.9	3.66	2.5	3011		
		.41		27		
total	1735	11.14	25.3	3434	0.55	160
		.19		33		
SV-M3(VC)						
15	129.5	5.27	2.9	1244		
		.14		11		
500	309.7	5.35	4.3	1694		
		.14		16		
300	59.70	-1.84	0.5	2905		
		.11		21		
total	498.9	4.47	7.7	1591	0.52	326
		.14		14		
SV-C1(VC)						
15	401.5	6.51	6.9	3432		
		.17		32		
300	1084	5.84	13.4	4956		
		.72		46		
300	185.2	1.39	1.8	4662		
		.29		39		
total	1671	5.51	22.1	4457	0.60	136
		.54		41		
SV-A1(VC)						
25	519.4	5.88	8.7	2938		
		.22		25		
500	512.2	9.50	6.6	3843		
		.42		32		
500	54.56	-5.34	3.1	1619		
		.44		3		
total	1086	7.02	18.4	3040	0.47	155
		.33		24		

SV-M1A(VC)						
25	141.1	4.02 .33	6.9	1199 11		
500	305.5	5.54 .14	8.0	2193 45		
500	72.64	-7.35 .18	1.5	1848 15		
total	519.2	3.32 .20	16.4	1743 28	0.25	145
SV-M1B(VC)						
25	135.3	1.99 .49	4.2	900 8		
500	230.4	-1.53 .97	3.9	1761 16		
500	51.63	-12.06 .22	0.5	2481 18		
total	417.3	-1.69 .72	8.6	1386 13	0.39	280
SV-C4(VC)						
25	n a	n a	14.3	463 5		
500	n a	n a	9.5	770 7		
500	n a	n a	0.7	1176 10		
Total			24.5	604 6		
SV-C5(VC)						
15	82.46	14.14 .37	7.3	496 5		
300	135.6	7.34 .30	6.4	847 8		
300	22.65	-14.95 .62	0.1	329 2		
total	240.7	7.56 .36	13.8	645 6	0.14	216
SV-C2(VC)						
25	n a	n a	6.3	2107 21		
500	n a	n a	7.4	3832 38		
500	n a	n a	1.9	3409 47		
Total			15.6	3082 32		
SV-A2(P)						
600	3295	12.06 .19	13.6	2022 135		
1200	1162	4.95 .28	4.1	402 .6		
1400	649.4	16.94 .24	1.2	332 .6		
1700	667.4	9.12 .29	0.8	1692 16		
total	5774	10.84 .23	19.7	1567 94	2.34	1496
		Ambadongar				
A-C1(VC)						
15	1176	7.01 .35	83.6	5301 103		

300	1452	2.37 .16	81.2	2770 54		
300	208.8	-3.44 .21	8.0	3537 65		
total	2837	3.87 .24	172.8	4030 78	0.13	33
A-C2(VC)						
15	640.6	8.02 .08	61.2	1468 29		
300	1304	2.48 1.34	78.9	2568 50		
300	182.9	2.95 .68	8.1	2869 55		
total	2128	4.19 .90	148.2	2130 41	0.11	54
A-C3(VC)						
15	235.9	10.30 .51	36.8	546 5		
300	369.3	14.15 .24	107.7	353 3		
300	43.04	-1.07 .31	6.1	427 5		
total	648.2	11.74 .34	150.6	403 4	0.03	85
A-C5(VC)						
15	19.85	-24.55 .69	7.2	563 10		
300	64.12	-5.95 .34	22.2	310 6		
300	15.19	-32.39 1.72	3.7	383 4		
total	99.16	-13.72 .62	33.1	373 7	0.03	64
A-C4(VC)						
15	721.5	4.01 .87	155.3	357 7		
300	575.2	-0.08 .004	125.3	401 8		
300	50.93	-12.63 .12	8.5	409 8		
total	1348	1.63 .36	289.1	378 7	0.04	99
A-C6(VC)						
15	134.3	-2.76 .32	12.6	1575 15		
300	407.4	-2.50 .58	9.6	3728 36		
300	54.59	-3.40 .27	2.2	790 7		
total	596.3	-2.64 .49	24.4	2347 22	0.20	83

*Combination of two consecutive steps when gas amount in any one step is too low .n a stands for not analyzed

The elemental ratios $N_2/^{36}Ar$ as well as $N_2/^{40}Ar$ can be very informative. As shown in Fig. 4.2, the $N_2/^{36}Ar$ ratio in all the samples are well above air. The $N_2/^{36}Ar$ value is

well known for air and UM, but that for the LM is still poorly constrained. The $N_2/^{36}Ar$ ratio constrained from the Kola carbonatites (Dauphas and Marty, 1999) should be only an upper limit for LM as N isotopic ratio clearly indicates presence of recycled N_2 in the source region. The $N_2/^{36}Ar$ ratios for the important terrestrial reservoirs are listed in Table 5.2. While $N_2/^{36}Ar$ involves both primordial isotopes, for $N_2/^{40}Ar$, the ^{40}Ar is radiogenic. The $N_2/^{36}Ar$ values of both the UM and LM must have been established early in the earth's history and any subsequent modifications must be due to the addition of recycled N. On the other hand variation between the $N_2/^{40}Ar$ ratio among different carbonatites of different ages may also be due to subsequent production of ^{40}Ar in the mantle with time. Thus the best constrain for $N_2/^{40}Ar$ ratios can be obtained only in terms of $N_2/^{36}Ar$ and $^{40}Ar/^{36}Ar$ ratios of the different reservoirs and are also tabulated in Table 5.2.

Table 5.2 List of $N_2/^{36}Ar$ and $N_2/^{40}Ar$ for the different terrestrial end members for magmatic samples. $N_2/^{36}Ar$ for Air, UM and Recycled taken from Mohapatra, 1998 and that for LM from Dauphas and Marty, 1999.

	Air	UM	LM	Recycled
$N_2/^{36}Ar(10^6)$	0.03	5	0.30(?)	16.67
$N_2/^{40}Ar$	83.3	125	38	~45000

While $N_2/^{36}Ar$ ratio can only be modified by the addition of recycled component, even if samples are poor in K as in the present case and there is no *in situ* ^{40}Ar, addition of crustal fluids can add ^{40}Ar to the source magma of the samples and affect the $N_2/^{40}Ar$ ratios. For example, in the two samples H-C1B and H-C4 where $N_2/^{40}Ar$ values of ~15 and 11 are observed (Table 5.1) may reflect some elemental fractionation between N and Ar. However since it is established that both N and Ar have comparable solubility (Libourel et al., 2003; Miyazaki et al., 2004), there should be an additional source of ^{40}Ar. One possibility is the presence of crustal fluids as we have seen from excess of other noble gas isotopes like ^{4}He, ^{22}Ne, ^{129}Xe and $^{131\text{-}136}Xe$ (see Chapter 4).

However, $N_2/^{40}Ar$ ratio is prone to be less affected in mantle samples by addition of air as compared to the $N_2/^{36}Ar$ values (Marty et al., 1995). This trend is very distinctly observed in the present study for Ambadongar where both calcitic as well as ferro carbonatites have been analysed. Ferro carbonatites are characterised by late stage air

borne hydrothermal fluids reflected in their air like $^{40}Ar/^{36}Ar$ ratios. The $N_2/^{40}Ar$ ratios of all the Ambadongar carbonatites show no systematic variation whereas their $N_2/^{36}Ar$ ratios are different by an order of magnitude between the calcitic carbonatite (~$15x10^4$) and the ferro carbonatites (~$3.2x10^4$), the later being almost air like. The $N_2/^{36}Ar$ ratio for the other carbonates range between (9-78)$x10^4$ clearly indicating presence of mantle and/or recycled components in the samples.

5.2B Apatites: The $\delta^{15}N$ for apatites during VC are negative for Hogenakal (-22.42±0.36‰), as well as Khambamettu (-15.88±0.31‰ for K-A2) and (-9.69±0.20‰ for K-A1) while it is positive for Sevattur (6.18±0.38‰) and Sung Valley (7.02±0.33‰). For Hogenakal and Khambamettu apatites the N contents are very low being ~59-140 ppb while for Sevattur and Sung Valley apatites the N contents are ~ 478 and 1086 ppb respectively, which is well within the range for the carbonates. However, in both the apatites in the final crushing step, the $\delta^{15}N$ signature is lighter, being 1.88±0.14‰ and -5.34±0.44‰ in SE-A1 and SV-A1 respectively, similar to many carbonates. The observations are in agreement to that seen from noble gases and discussed in the previous chapter:

- Melts responsible for the generation of apatites are different from the carbonates which are reflected not only in their $^{40}Ar/^{36}Ar$ ratios but also in their negative $\delta^{15}N$ values atleast for Hogenakal and Khambamettu.
- Vesicles in the same sample may house different magma components that have not homogenised and are trapped in vesicles of different sizes. It is likely that the light nitrogen component is trapped in the smaller vesicles and released in the final step of crushing in most samples, while the larger vesicles trap a component that has a relatively heavy N isotopic signature. Vesicle formation in magma is believed to be a non equilibrium process and may not reequilibrate with dissolved magmatic volatiles. Thus they may preserve the volatile compositions at different times during magma history as found in the bubble-by-bubble difference in the volatile elemental and isotopic ratios from analyses of Mid-Atlantic Ridge basalts (Burnard, 1999).

The $N_2/^{36}Ar$ trapped ratio for the apatites as obtained by VC lie in the range of (7-47) x 10^4 implying mixing between air and mantle components. The $N_2/^{40}Ar$ values lie in the range of 42-155 as also expected for mixing between different trapped mantle

components. The only exception is H-A where the $N_2/^{40}Ar$ value of ~ 14 indicates addition of crustal ^{40}Ar to the samples.

5.2C Magnetites: The $\delta^{15}N$(‰), N (ppb) for the three magnetites analysed from Sung Valley are 4.47±0.14, 499(SV-M3), 3.32±0.20, 519(SV-M1A) and -1.69±0.72, 417 (SV-M1B). Similar to the carbonates and apatite, they also show the presence of a light nitrogen component in the smaller vesicles observed mostly in the final crushing step. Their $N_2/^{36}Ar$ values are in agreement with mixing of air and mantle components.

5.3 Release pattern of nitrogen during pyrolysis (apatites)

The release pattern of $\delta^{15}N$ during stepwise heating has been shown for all the five apatites analysed from Hogenakal, Khambamettu, Sevattur and Sung Valley in Fig. 5.1. Except for the Khambamettu apatites where the progressive increase in $\delta^{15}N$ with increasing temperature steps may simply reflect reducing contamination of air to the single N component in the sample with $\delta^{15}N$ value of ≥6.55±0.37‰ in KA-2 and ≥11.52±0.11‰ in KA-1 (the highest $\delta^{15}N$ values observed at their melting steps), presence of two or more components can be easily visualised from the other apatites in Fig. 5.1.

For all the samples the initial temperature step (600°C for Hogenakal and 950°C for Khambamettu) wherein measurable gas amounts are released, might still have some air contamination for N thus explaining their low $\delta^{15}N$ value (as compared to the next higher temperature fraction). However, in addition, Hogenakal apatite shows the presence of two N components, one with a positive $\delta^{15}N$ value of 12.55±0.18‰ observed at temperatures of 950-1400°C, while a negative $\delta^{15}N$ component (-3.03±0.16‰) is seen at a higher temperature step of 1600-1800°C. Although the negative $\delta^{15}N$ component is not observed for either SE-A1 and SV-A1, in both the apatites we do see the presence of lighter N in the melting step (as compared to the highest $\delta^{15}N$ observed in lower temperature steps of 950-1400°C). Presence of more than one N component is also obvious from Fig. 5.2 where fraction of N and Ar released during VC and P has been compared for all the apatites. While a large fraction of Ar is released from the vesicles during crushing and must be essentially of trapped origin, the N is definitely hosted at two different sites in the minerals. A very small fraction of N as seen from Fig. 5.2 is hosted in the vesicles while most of the N resides in lattice of the minerals.

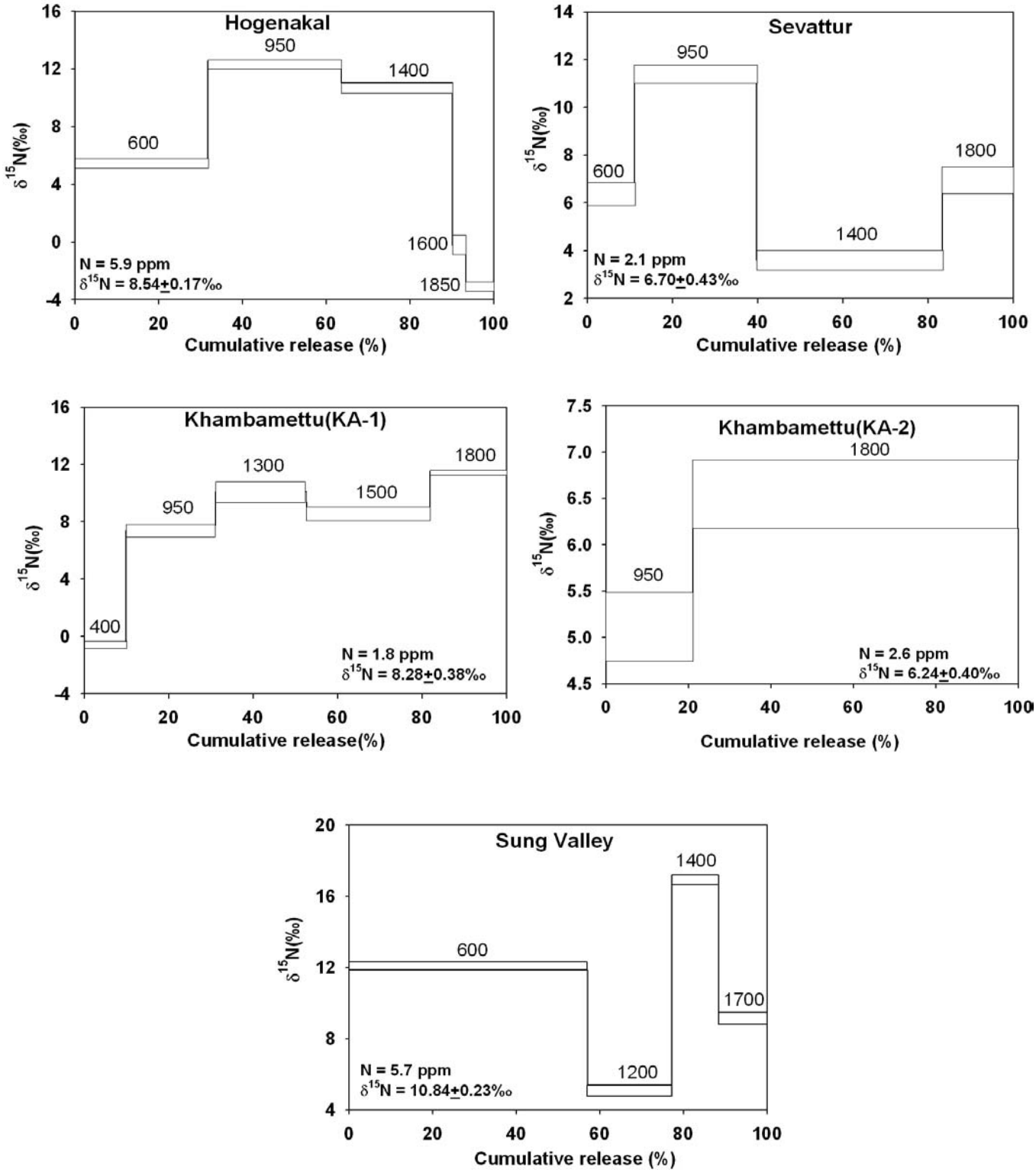

Fig. 5.1 $\delta^{15}N$ variation vs. cumulative release of N during pyrolysis of apatites from Hogenakal, Sevattur, Khambamettu and Sung Valley. Temperature in °C for each step is indicated. Presence of more than one component in all the apatites, except Khambamettu is clearly seen.

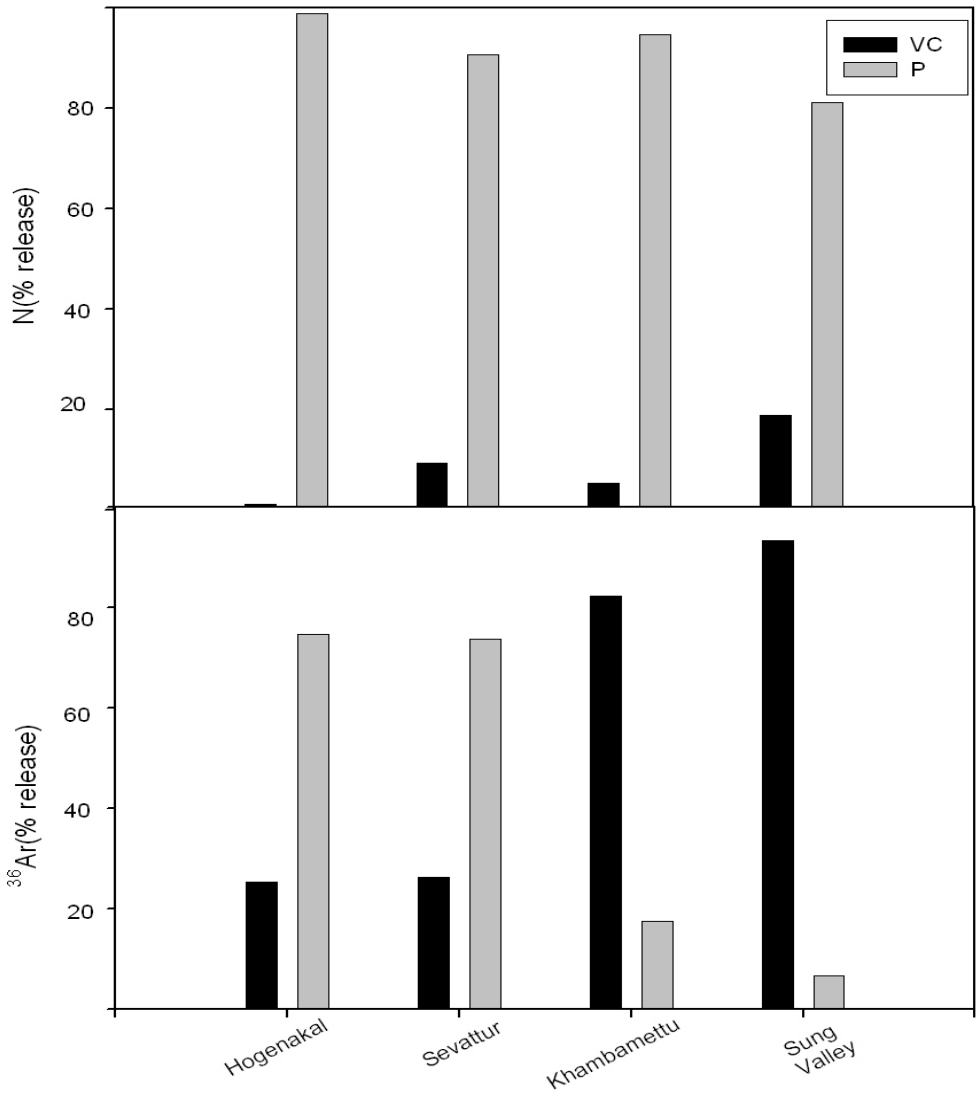

Fig. 5.2 Comparison of % release of N and ^{36}Ar between VC and P. While most of the N is released during P, a considerable fraction of ^{36}Ar is released during VC

5.4 Isotopic fractionation

It is important to assess and understand the role of isotopic fractionation for N during the processes of vesciculation, degassing, gas partitioning between melt and residual phases etc. that occur in the process of magma generations, ascent and emplacement, to be able to decouple and correct for such effects. So, a brief discussion on isotopic fractionation is pertinent before the actual discussion of the N and Ar results. In the current state of knowledge no definite conclusion can be reached regarding isotopic fractionation of N. Cartigny and Ader (2003) argue that MORB vesicles are depleted by about 1.5‰ relative to dissolved N, while Marty and Dauphas (2003) consider such fractionation to be negligible. Theoretical study of fractionation of N isotopes between N radicals and N_2 indicates a maximum depletion of 1.5‰ at 1300°C in N_2 relative to the radicals (Richet et al., 1977) which is of relevance if N in the mantle

occurs in some form of a N rich mineral. However the fractionation is not very large. Also since N is incompatible, even if N fractionation takes place during extraction from the mantle source, the net effect would not be observable due to quantitative extraction of N.

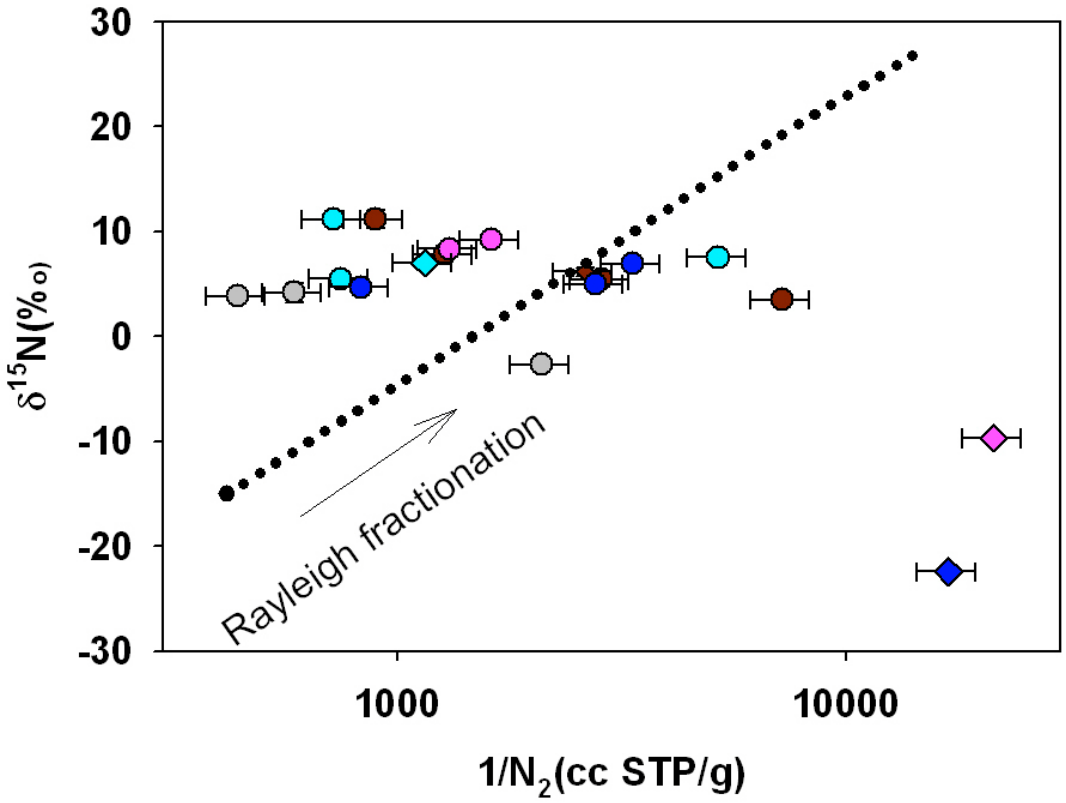

Fig. 5.3 $\delta^{15}N$ vs. $1/N_2$ for different carbonates(circle) and apatites(diamonds) studied by VC from Hogenakal(blue), Sevattur(dark red), Khambamettu(pink), Sung Valley(cyan) and Ambadongar(grey). The Rayleigh fractionation trend from a starting initial composition with $\delta^{15}N_0$~-15‰ and N~3 ppm is also shown. None of the carbonatites can be explained by such fractionation

N isotopic fractionation in diamonds during growth has also been ruled out (Cartigny et al., 2003). Another possibility of isotopic fractionation may arise during metamorphism of rocks. In fact petrological study of Sevattur carbonatites show the effect of tectonic stress as reflected in the development of boudinage structures, elongated and sheared xenoliths and deformed calcite twin lamellae (Pandit et al., 2002). But available data for metamorphic rocks have shown that the effect of metamorphism on N isotopic fractionation is very limited and can be of the order of 1-3‰ if any (Busigny et al., 2003).

Isotopic fractionation of N during any process like degassing or metamorphism should show a correlation between $\delta^{15}N$ and N contents of the samples. Isotopic fractionation during any of these processes should show a Rayleigh trend which for reference is also shown in Fig. 5.3. For the referred trend an assumed $\delta^{15}N_0$ value of -15‰(close to the lowest and therefore most pristine value obtained from the following study) and N content of 3 ppm which is again the highest value of trapped N for any sample in the present study have been considered. The vapour to melt partition coefficient value of ~0.988 used here refers to that at temperature of 1800°C (Tonks and Melosh, 1990). In case of any fractionation effect the residual melt should be more enriched in ^{15}N and therefore fractionation should reflect increasing $\delta^{15}N$ with decreasing N content. However it is obvious that no such correlation is observed for the presently studied carbonatites and it can be thus concluded that even if any isotopic fractionation has occurred in the samples for N, it is very insignificant.

5.5. Comparison of vacuum crushing and pyrolysis for apatite

Table 5.3 lists the comparison between VC and P of apatites. From Table 5.3 it is obvious that N released from the melt is far in excess than that from the vesicles. N in the vesicles can only account for ~1.2%(Hogenakal), 5.2%(Khambamettu) 19%(Sung Valley) and 23%(Sevattur) of the total gas in the samples while a considerable amount of Ar is hosted in the vesicles. This is also seen very clearly in Fig. 5.2. The $\delta^{15}N$ signature of the vesicles as observed during VC is also grossly different from the total as seen from the P of the samples. While the vesicles host a depleted N component as seen for the apatites of Hogenakal and Khambamettu, the $\delta^{15}N$ of the N released during P is positive. Although the light N component is not seen during VC of SV-A1 and SE-A1, the $\delta^{15}N$ is lower for SV-A1 and comparable for SE-A1. As discussed in previous chapter, the isotopic disequilibrium between the vesicles and the melt is also observed for the $^{40}Ar/^{36}Ar$ ratios. While the values are higher and therefore closer to mantle ratios for H-A, K-A2 and SV-A1 during VC, for SE-A1 both VC and P values are comparable in agreement with isotopic equilibrium observed for $\delta^{15}N$ also in this sample.

If we compare the $N_2/^{36}Ar$ ratios of the samples between VC and P, it is obvious that while the elemental ratios can be generally explained by mixing between air and mantle components during VC, they are significantly higher by order of magnitude in case of P.

Table 5.3 Comparison of N and Ar, isotopic and elemental ratios between VC and P for apatites

Sample	N(ppb)	$\delta^{15}N$(‰)	$^{40}Ar/^{36}Ar$	$N_2/^{36}Ar$ (10^4)
H-A(P)	5916	8.54 ±.17	2787 ±6	191
H-A(VC)	73.8	-22.42 .36	4679 38	7
SE-A2(P)	2079	6.70 .43	3350 6	256
SE-A1*(VC)	478	6.18 .38	3549 33	15
K-A2(P)	2626	6.24 .40	2347 16	1236
K-A2(VC)	140	-15.88 .31	4468 32	28
SV-A2(P)	5774	10.84 .23	1567 94	235
SV-A1*(VC)	1086	7.02 .33	3040 24	47

*These apatites are from different samples as compared to their pyrolyzed counterparts

Similar trends between VC and P were also observed from some MORB analyses (Marty et al., 1995) though $\delta^{15}N$ was not analyzed in that study. However the authors had attributed all the N_2 released during P to be secondary while the original mantle N was believed to be only preserved in the vesicles. Source of such N contamination can come from preferential adsorption or incorporation of surface derived N (organic N, N rich alteration phase), but such attribution without $\delta^{15}N$ measurements is improper. But unlike in the case of the MORB samples, where only at low temperature steps of around ~600°C the high N_2/Ar values of 850-44000 are observed accompanied with air like $^{40}Ar/^{36}Ar$ ratios, in the present study all the apatites show high $N_2/^{36}Ar$ as well as high $N_2/^{40}Ar$ values even up to the melting temperature of 1800°C, and are accompanied by non-air like (>1000°C) $^{40}Ar/^{36}Ar$ ratios. Also non equilibrium between melt and vesicles have been observed earlier between crushed and melted MORBs where addition of atmospheric component resulted in the melt being more depleted in the mantle component than the vesicles (Fischer, 1997). There are many

other reasons why stepped heating data cannot be simply neglected as argued by Mohapatra and Murty (2004). The stepped heating data may be discarded on the ground that isotopic fractionation can result during stepwise heating and extreme signals, both positive and negative may be generated by various organic contamination. However all the samples have been combusted at 400°C initially. Besides, fractionation predicts that one should observe light N in the low temperature extraction steps, while heavy N should be observed in the higher temperature fractions. But contrary to that, heavy N is observed in the low temperature fractions while light N is only seen in the higher temperature steps. Another possibility is the fractionation of N during degassing leaving the vesicles depleted in ^{15}N relative to the residual melt (Cartigny et al., 2001b). However the extent of fractionation observed in the present cases for the various samples between melt and vesicles cannot be accounted for by simple Rayleigh fractionation assuming that the vesicles have been formed from the melt and the N released from the lattice represents the residual melt after vesicle formation. For initial composition of the melt, it is assumed to be similar to that of the vesicles while the actual initial composition should be equal to or lower than this. Accordingly the $\delta^{15}N$ of the residual melt remains almost unchanged for the small fraction of N removed during vesicle formation for each of the samples. So the N excess observed during P of apatites in the present study is likely to be an indigenous component in the sample rather than being the effect of any contamination or fractionation.

5.6 Crustal contamination

Carbonatite melts are presumed to remain unaffected by crustal contamination because of their low temperatures of 600-770°C (Secher and Larson, 1980). Also, as they are derived from a volatile enriched source, they should contain large amounts of noble gases and nitrogen. Thus they should not be significantly affected by crustal contamination. Besides, since they are low viscosity melts their transport through crust is expected to be rapid. The interaction may result in incorporation of crustal xenoliths in the melt by forceful injection, but crustal melt incorporation into the parent carbonatitic melt is not expected. Indeed, Hogenakal carbonatites contain xenoliths of amphibolite and quartzite country rocks (Pandit et al., 2003). The Sevattur carbonatites also contain deformed feldspar grains (derived from country rocks) as well as a number of xenoliths of basement gneisses, syenites and

pyroxenites (Pandit et al., 2003). However there are no reports of the presence of any crustal xenocrysts in these carbonatites.

There are numerous lines of evidences to rule out crustal contamination in mantle samples. Mineralogy and Sr isotopic records can be very useful. In the Sung valley carbonatites the initial $^{87}Sr/^{86}Sr$ and $^{143}Nd/^{144}Nd$ of carbonatites and associated crustal rocks do not show any effect of crustal contamination (Veena et al., 1998; Veena et al., 1991.). However initial $^{87}Sr/^{86}Sr$ variation in alkaline rocks of Ambadongar is consistent with an open system evolution of the complex through assimilation of lower crustal granulite by the parent carbonated silicate magma from which the carbonatites evolved by liquid immiscibility followed by fractional crystallization (Ray et al., 2000).

Trace element abundance and isotopic ratios rule out any crustal contamination for the Hogenakal carbonatites (Pandit et al., 2003). The mantle $\delta^{13}C$ values, positive ε_{Nd} and low $^{87}Sr/^{86}Sr$ characterises their derivation from a depleted mantle source. Some crustal component was identified in the Sevattur carbonatites based on the Pb isotopes, and two component mixing was advocated between the crustal component and the mantle source (Schleicher et al., 1998). The crustal component has been identified to be the subducted Dharwar crust at the source region itself (Pandit et al., 2003) and not a component incorporated during the uprise of the magma. This also accounts for the enriched ^{13}C, higher $^{87}Sr/^{86}Sr$ and negative ε_{Nd} values for Sevattur pointing towards the presence of an enriched mantle source resulting from the recycled Dharwar crust. However, even for the Sevattur carbonatites, crustal contamination during uprise of the magma can be ruled out as major, minor and trace elements are comparable to that of the typical carbonatite (Krishnamurthy, 1988). Also the $\delta^{18}O$ value of ~ 7‰ is typical of pure mantle sources and there are no evidences of progressive crustal contamination as Sr ratios are identical in the early formed pyroxenites as well as the later carbonatites (Kumar and Gopalan, 1991).

5.7 N components

More than one N component in the samples are indicated from the presence of both depleted and enriched N signature during the crushing of the carbonates and apatites. Compelling evidences come from comparison of VC and P results of the apatites discussed above, where VC seems to release the light N component hosted in the vesicles that have not equilibrated completely with the heavy N released from the

lattice of the apatite during P. Also it is clearly seen from Fig. 5.2 that the heavy N component is dominant and constitutes most of the N in the apatites. Therefore it may not always be easy to identify the mantle N component sited in the vesicles as a small contribution from the dominant heavy N component mostly residing in the lattice may dilute its signature even during VC. Contribution of lattice sited gases during VC is not unusual as we have seen from the release of *in situ* noble gases during crushing. However we do see the presence of the lighter component during P for all the samples. During P, the depleted component is clearly identifiable only in case of H-A in the final melting steps. Depleted N signature due to contamination from surficial gases as well as organic contaminants may be a possibility but may be ruled out in the following cases from the observation of light N at a high temperature in H-A, accompanied by mantle $^{40}Ar/^{36}Ar$ ratios. In fact, a comparatively lighter N component has been observed at higher temperature for all the apatites studied. For Hogenakal, the $^{40}Ar/^{36}Ar$ of the melting step accompanied by depleted $\delta^{15}N$ signature is also in agreement with the $^{40}Ar/^{36}Ar$ of the VC that releases light N trapped in the vesicles. Similar evidences of noble gases trapped in fluid inclusions, and released during VC and 1800°C pyrolysis have been observed from some Jwaneng diamonds (Honda et al., 2003). However, it should be mentioned here release of indigenous gases from diamonds will only occur at graphite diamond transition temperature of ≥ 1800°C.

5.7A Recycled nitrogen: a solid inorganic form (?): Crustal contamination has been already ruled out for all the carbonatites studied. For Ambadongar addition of granulite crust can only account for $\delta^{15}N$ value of +2‰. Thus the higher $\delta^{15}N$ value observed from the different complexes reflects addition of a subducted component. In the apatites, the high amount of N released during P also have enriched isotopic signature and can therefore be attributed to subduction. This accounts for the lower $^{40}Ar/^{36}Ar$ ratio and higher $\delta^{15}N$ for P of apatites than VC as subducted component can transport air like Ar and enriched N into the mantle (Staudecher and Allegre, 1988; Mohapatra and Murty, 2000a,b).

The recycled N component that is mainly hosted in the lattice as seen from the P of the apatites has very high $N_2/^{36}Ar$ and $N_2/^{40}Ar$ ratios compared to mantle values that we attribute to some indigenous sample N rather than contamination effect (discussed earlier). Possibility of a subducted component enriched in N is most likely (Basu and Murty, 2002). The low content of ^{36}Ar accompanying the subducted N for all the

samples in Fig. 5.2 has important implication as to the nature of this recycled component. While Ar can only exist in gaseous speciation in mantle, it is not unlikely for the N to be present in some other speciation as well. On the surface of the earth N is present both in organic as well as inorganic forms. Organic N is most commonly present in sediments and sedimentary rocks where they are mostly derived from decay of buried organic material and when exposed to oxygen gets converted to NO_3^-. Another form of N is the NH_4^+ that is present in igneous and metamorphic rocks substituting for K^+ in silicate minerals. In sedimentary rocks also NH_4^+ may be present either adsorbed on mineral surfaces, or substitutes for K. In fact, an excellent correlation has been observed between N and K from metasediments of Schistes Lustres nappe, Western Alps (Busigny et al., 2003). From the same study it has been shown from the constancy of the ratios of fluid mobile elements like K/N, K/Rb and K/Cs that they were retained in the subducting veneer atleast to the depth locus of island arc magmatism. These evidences imply that recycled N may be retained as such for a considerable depth in the mantle in solid speciation without getting converted to other forms.

Presence of crustal fluids as seen from our noble gas studies implies that subduction was restricted to shallow depths of <30 km (see Chapter 4). From existing evidences, it is therefore possible that N was subducted as NH_4^+, most probably in some inorganic form in some silicate minerals substituting for K^+ that was retained till considerable depth and therefore not homogenised with other mantle gases like Ar before being incorporated in the magma source. Thus as seen from Fig. 5.2, the N released during P is accompanied by very little Ar.

5.7B Mantle nitrogen: Presence of a light N component released during VC of apatites as well as during the final crushing steps of the different carbonates and magnetites point towards the presence of mantle gases in the samples. The depleted N signature was preserved in some samples and not in others probably owing to their different magmatic history. Or it may be possible that the light N is very minor in these samples and is easily masked by the dominant recycled component. Thus, it is not always possible to clearly identify the mantle N in all steps of VC or P even if it is present. Release of light N in the final crushing step implies that mantle N is preferentially preserved in the smaller vesicles. No isotopic fractionation process can account for the variation up to 14‰ between the lattice and vesicle sited N in the Hogenakal and Khambamettu apatites. Thus both the N components cannot be related

to fractionation process and represent two components indigenous to the samples. Presence of light N with $\delta^{15}N$ as low as -25‰ has been observed in some peridotitic diamonds from Fuxian, China and attributed to mantle component (Cartigny et al.,1997). Also some geothermal gases sampled in the Hengill area Iceland show $\delta^{15}N$ ranging from -0.5 to -10.5‰ that has been explained by presence of plume derived light N (Marty et al., 1991).

5.8 Mixing plots

Fig. 5.4 is a mixing plot of $N_2/^{36}Ar$ vs. $^{40}Ar/^{36}Ar$ where the mantle, air and recycled end members have been shown. Fig. 5.4A is for the South Indian carbonatites where mantle components involve both UM and LM (based on Ne and Ar systematics as discussed in Chapter 4). Fig 5.4B is for the plume related carbonatites Sung Valley and Ambadongar where Ne, Ar and Xe systematics indicate involvement of air and LM components (also discussed in Chapter 4). From both the plots it is obvious that in addition to the mantle components a subducted component is present in the samples

5.9 $\delta^{15}N$ of LM

Fig. 5.5 is a plot of $\delta^{15}N$ vs. $^{40}Ar/^{36}Ar$. The first panel involves Sung Valley and Ambadongar whereas the second panel is for the South Indian carbonatites. The value of R for the mixing curves is defined as $(^{14}N/^{36}Ar)_{mantle}/(^{14}N/^{36}Ar)_{air/recycled}$. For Ambadongar and Sung Valley previous results clearly indicate the presence of air, recycled and LM components while for the South Indian carbonatites an additional UM component is required. It is obvious from the data points from Fig. 5.5 that the LM component present should have a similar depleted signature of $\delta^{15}N$ ~-5 to -15‰ obtained from the OIBs (Mohapatra,1998). In fact other isotopic signatures of carbonatites share similarities with OIBs suggesting similar sources and processes (Bell and Blenkinsop., 1989; Grunenfelder et al.,1986; Kwon et al.,1989; Nelson et al.,1986). We have independently seen that apatites from Hogenakal and Khambamettu are derived from a LM source. Thus the trapped N depleted gases in their vesicles should also reflect the $\delta^{15}N$ of the LM. Thus in the light of the recent results it may be suggested that the $\delta^{15}N$ value of LM $\leq$ -15‰ and based on $\delta^{15}N$ obtained from H-A, it is most likely that LM $\delta^{15}N \leq$ -22‰ (Basu and Murty, 2003). The value of ~+3‰ obtained from the Kola carbonatites and attributed to LM (Dauphas and Marty, 1999) is erroneous as the authors have considered the N to be a

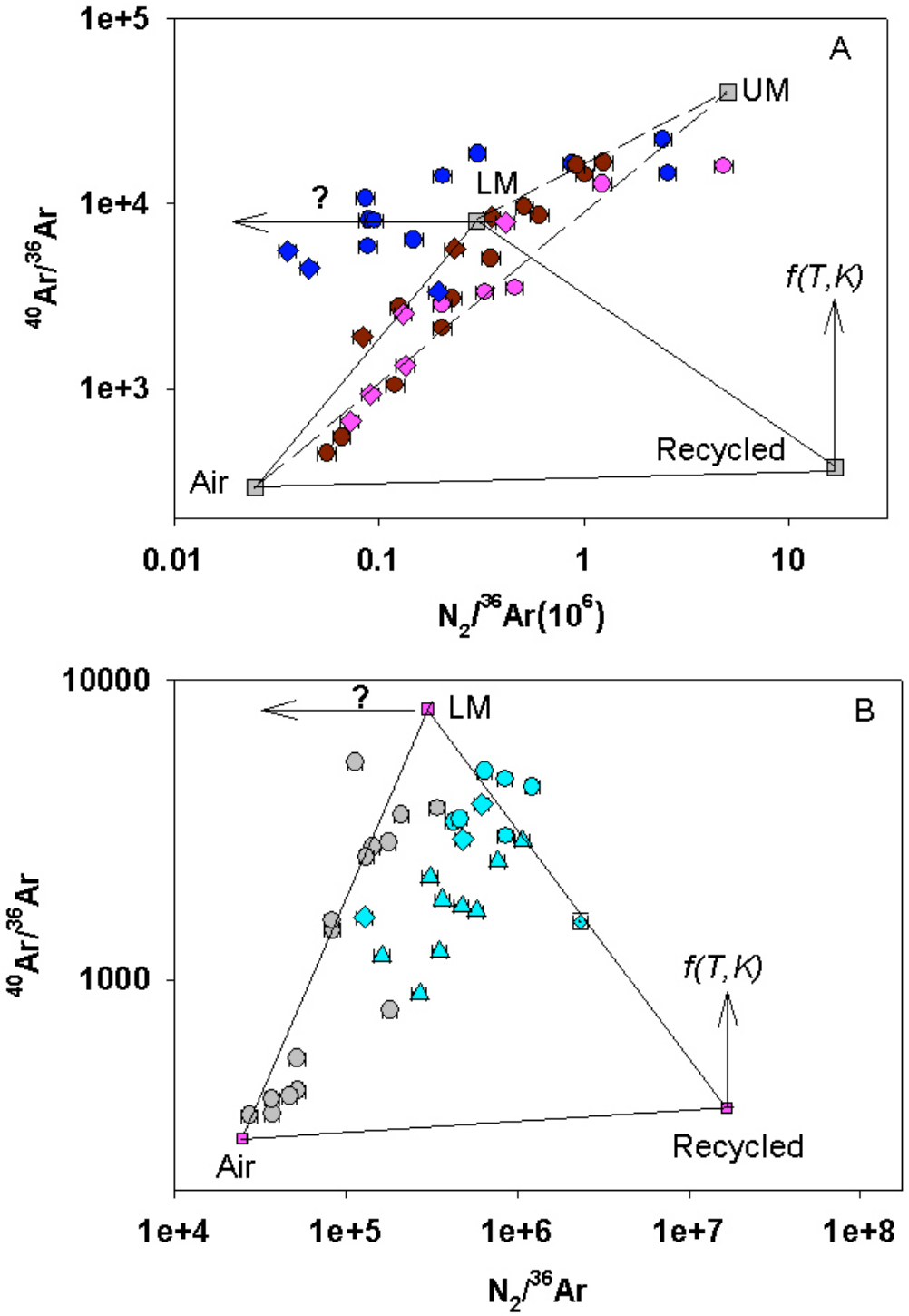

Fig. 5.4 Plot of $N_2/^{36}Ar$ vs. $^{40}Ar/^{36}Ar$ for a)South Indian carbonatites Hogrnakal (blue), Sevattur (brown) and Khambamettu (pink) b)Plume related carbonatites of Sung Valley (cyan) and Ambadongar (grey). Samples represented by circles(carbonates), diamonds(apatites) and triangles(magnetites). Presence of air, LM and recycled components observed in all. In addition, South Indian carbonatites also incorporate some UM volatiles.

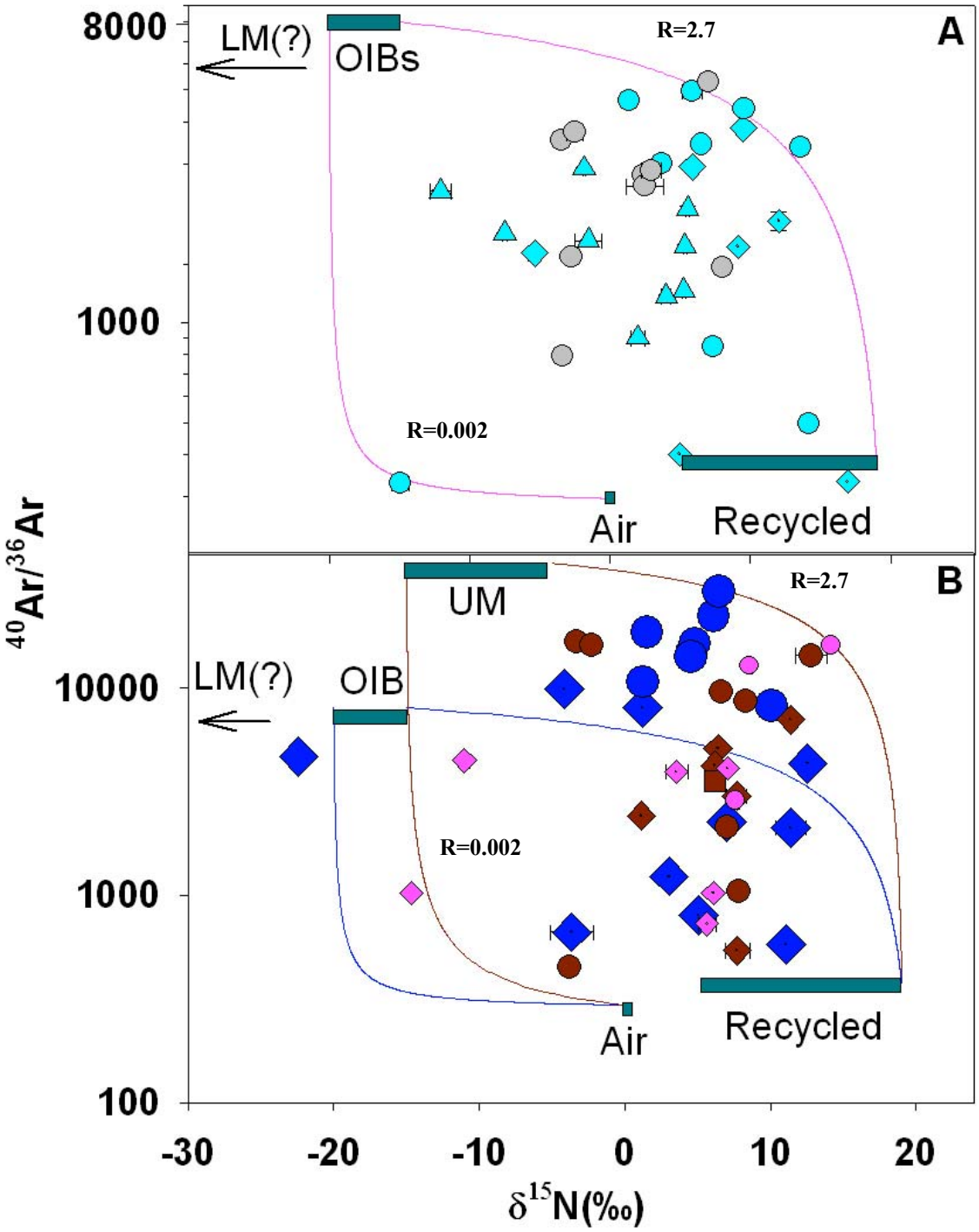

Fig. 5.5 VC and P results for A) Plume related carbonatites B) South Indian carbonatites. Symbols and colours as in Fig. 5.4, symbols with a dot in the centre represent P results. Value of R indicated against mixing trends. For discussion see text.

single LM component. A realistic possibility is that the Kola carbonatites have an overwhelming contribution to N from recycled component having $\delta^{15}N \geq 15‰$.

5.10 Secular changes in N and Ar, isotopic and elemental ratios in the mantle

Since the carbonatites studied cover a range of ages from 2400Ma (Hogenakal) to 65Ma (Ambadongar), they might provide a window to the continental mantle to study any temporal variation of N and Ar for both isotopic and elemental ratios. For example, if recycling of N into the mantle is considerable, both $N_2/^{36}Ar$ as well the $\delta^{15}N$ values should show an enhancement with time. Also, significant magma degassing with time should be reflected in increasing $\delta^{15}N$ values. However, as seen from Fig. 5.6 where only trapped gases in the vesicles have been considered, no systematic changes with sample ages for either of these parameters are observed.

The $^{40}Ar/^{36}Ar$ value of ~40000 for UM and ~8000 for LM has been constrained from the study of the oceanic basalts that are <200 Ma years old. The constrained $^{40}Ar/^{36}Ar$ end member value should hold good for the younger carbonatites of Sung Valley (107 Ma) and Ambadongar (65 Ma). However, for the considerably older carbonatites of Hogenakal (2400 Ma), Sevattur (770 Ma) and Khambamettu (523 Ma), the end member $^{40}Ar/^{36}Ar$ ratio will not hold true as ^{40}Ar is produced from the decay of ^{40}K and must be a function of time. Such an evolution of $^{40}Ar/^{36}Ar$ ratio with time has been constrained by Sarda et al., (1985).

The equation for average mantle Ar isotopic composition at time t is (Porcelli and Ballentine, 2002)

$$(^{40}Ar/^{36}Ar)_m = \{\lambda_{40}/(\alpha-\lambda_{40})\} * \{e^{(\alpha-\lambda 40)t}-1\} * \{(y^{40}K_m e^{\lambda 40t})/^{36}Ar_{m0}\}$$

where

K = 270 ppm (BSE)

α = $1.82*10^{-10}$ (degassing constant)

y = 0.1048 (yield for ^{40}Ar)

$\lambda_{40} = 5.543*10^{-10}a^{-1}$ (decay rate of ^{40}K)

$^{36}Ar_{m0} = {}^{36}Ar_{atm}/(1-e^{-\alpha t})$ ($^{36}Ar_{m0}$ is the initial concentration of ^{36}Ar in the mantle, $^{36}Ar_{atm}$ is the concentration in the atmosphere after mantle degassing

For early catastrophic degassing, $^{36}Ar_{m0} = (1-f)\ ^{36}Ar_{m0}$ where f is the fraction of the ^{36}Ar removed from the mantle into the atmosphere and has been estimated to be ~99% (Javoy, 1997), an effect likely to be more pronounced in the UM.

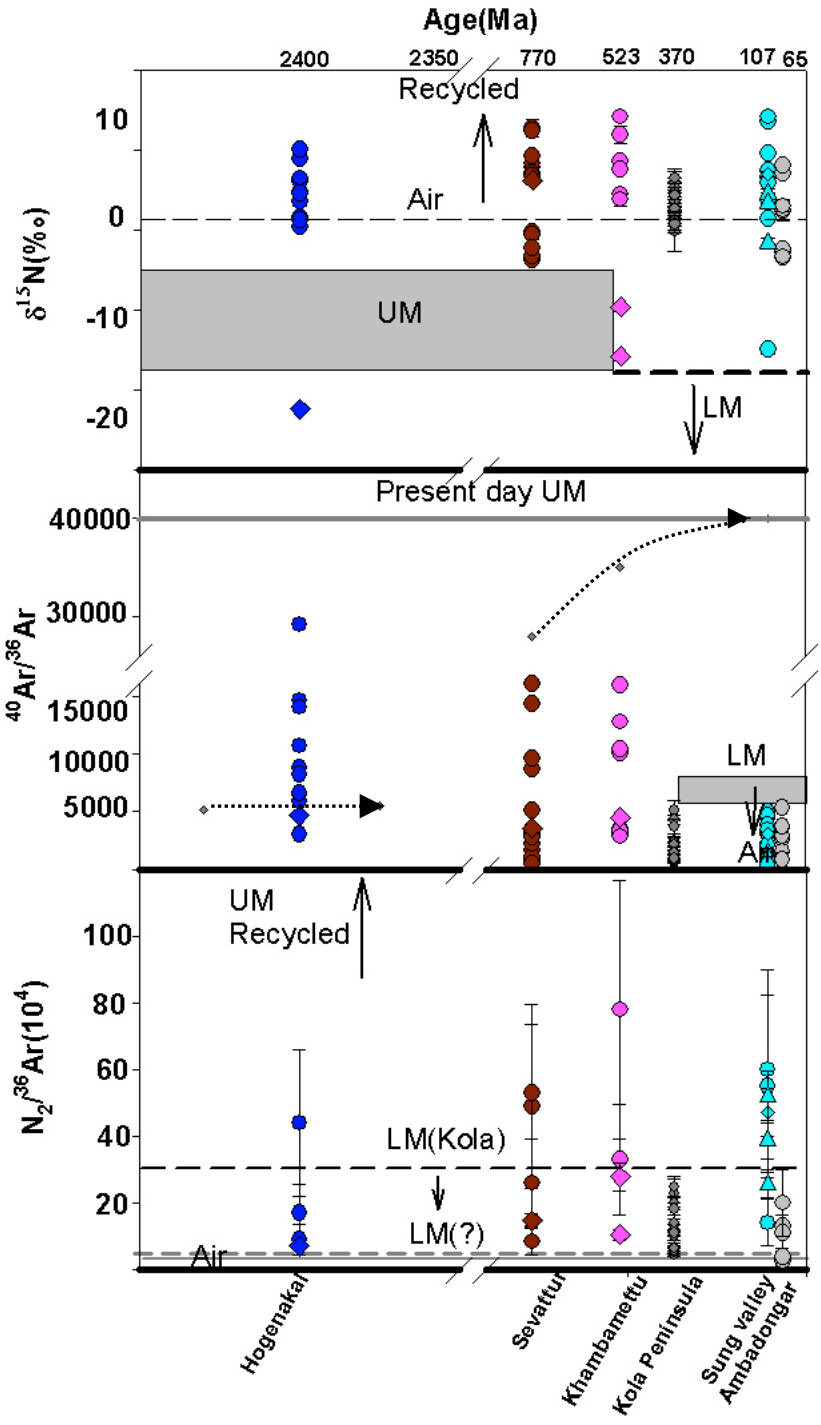

Fig.5.6. Plot of $\delta^{15}N$, $^{40}Ar/^{36}Ar$ and $N_2/^{36}Ar$ of samples from carbonatite complexes of different ages. The X-axis represented by the sample locations denote decreasing age from Hogenakal(2400 Ma) to Ambadongar(65 Ma). Data from Kola carbonatites(370 Ma) also plotted (Dauphas and marty., 1999). In second panel dotted arrow represents mantle evolution of $^{40}Ar/^{36}Ar$ (see text for details). However no systematic elemental or isotopic variation with age is observed. Colour representation and symbols same as previous figures

The evolutionary curve for $^{40}Ar/^{36}Ar$ in the Earth is shown in Fig. 5.6. The assumption is that of the simplest case of atmosphere formation by unidirectional degassing from a single solid Earth reservoir. It is also assumed that the mantle is well mixed and has been melted and degassed at a constant rate at the MORB source without any return flux from the atmosphere by subduction. From the above calculations as represented by the evolutionary curve, the $^{40}Ar/^{36}Ar$ ratio for the Khambamettu and Sevattur carbonatite sources should have evolved to ~35000 and ~29000 respectively, well in the range of UM. However Hogenakal, the end member $^{40}Ar/^{36}Ar$ ratio of the source should have evolved only to ~5000. However, the highest $^{40}Ar/^{36}Ar$ ratio observed from the present study is ~29000(HC-1A). In fact, for all the carbonates analysed, the measured $^{40}Ar/^{36}Ar$ ratio is >10000. This could be due to these two possibilities:

- Ingrowth of *in situ* ^{40}Ar produced in the samples from K after their crystallisation. However the measured K content in the samples is in the range of 18-30 ppm and therefore, cannot account for substantial ^{40}Ar production in the samples.
- Incorporation of ^{40}Ar from crustal fluids. This may be due to the residence time of some ancient subducted crust in the mantle. However, since the age of the carbonatite is considerable, the time elapsed before incorporation of such a subducted component into the source of the carbonatitic magma would be insufficient to account for all the excess ^{40}Ar. Crustal contamination during uprise has already been ruled out (see section 5.6). Also because Hogenakal carbonatite intrudes into the crust that is only 150 Ma (Kumar et al., 1998), it cannot account for sufficient ^{40}Ar from decay of K.

In view of the inability of the above mechanisms to account for the high $^{40}Ar/^{36}Ar$ ratio of the Hogenakal, the other possibilities could be loss of a greater fraction of ^{36}Ar during degassing. The $^{40}Ar/^{36}Ar$ ratio is very sensitive to degassing and loss of 99.75% of ^{36}Ar (instead of the generally accepted 98.6%) can explain the high $^{40}Ar/^{36}Ar$ ratio of Hogenakal. However, in that case the expected $^{40}Ar/^{36}Ar$ value far exceeds the well constrained present value of UM. An alternative could be loss of 99.75% of ^{36}Ar during early degassing but its gradual build up by subduction progressively. Indeed recycling of Ar into the deep mantle has already been proposed. The aspect of gradual addition of ^{36}Ar into the mantle needs to be investigated carefully. It may also be possible that the rate of degassing reflected in the degassing

constant (α) was much higher than $1.82*10^{-10}$ and could have been as high as ~$9.2*10^{-10}$. This also implies that the present day $^{40}Ar/^{36}Ar$ ratio is >40000 inferred from MORBs for the UM. Indeed values of $^{40}Ar/^{36}Ar$ much greater than the generally accepted ratio of ~28000, as high as 400000 have been suggested by some authors (Burnard et al., 1997).

5.11 Summary

Volatiles in carbonatites are multi-component mixtures with contributions from air, mantle and recycled gases. However due to very limited equilibration between the melt and the vesicles, and between the earlier and later formed vesicles, the depleted signature of mantle gases are preserved in some apatites and in some smaller vesicles of some carbonates as well. This is possibly due to very short duration of exchange between the melt to which the subducted component was added at a late stage only at a shallow depth, and earlier formed vesicles hosting trapped gases. Homogenisation between the inorganic N from the crustal fluid and air containing subducting slab and the gaseous mantle N was also incomplete. As a result both recycled as well as pristine N retained to some extent their original signatures. It was possible to identify a depleted N signature of ≤-15‰, possibly as low as ≤-22‰ in the LM from our study, which is very close to the pristine N of the E-chondritic building blocks.

The magmatic model that can be inferred from the N and Ar study of carbonatites is in agreement with that predicted from their noble gas study. The apatites are all derived from a LM magma source. Preservation of their mantle signatures in the vesicles imply disequilibrium between the melt and the vesicles possibly due to short interaction time between the inclusions and the melt after introduction of the subducted component. This is possible if subducted N component is introduced at a shallower depth probably as inorganic NH_4^+ (substituting for K^+) and is not able to completely homogenize with the gaseous component present. Introduction of subducted component can account for the presence of crustal fluids as seen from the excess ^{4}He, ^{40}Ar, $^{21,22}Ne$ and $^{131\text{-}136}Xe$ in the samples. Introduction of such a recycled slab into the mantle may as well change the $^{40}Ar/^{36}Ar$ ratios of the magma depending on the residence time of the slab in the mantle region as well as its K content. In the present study for all the samples it is evident from the P of the apatites that introduction of the recycled component into the mantle lowers the Ar ratios closer to air like values. In Sevattur and Sung Valley, probably because of longer duration of

interaction between vesicles and the residual melt to which the recycled component was added, the equilibration between the two was to a greater extent. This explains why the pristine signatures in the apatites from these carbonatites were less preserved. However the smallest vesicles which were last formed still retained the depleted mantle signatures because their equilibration time with the melt was the least. This is true for all the complexes where the smallest vesicles, even in carbonates and magnetites are able to retain part of their mantle signatures. In the South Indian carbonatites, while the apatites were able to preserve their mantle signature in the vesicles, carbonates were not. This may be due to their derivation from a second batch of magma where the vesicles equilibrated more with the melt to which the subducted component has been added.

Chapter 6

Implications of the present study

6.1 Introduction

The present study of noble gases and nitrogen on some carbonatites of India has some implications on the petrogenetic models for these rocks. The study also has some implication on the N budget in the mantle. Both these aspects are discussed briefly in this chapter in the subsequent sections. Also there is a brief discussion on the futuristic aspects of the present thesis.

6.2 Petrogenetic models

Most carbonatites world over are rift related. Impacting plume heads carrying excess heat may contribute to lithospheric thinning, delamination, rifting and magmatism. Noble gases from the present study suggest the presence of LM volatiles in the Sung valley carbonatites. Earlier, Sr-Nd-Pb isotopic ratios of Sung valley (Veena et al., 1998; Ray et al., 2000) have indicated a plume origin for these carbonatites. Such HIMU-EM-I signatures have also been reported from the East African carbonatites (Bell and Tilton, 2001). Like the east African carbonatites, in the present case also the source of the LM volatiles can be the D" layer at the core-mantle boundary. Migration of volatiles during plume ascent and their interaction with either HIMU or EMI components can explain all the isotopic signatures observed in the Sung valley carbonatites. From Sr and Nd isotopic results, no DMM component is reported from these rocks, in agreement with the noble gas isotopic ratios that do not indicate any UM volatiles to be present in the samples. This also seems to suggest that both the HIMU and EMI components originate in the LM as postulated for the African carbonatites, in the deep lower 1000 km or possibly near the core-mantle boundary (Bell and Tilton, 2001).

For the Ambadongar carbonatites, initial $^{87}Sr/^{86}Sr$, $^{143}Nd/^{144}Nd$ and Pb isotopic ratios are explained by mixing of three distinct mantle components- namely the Reunion plume, continental lithosphere and asthenosphere (Indian MORB-like) (Simonetti et al., 1998). Our noble gas data also show the presence of LM volatiles, indicating presence of a plume component in the samples. However presence of UM volatiles

(from MORB asthenosphere and lithosphere) in the samples cannot be entirely ruled out. Experimental results in the past have indicated that entrainment of ambient mantle during ascent of thermal plumes is possible because of coupling between heat conduction and laminar stirring driven by plume motion (Griffiths and Campbell, 1990). From the noble gas results of the present study, it is obvious that even if UM volatiles are present in the samples they must be insignificant. It has been proposed that input from the Reunion plume and lithospheric component varied with progressive stages with input from the plume being dominant in the early stages. In the later stages with increased heating of the lithosphere and its consequent thinning resulted in higher degrees of partial melting and more input from the lithospheric component (Simonetti et al., 1998). Thus the Ambadongar carbonatites must have been related to the early stages of the Reunion plume. Another strong possibility is that while the Sr and Nd are derived from different sources reflecting more than one kind of mantle component, the volatile elements are derived from a common source in the LM. Presence of such primitive volatiles from the deep mantle but quite different Sr and Nd isotopic signatures reflecting both enriched and depleted sources have also been observed from the Brazilian and Canadian carbonatites (Sasada et al., 1998).

Both Sung valley and Ambadongar carbonatites, as well as those from Brazil and Canada are related to flood basalt provinces temporally and spatially. Generation of melts by different degrees of partial melting of plume volumes characterized by localized CO_2/H_2O ratios has been proposed to explain this association in these provinces (Bell, 2002). This model attributes that generation of melt in response to plume ascent is essentially within the plume itself. This is in agreement with the presence of LM volatiles that we observe from our studies without the involvement of the lithospheric mantle in this process of melt generation. The model favours the role of lithosphere only to concentrate the volatile rich fluids or melts as well as the large-ion-lithophile-elements incorporated into an upwelling plume head. Presence of crustal fluids in the Sung valley and Ambadongar carbonatites can be explained by interaction with subducted crustal material and other fluids during the ascent of the plumes. Late stage low temperature hydrothermal activity and resulting ^{18}O depleted signatures (Viladkar and Schidlowski, 2000) accounts for the air like Ar ratios in the ferrocarbonatites.

The carbonatitic complexes of Hogenakal and Sevattur in Southern India are emplaced within the Precambrian granulite terrain (Subramanian et al., 1978;

Viladkar and Subramanian, 1995) and are believed to be asssociated with the Precambrian magmatism within the Eastern Ghat Mobile Belt (EGMB) of eastern and southern India (Schleicher et al., 1998). No plume associations are as yet reported for them. Our noble gas data for these carbonatites are different from the plume related Sung Valley and Ambadongar carbonatites discussed earlier and do not suggest the presence of any plume component in these rocks. From their Sr and Nd isotopic results, their evolution from a lithospheric mantle source has been suggested (Kumar et al., 1998). While the Sevattur carbonatites are believed to be derived from an enriched source (EM-I type), (Kumar et al., 1998; Pandit et al., 2002), the source for the Hogenakal cabonatites has been advocated to be enriched by Kumar et al.,(1998) but depleted by Pandit et al.,(2002). Our noble gas data are identical in all the South Indian carbonatites and consistent with their derivation from the lithospheric mantle region with UM Ar isotopic ratios. However presence of primitive volatiles reflected by $^{129}Xe/^{132}Xe$ ratios in the samples suggests the involvement of asthenospheric MORB like sources for the volatiles, while Sr and Nd may have been derived from the lithospheric mantle. But the apatites in these carbonatites seem to trap volatiles from the LM and more than one pulse of magma injections is suggested.

To summarize the main implications from this study in terms of the genesis of carbonatites are:

- Carbonatites trap volatiles from the LM. Like that of some African carbonatites, even the core-mantle boundary may be the source of such primitive volatiles present in the carbonatites from Sung valley and Ambadongar.
- However all carbonatites may not be plume related and may trap volatiles from other sources as well. From our present study, it is observed that the South Indian carbonatites trap volatiles from the UM.
- Mineral phases like apatites present in these South Indian carbonatites are related to the LM implying more than a single pulse of magma generation for these rocks.

6.3 Lower mantle $\delta^{15}N$ and its implications

One of the main objectives of the present thesis is to constrain the $\delta^{15}N$ of the LM. So far the only available value for $\delta^{15}N$ of the LM was constrained to be $\approx$+3‰ from the study of Kola carbonatites (Dauphas and Marty, 1999) by VC. However assigning this

value to the LM end member may be erroneous as seen from the following discussion. The Kola carbonatites show a range in $\delta^{15}N$ values from -0.2±2.5‰ to 6.5±1.2‰ while the accompanying $^{40}Ar/^{36}Ar$ ratios vary from 532±51 to 5103±899. A careful inspection of the data reveals that the range of $\delta^{15}N$ values is unexplainable simply as a two component mixing between air and mantle gases in varying proportions as assumed by Dauphas and Marty (1999). For example, the $\delta^{15}N$ value of 5.3±1.1‰ for a calcitic carbonatite and 6.5±1.2‰ for a dolomitic carbonatite, both from Seblyavr complex, Kola are accompanied by $^{40}Ar/^{36}Ar$ ratios of 532±51 and 745±89 respectively. On the other hand, from the same complex lower $\delta^{15}N$ values of -0.2±2.5‰ of the pyroxenite and 1.1±1.2‰ from the apatite-diopside-phlogopite have higher $^{40}Ar/^{36}Ar$ ratios of 1485±201and 1456±132 respectively. The only explanation for such a trend could be addition of recycled component to mantle volatiles that shifts the mantle N towards more positive $\delta^{15}N$ but lowers the $^{40}Ar/^{36}Ar$ ratio of the mantle by introducing air like Ar into the magma via the subducting slab. In fact, the authors identify the presence of three components, namely mantle, air/air-saturated-water and sediments in the samples from the plot of $\delta^{15}N$ vs. $^{40}Ar/^{36}Ar$. Thus from the $\delta^{15}N$ and $^{40}Ar/^{36}Ar$ trend of the Kola carbonatites it is evident that the value of ≈ +3‰ advocated to the LM $\delta^{15}N$ simply reflects addition of a recycled component to the mantle and $\delta^{15}N$ of the mantle must be lower than +3‰.

From the present study it was possible to constrain the $\delta^{15}N$ of the LM to be <-15.9±0.3‰. But this value could be as low as -22.4±0.3‰ if we consider the lightest N found in the apatite of Hogenakal as the real end member. This fits well with the evolutionary model of N as well as agrees with values as low as ≈-25‰ in Fuxian diamonds (Cartigny et al., 1997). The $\delta^{15}N$ of the UM has been constrained to be (-5 to -15)‰ (Marty and Humbert, 1997; Mohapatra and Murty, 2004).Since the deep LM is supposedly less degassed than the UM as suggested from noble gases, it is not unreasonable to expect a $\delta^{15}N$ value < -15‰ in the LM. The value of $\delta^{15}N$ <-15.9±0.3‰ for the LM from the present study fits well into the evolutionary history of N in the Earth as will be subsequently discussed.

The present estimate of N varies between 1-3 ppm for UM from $N_2/^{36}Ar$ and $^{40}Ar/^{36}Ar$ covariations in the MORBs (Marty, 1995). However such a covariation termed a 'good correlation' has been recently questioned (Mohapatra and Murty, 2004). Some

other estimates of N propose the value to be 2 ppm. For diamond source that can be as high as 36 ppm if N is compatible in the mantle (Cartigny et al., 2001a). These estimates are very sensitive to the assumed $\delta^{15}N$ value of the mantle, and with better constraints of $\delta^{15}N$ available now for both UM and LM, the N content in the mantle should be reevaluated. From the results obtained in this study and using the existing model of terrestrial N evolution (Javoy, 1997; Tolstikhin and Marty, 1998; Javoy, 1999) an approximate N budget of the LM has been estimated.

The evolutionary model for terrestrial N consists of the following major steps (Fig. 6.1):

- Initial phase of accretion of the Earth from building materials that are generally considered to be the reducing E-chondrites. This choice is basically based on their remarkable identity to the Earth in terms of stable isotopes. In fact, for O isotopic composition an exact identity is seen (Javoy and Pineau, 1983). During accretion, impact degassing is believed to have released ~95% of the initial rare gases present, but release of N must have been less efficient due to prevailing reducing conditions.
- The major phase of accretion was followed by metallic core segregation when the migrating metallic blobs reach a reasonable size and reequilibration with mantle silicates is therefore impeded. The noble gas amount in the core is difficult to estimate due to the fact that partitioning of elements between metal and silicate is poorly constrained. However since N is a siderophile element, it must have been considerably sequestered into the core during this process. But since core formation was an equilibrium process at higher temperature, it should not significantly affect the isotopic composition.
- After the major phase of accretion and core formation the mantle or part of it was partially melted by impacts/giant impact leading to degassing and loss of N along with other volatiles. This must have left the residual N in the mantle isotopically fractionated, making it heavier with respect to the starting composition of ~-35‰. Although >90% of noble gases are estimated to have been lost in the process of degassing from the UM, since the solubility of N in silicate melts would be higher under prevailing reducing conditions, it may not have been lost to that extent. Also model calculations generally suppose that only the upper 400 km of the mantle has been affected by processes like

magma degassing and therefore it is not too unreasonable to consider that the LM, or atleast a portion of it may not have been affected significantly. Some recent estimates suggest a ~50% retention of N in the mantle after degassing.

- ✶ The Earth's evolution was concluded by a final stage of addition of a late veneer. This is necessitated by the absence of expected fractionated pattern as well as presence of high content of siderophile elements like Ir, Pt, Au etc in the mantle. However the estimated mass of the veneer is only 0.75% of the mantle's mass and should not affect its volatile budget significantly as most of their volatiles are already degassed into the atmospheric reservoir.

From analogue with E-chondrites the initial N content of the Earth must be ~300 ppm while the initial $\delta^{15}N$ is~-35‰. However the surficial terrestrial reservoirs can only account for 1 ppm. This raises the possibility that N has been lost from the system by hydrodynamic escape, and/or sequestered in the core and/or locked up in the mantle. From simple mass balance calculations if N is sequestered into the core,

$f_mN_m+f_cN_c = 300$ where f_m and f_c are the mass fractions of accreted mass of core and mantle, while N_c and N_m represents the concentrations of N in the core and mantle respectively. A close analogue of the mantle and the core are the pallasites for which the $N_c/N_m \sim 8.3$ has been estimated (Prombo and Clayton., 1993). The core constitutes 32.54% by mass of the total Earth, while the mantle makes upto 67% of it (Javoy, 1999). Accordingly, the N in the mantle may be estimated to be ~ 80 ppm. Both the concentration as well as isotopic ratios of mantle N may be modified by present day processes like degassing during magmatism and subduction. But mass balance flux of N indicates that global outgassing flux is much lower than the subducting flux, so the resulting effect would be addition of enriched N into the mantle. This would further increase the N concentration in the mantle. Recently there are several evidences of recycling of N into the deep mantle (Sano et al., 2001; Busigny et al., 2000). The Kola carbonatites also indicate that subducted N may penetrate up to LM depths (Dauphas and Marty, 1999). Also outgassing fluxes from hot spots that sample the deep regions of the mantle are considerably lower than the MORBs, island arcs or back arc basins (Sano et al., 2001). Therefore degassing form LM can be considered negligible. In the present study, presence of pristine N has been clearly identified in the LM (Chapter 5) from the carbonatites of Sung Valley and Ambadongar, as well as the apatites of South India. This is an attempt to estimate the LM N that may be present in these

samples, and therefore in their source LM itself from simple mass balance calculations.

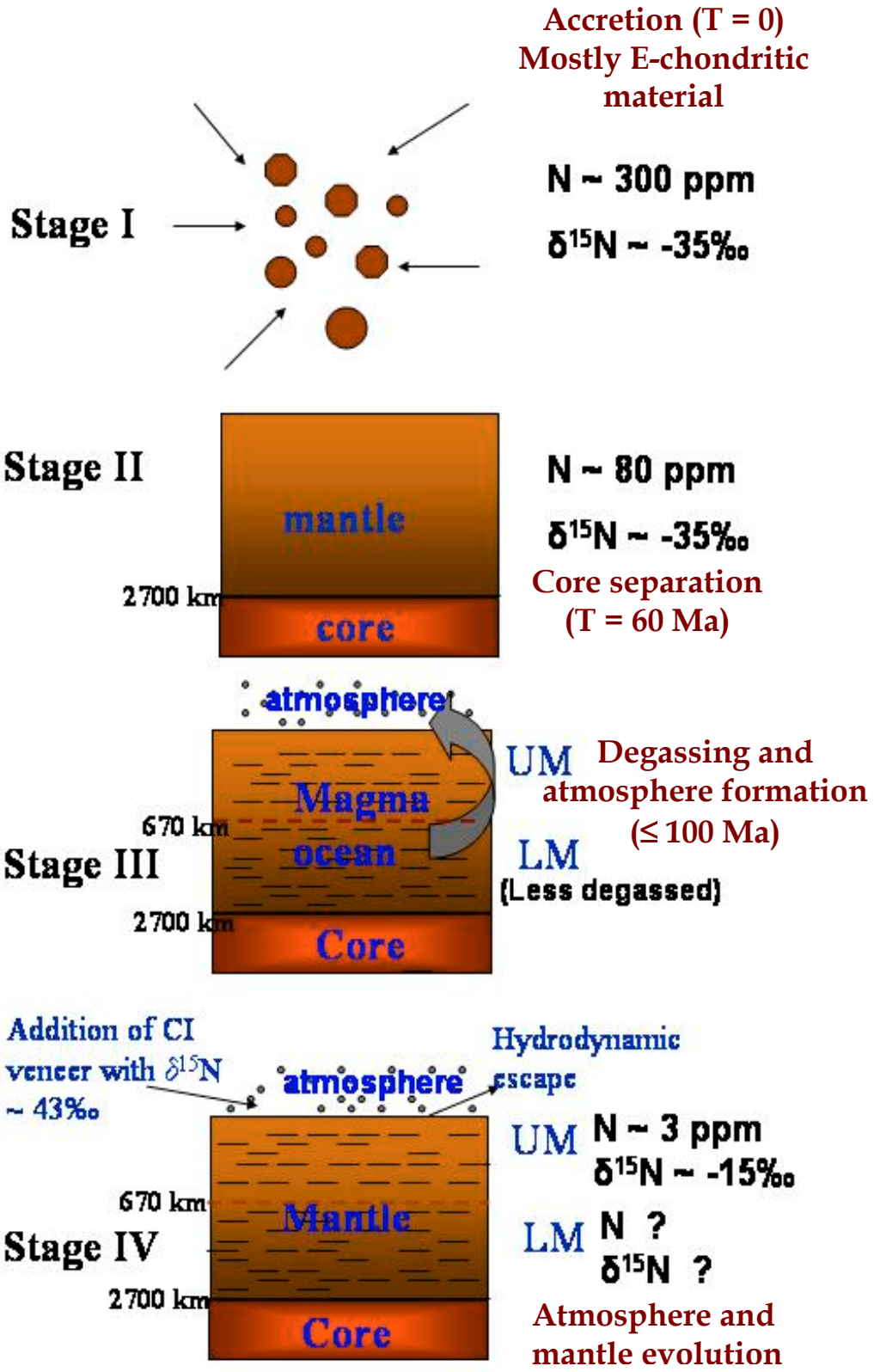

Fig. 6.1 Evolution of terrestrial N (modified after Mohapatra, 1998).

Following the discussion in chapter 5, based on combined N, Ar isotopic systematics, the N in the samples can be considered a mixture of three components namely air(A), recycled(R) and mantle(M). Simple mass balance calculations using the equations given below can yield the proportion of each component in the samples:

$A + M + R = 1$

$\delta^{15}N_{sample} = \delta^{15}N_{air}A + \delta^{15}N_{mantle}M + \delta^{15}N_{recycled}R$

$(^{40}Ar/^{36}Ar)_{sample} = (^{40}Ar/^{36}Ar)_{air}A + (^{40}Ar/^{36}Ar)_{mantle}M + (^{40}Ar/^{36}Ar)_{recycled}R$

The present study has clearly shown that addition of crustal fluids that are carried by the subducting slab has been added to the mantle source at very shallow depth, probably < 30 km so as to retain their typical noble gas signatures, even for the lighter isotopes like ^{4}He. Also from the study it is evident that N in the mantle may not exist as a homogeneous gaseous component. Clear identification of an inorganic form of subducted N that retains its signature at shallow depths has been seen. From the absence of complete homogenization between the different components in the samples, it is not very unexpected that pristine signatures of trapped gases have been retained to some extent in some of the fluid inclusions and modified depending on equilibration between inclusions hosting the primordial trapped fluids and melt bearing subducted crustal component. Preservation of such heterogeneous fluid inclusions have been seen from the study of both apatites and calcites from carbonatites of Ambadongar (William-Jones and Palmer, 2002). For most of the samples studied, the recycled component is the dominant constituent, and thus it is difficult to estimate the proportion of any mantle gases, even if present in them. Only for a few samples where a measurable proportion of the gas present can be from the mantle has been listed in Table 6.1. For samples like H-A, K-A1 and K-A2 where pristine signatures have been preserved as seen from their VC, it is the mantle component that is dominantly released during VC and therefore estimating the other components namely recycled and air that may be present are difficult. For practical purposes, all the N released from these samples during VC (60-140 ppb), can be considered to be mainly from the mantle itself. From Table 6.1, an estimate of N in the LM is ~0.7 ppm. A similar exercise for the carbonates from South India that are derived from an UM source also yields the various proportions of mantle, recycled and air components in the samples and are listed in Table 6.1. This gives an estimate

of N in the UM to be ~0.4 ppm. This is considerably lower than the existing estimate of ~3 ppm for UM. Therefore the N content of 0.7 ppm derived for LM in the present case is only a lower limit.

Considerable volatiles must have been lost from the systems during magma evolution. Since the range of mantle N content for both UM and LM samples are identical, assuming that the magmatic process involved in the generation of the carbonatites in all the settings are grossly similar, the LM N content should also be ~3 ppm. The value can be higher as the ascent time and distance was much more for the LM carbonatites. Considerable loss of volatiles by the process of vesciculation has been identified for both MORB and plume samples (Moreira and Sarda, 2000). In fact, the loss for Ar in plume samples is about 87% where the vesciculation occurs in an open system and leaves the magma shortly after their generation. Since N and Ar, both behave identically, the loss for N from the system should have also been considerable. Accordingly, correcting the total N for 87% loss from the sample, the mantle N has been re-estimated for all the samples and tabulated in Table 6.1. The highest value of N for the UM obtained from H-C1A is ~3 ppm in agreement with the expected value. From the Ambadongar and Sung Valley carbonatites, at least 5 ppm of N is expected in the LM.

Preservation of pristine signatures from homogenisation by mantle convection is possible even in the UM as seen from $\delta^{15}N$ values. Residual $\delta^{15}N$ isolated from convection may be preserved in portions of sublithospheric mantle below continental blocks (Cartigny et al., 1997). In LM it has been proposed that a layer of material which is intrinsically about 4% denser than the overlying mantle is dynamically stable and advocated as the D" layer (Kellogg et al., 1999). Plumes from such a layer isolated from mantle convection may contain primordial gases in them. Thermal constraints have also shown that primitive material may exist as blobs in the LM which persist in convective cells because of their high viscosity and are therefore not deformed or mixed with the surrounding flow (Becker et al., 1999). Another possibility is that of addition of outer core material bearing pristine volatiles like N that got segregated into it during core formation to the D" layer and subsequent upwelling of the mixtures as plumes (Brandon et al., 1998).

The $N_2/^{36}Ar$ estimate of ~3 x 10^5 for the LM by Dauphas and Marty (1999) should be an upper limit as it also involves substantial contribution from recycled component.

The measured value of $N_2/^{36}Ar$ for H-A which preserves very pristine $\delta^{15}N$ signature is 0.7 x 10^5 should be a closer representative of the LM ratio. K-A1 and K-A2 also preserves some of the pristine N as indicated from $\delta^{15}N$ values. The $N_2/^{36}Ar$ ratios for these two samples are 1.1 x 10^5 and 2.8 x 10^5 respectively. The values are definitely lower than ~50 x10^5 constrained for that of the UM (Dauphas and Marty., 1999). This may be due to the fact that LM is less degassed than the UM. Another probability could be that UM is more influenced by recycled component than the LM. It is more likely that a combination of both these effects come into play as reflected by the $\delta^{15}N$ ratio of~ -20‰ likely for LM as seen from the present study, while that for the UM is ~-15‰ (Mohapatra and Murty, 2004).

Table 6.1. Proportion of recycled (R), mantle(M) and air(A)components in carbonates and magnetites from different carbonatites. The N content in the mantle source has been calculated from M derived

Name of sample	R	M	A	N_{mantle} (ppb)	$N_{corr}^{\bullet}$ (ppm)
SV-M3	0.46	0.16	0.38	81.5	0.6
SV-M1A	0.41	0.18	0.41	95.4	0.7
SV-M1B	0.03	0.14	0.83	58.9	0.4
AC-2	0.51	0.23	0.26	495.4	4
AC-6	0.09	0.27	0.65	158.2	1
H-C1A	0.58	0.27	0.15	406.0	3
H-C4	0.72	0.26	0.02	97.2	0.7
SE-C5	0.58	0.22	0.20	96.1	0.7
SE-C7	0.68	0.16	0.16	157.0	1
K-C3	0.66	0.10	0.24	95.3	0.7
K-A2*	0.68	0.26	0.06	681	5

*Only sample for which P analysis has been considered to estimate N in mantle. For all other P analyses of apatites, the recycled component is so dominant that mantle gases are difficult to identify. $N_{corr}^{\bullet}$ refers to N content in mantle after correcting the samples for 87% loss of N from the system.

6.4 Future aspects

- There is immense possibility of loss of volatiles from any magmatic system by degassing. This should apply for carbonatitic melt as well. This might be a closed system process when the vesicles are created in equilibrium with the magma and

then subsequently lost during its residence time in the mantle. This is essentially a solubility controlled process where $(He/N) = (He/N)_0(S_{He}/S_N)$ where S_{He}/S_N is the ratio of the solubilities of the two elements and $(He/N)_0$ represents the initial elemental ratio. From He/N measured in the samples that will represent the composition of the final residual melt, the $(He/N)_0$ may be estimated. Since He fluxes from the MORBs and plumes are well documented, accordingly an estimate for N may be made. If degassing is in an open system it can be modeled by Rayleigh distillation law where $(N/He)_{magma} = (N/He)_0 g^{(1-\alpha)}$, where $g=(N/N_0)$ that is the fraction of N remaining in the melt after degassing, and α represents the ratio of their solubilities. To an approximation, $(N/He)_{magma}$ may be represented by the matrix composition of the samples while $(N/He)_0$ may be obtained from the study of the vesicles. The N_0 can be accordingly calculated. In the present study this modeling was impeded due to lack of enough He numbers, and more important because it was seen that the matrix was dominated by a N component that has not homogenized completely with the mantle volatiles. Study along this line would be very useful to obtain the upper limit of LM content of N, as in the present study only a lower limit could be given. Also, in this respect it will be required to initially model the degassing process, open or closed, using suitable volatile elemental ratios (Moreira and Sarda 2000; Cartigny et al., 2001b).

Study of vesicularity in the samples may also be very useful to obtain the initial N content(N_0) of the magma as Rayleigh distillation predicts $(N_{melt}/N_0) = [(\rho S_i T_c/T_0)/(V^*+\rho S_i T_c/T_0)]$. Here N_{melt} is represented by the N content in the sample, ρ represents the melt density, in this case that of the carbonatitic melt, V* represents the vescicularity and T_c and T_0 stand for the closure and standard temperatures respectively.

- One of the debatable questions about carbonatites is the huge amount of C present in these rocks in several per cent level while that in the mantle occurs in trace quantities. Many experts advocate a recycled source for the C (Ray et al., 1999) while others believe it to be primordial from mantle (Sasada et al., 1998). The carbonatites in the present study suggest addition of subducted N only at a late stage that may not have completely homogenized with the source mantle volatiles. But carbonatites from Kola document a well mixed source with a homogenized recycled N component. In such carbonatites where recycled and mantle gases are

well mixed, a conjugate $\delta^{13}C$-$\delta^{15}N$ study may provide some light to the source of the C, recycled or otherwise. Such a coupled study was used to rule out subduction related processes for diamond formation for many samples of different locations (Cartigny et al., 1998). In case of subducted (biogenic) origin of C in the mantle, very light $\delta^{13}C$ value should be associated with positive $\delta^{15}N$. Absence of such association as seen in the case of diamonds (Cartigny et al., 1998) where the associated $\delta^{15}N$ values are negative imply either high temperature isotopic fractionation process or may be related to primordial mantle isotopic heterogeneity. Thus a simple tool to identify subducted C if any in the carbonatites would be to look for $\delta^{15}N > 0$, associated with $\delta^{13}C$ signatures signifying subduction.

- Our recent study on some of the Indian carbonatites as well as other carbonatites from different parts of the world indicates a plume origin for these rocks. These plumes seem to originate from the LM and maybe from as deep as the core-mantle boundary. Carbonatites can therefore be appropriate samples to look for evidences of entrainment of outer core metal to the D" layer, the probable source for these carbonatites. This should be reflected in coupled enrichment of ^{186}Os and ^{187}Os and a positive correlation between the two ratios $^{186}Os/^{188}Os$ and $^{187}Os/^{188}Os$ should be observed. Such a trend for Os isotopes has been observed from isotopic analyses of picritic lavas from Hawaii (Brandon et al., 1998). By corollary observation of such enrichments in carbonatites would confirm their origin from the D" layer and occurrence of core-mantle interaction.
- The origin of carbonatites, whether from a carbonated primary magma or from carbonate-silicate melt immiscibility has been a matter of debate. Noble gas isotopic studies of trapped gases in the associated alkaline rocks and comparing them with that of the carbonatites may provide a straightforward answer. In case they are derived from the same source by liquid immiscibility, the isotopic ratios would be identical for both, but concentration of noble gases should be higher for the carbonatites as noble gases tend to partition into CO_2 and carbonated melts from coexisting silicates (Patterson et al., 1994).
- A point of much discussion presently is the fractionation of N isotopes during degassing. Such a fractionation has been advocated from the study of MORB vesicles and melts (Cartigny et al., 2001b). Fractionation during outgassing should

see the vesicles depleted in ^{15}N relative to the residual melt. Carbonatites with phases like calcites and apatites that are rich in fluid inclusions would be appropriate samples for such study. A coupled N and noble gas study would be necessary as noble gas isotopic ratios can indicate if melt and vesicles are in equilibrium, and if the non equilibrium exist due to some other processes like late addition of air/recycled component. In case if both vesicles and melt are in equilibrium for noble gases, disequilibrium for N isotopic composition may be investigated for fractionation during processes like degassing.

Appendix

Some technical terms used in the body of the thesis have been abbreviated for the sake of convenience. They have been explained in this appendix.

δ value to express isotopic composition of N: Nitrogen is an element with two stable isotopes namely ^{14}N and ^{15}N, of which ^{14}N is far more abundant (99.63%). The terrestrial atmosphere with a uniform $^{15}N/^{14}N$ ratio of 0.003676 serves as the standard for the nitrogen isotopic measurements. The N isotopic composition of a sample is expressed as the deviation of the $^{15}N/^{14}N$ ratio from that of the terrestrial atmosphere (Air), Symbolically it is represented as

$$\delta^{15}N(‰) = \left[\frac{\left({}^{15}N/{}^{14}N \right)_{sample}}{\left({}^{15}N/{}^{14}N \right)_{air}} - 1 \right] \times 10^{3}$$

The multi component mantle: The dominant rock type of the mantle is believed to be the peridotites. They are predominantly made up of olivine $(MgFe)_2SiO_4$, with lesser amounts of orthopyroxene $(MgFe)SiO_3$ and clinopyroxene $Ca(MgFe)Si_2O_6$. Plate tectonics is driven by solid state mantle convection which carries deep mantle material upward till it melts. The melt rises to the surface and extrudes as basaltic lavas. **Basalts** are rocks formed by 2-5% melting of peridotite under ridges (MORBs) and ocean islands(OIBs). **EM-1** and **EM-2** basalts are enriched OIBs having isotopic similarities with that of recycled continental materials while **HIMU** basalts are OIBs having similarities with that of recycled oceanic crust. When the mantle melts some elements (incompatible) are concentrated in the liquid state while others (compatible) remain in the solid minerals. This results in elemental fractionation that eventually manifests as isotopic differences. The EM-1 basalts are characterized by high Rb/Sr, and low U/Pb and Sm/Nd ratios. The EM-2 basalts have high Rb/Sr(> EM-1) and U/Pb, with low Sm/Nd ratios. HIMU (High-mu i.e. $^{238}U/^{204}Pb$) basalts represent mantle sources with high U/Pb ratios. DMM represents depleted MORB source having low Rb/Sr and U/Pb with high Sm/Nd ratios. Elemental fractionation also occurs depending on whether the elements are lithophile

(bond with oxygen and are concentrated in the silicate earth) or **siderophile** (dissolve readily in metallic iron under moderately reducing conditions and are concentrated in the core of the Earth).

Andesites: During the process of subduction, the lithosphere slides back into the mantle beneath island arcs often at an angle of 45°. Subsequently, it might be stored in the mantle or reappear as volcanism. **Andesites** are rocks with higher SiO_2 than basalts and are produced in such subduction zone settings. They are mostly composed of plagioclase feldspars and amphiboles and are generally believed to be the partial melt products of water rich subducting oceanic crustal basalts or the intervening wedge of the lower crustal rocks above the subducting plate.

Phase transformations in the mantle: Experimental evidences suggest that the olivine component of the peridotite undergoes successive pressure dependent transformations to the spinel structure **(ringwoodite)** and ultimately breaks down to form perovskite magnesiowustite. The transformations that occur in the mantle are the following:

$(MgFe)_2SiO_4 = (MgFe)_2SiO_4$ (13-14 GPa, depth - 410 km)
Olivine **Wadsleyite**
$(MgFe)_2SiO_4 = (MgFe)_2SiO_4$ (18 GPa, 520 km)
Wadsleyite = Ringwoodite
$(MgFe)_2SiO_4 = (MgFe)SiO_3 + (MgFe)O$ (23 GPa, depth - 660 km)
Perovskite magnesiowustite

The pressure and depths of the transformations have also been indicated. The depths of the transformations can be related to major global seismic discontinuities.

References

Allegre C.J. (1997) Limitation on the mass exchange between the upper and the lower mantle: the evolving convection regime of the Earth. *Earth. Planet. Sci. Lett.* **150** 1-6.

Anderson T. (1987) Mantle and crustal components in a carbonatite complex, and the evolution of carbonatite magma: REE and isotopic evidence fro the Fen complex, southeast Norway. *Chem Geol* **65** 147-166.

Andrews J.N., Hussain N. and Youngman M.J. (1989) The in situ production of radioisotopes in rock minerals with particular reference to the Stripa granite. *Geochim. Cosmochim. Acta.* **53** 1803-1805.

Ballentine C.J. and Barford D.N. The origin of air-like noble gases in MORB and OIB. *Earth. Planet. Sci. Lett.* **180** 39-48.

Basu A.R., Renne P.R., Das Gupta D.K., Teichman F. and Poreda R.J. (1993) early and late alkali igneous pulses and a high 3He plume origin for the Deccan flood basalts. *Science* **261** 902-906.

Basu S. and Murty S.V.S. (2003) Mantle gases in carbonatites. *Geochimica Cosmochimica Acta.* **A34,** 67.

Basu S. and Murty S.V.S.(2002) Nitrogen and argon in carbonatites from India. *18th General meeting of the International Mineralogical Association, Edinburgh.* **MT6,** 246.

Basu S., Murty S.V.S. and Kumar A.(2003) U, Th-^{21}Ne.dating and its applications. *Proc. Of the ISMAS Silver Jubilee Symposium on Mass Spectrometr.* 581-584.

Beaumont V. and Robert F. (1999) Nitrogen isotopic ratios of kerogens in Precambrian cherts: A record of the evolution of atmosphere chemistry? *Precamb. Res.* **96** 63-82.

Bebout G.E. and Fogel M. (1992) Nitrogen isotope compositions of metasedimentary rocks in the Catalina Schist, California: implications for metamorphic devolatilization history. *Geochim. Cosmochim. Acta* **56** 2839-2849.

Becker T.W., Kellogg J.B. and O'Connell R.J. (1999) Thermal constrains on the survival of primitive blobs in the lower mantle. *Earth. Planet. Sci. Lett.* **171** 351-365.

Bell K. (2002) Probing The Mantle: The Story From Carbonatites. *EOS, Transactions, American Geophysical Union* **83** no. 25.

Bell K. and Blekinshop J. (1989) Neodymium and Sr isotope geochemistry of carbonatites. In *Carbonatites: Genesis and evolution* (ed. K. Bell) Unwin Hyman Ltd, London 278-297.

Bell K. and Tilton G.R. (2001) Nd, Pb and Sr Isotopic Compositions of east African Carbonatites: Evidence for Mantle mixing and Plume Inhomogeneity. *J. Petrol.* **42** 1927-1945.

Boyd S.R., Hall A. and Phillinger C.T. (1993) The measurement of $\delta^{13}C$ in crustal rocks by static vacuum mass spectrometry: applications to the origin of the ammonium in the Cornubian batholith, S.W. England. *Geochim. Cosmochim. Acta* .**57** 1339-1347.

Brandon A.D., Walker R.J., Morgan J.W., Norman M.D. and Prichard H.M. (1998) Coupled ^{186}Os and ^{187}Os Evidence for Core-Mantle interaction. *Science* **280** 1570-1573.

Brooker R.A. (1998) The effect of CO2 saturation on immiscibility between silicate and carbonate liquids.: an experimental study. *J. Petrol.* **39** 1905-1915.

Browne J.C. and Berman B.L. (1973) Neutron-capture cross sections for ^{128}Te and ^{130}Te and the Xe anomaly in old tellurium ores. *Phys. Rev. C* **8** 2405-2411.

Burnard P. (1999) The bubble-by-bubble volatile evolution of two mid-ocean ridge ridge basalts. *Earth. Planet. Sci. Lett*. **174** 199-211.

Burnard P., Graham D. and Turner G. (1997) Vesicle-Specific Noble Gas Analyses of "Popping Rock": Implications for Primordial Noble Gases in Earth. *Science* **276** 568-571.

Busigny V., Cartigny P., Philippot P., Magali A. and Javoy M. (2003) Massive recycling of nitrogen and other fluid mobile elements (K, Rb, Cs, H) in a cold slab environment: evidence from HP to UHP oceanic metasediments of the Schistes Lustres nappe (western Alps, Europe). *Earth. Planet. Sci. Lett*. **6809** 1-16.

Cartigny P. and Ader M. (2003) A comment on "The nitrogen record of crust-mantle interaction and mantle convection from the Archean to Present". *Earth. Planet. Sci. Lett*. **6836** 1-8.

Cartigny P., Boyd S. R., Harris J. W. and Javoy M. (1997) Nitrogen isotopes in peridotitic diamonds from Fuxian China: the mantle signature. *Terra Nova* **9** 175-179.

Cartigny P., Harris J. W. and Javoy M. (2001a) Diamond genesis, mantle fractionations and mantle nitrogen content: a study of δ^{13}C-N concentrations in diamonds. *Earth. Planet. Sci. Lett*. **185** 85-98.

Cartigny P., Harris J. W., Taylor A., Davies R. and Javoy M. (2003) On the possibility of a kinetic fractionation of nitrogen stable isotopes during natural diamond growth. *Geochim. Cosmochim. Acta* .**67** 1571-1576.

Cartigny P., Harris J.W., Pineau F., Phillips D., Girard M. and Javoy M. (1998) Subduction related diamonds? - The evidence for a mantle-derived origin from coupled δ^{13}C-δ^{15}N determinations. *Chem Geol* **147** 147-159.

Cartigny P., Jendrzejewski N., Pineau F., Petit E. and Javoy M. (2001b) Volatile (C, N, Ar) variability in MORB and the respective roles of mantle source heterogeneity and degassing: the case of the Southwest Indian Ridge. *Earth. Planet. Sci. Lett*. **194** 241-257.

Condie K.C., Allen P. and Narayana B.L. (1982) Geochemistry of the Archean low to high grade transition zone of Southern India. *Contrib. Mineral. Petrol.* **81** 157-167.

Dauphas N. and Marty B. (1999) Heavy Nitrogen in Carbonatites of the Kola Peninsula: A possible signature of the Deep Mantle. *Science* **286** 2488-2490.

Eikenberg J., Koppel V., Labhard T. and Signor P. (1989) U-Pb, U-Xe and U-Kr systematics of a greenschist facies metamorphic uranium mineralisation of the Siviez-Mischabel nappe (Valais, Switzerland). *Schweiz. Mineral. Petrogr. Mitt.* **69** 331-344.

Eikenberg J., Signer P. and Weiler R. (1993) U-Xe U-Kr and U-Pb systematics for dating uranium minerals and investigations of the production of nucleogenic neon and argon. *Geochim. Cosmochim. Acta.* **57** 1053-1069.

Farley K. A., Wolf R. A., and Silver L. T., (1996) The effects of long alpha-stopping distances on U-Th/He ages. *Geochim. Cosmochim. Acta.* **60** 4223-4229.

Farley K.A. (2000) Helium diffusion from apatite: General behaviour as illustrated by Durango fluorapatite. *J. Geophys. Res.* **105** 2903-2914.

Farley K.A., Poreda R.J. and Onstott T.C. (1994) Noble Gases in Deformed Xenoliths from an Ocean Island: Characterization of a Metasomatic Fluid. In *Noble Gas Geochemistry and Cosmochemistry* (ed. J. Matsuda) Terra Scientific Publishing Company, Tokyo 159-178.

Fischer T. P., Hilton D.R., Zimmer M.M., Shaw A.M., Sharp Z.D. and Walker J.A. (2002) Subduction and Recycling of Nitrogen Along the Central American Margin. *Science* **297** 1154-1157.

Fisher D.E. (1997) Helium, argon, and xenon in crushed and melted MORB. *Geochim. Cosmochim. Acta.* **61** 3003-3012.

Frick U. and Pepin R.O. (1981) Microanalyses of nitrogen isotopes abundances: association of nitrogen with noble gas carriers in Allende. *Earth. Planet. Sci. Lett*. **56** 64-81.

Gerling E.K. and Shukolyokov Yu. A. (1960) The composition and contents of xenon isotopes in uranium minerals. *Radiochemistry* **1** 106-118.

Grady C. (1971) Deep main faults in South India. *J. Geol. Soc. India.* **12** 56-62.

Graham D.W. (2002) Noble Gas Isotope Geochemistry of Mid-Ocean Ridge and Ocean Island Basalts: Characterization of Mantle Source Reservoirs. In *Noble Gases in Geochemistry and Cosmochemistry* (ed. D. Porcelli., C.J. Ballentine and R.Weilers) Mineralogical Society of America Washington DC 247-318.

Griffiths R.W. and Campbell I. A. (1990). Stirring and structure in mantle starting plumes. *Earth. Planet. Sci. Lett*. **99** 66-78.

Grunenfelder M.H., Tilton G.R., Keith B. and Blekinson J. (1986) Lead and strontium isotope relationships in the Oka carbonatite complex, Quebec. *Geochim. Cosmochim. Acta* .**50** 461-468.

Haendel D., Muhle K., Nitzsche H., Stiehl G. and wand U. (1986) Isotopic variations of the fixed nitrogen in metamorphic rocks. *Geochim. Cosmochim. Acta* .**50** 749-758.

Hanyu T. and Kaneoka I. (1997) Magmatic processes revealed by noble gas signatures: the case of Unzen volcano Japan. *Geochem. J.* **31** 395-405.

Harrison D., Burnard P.G., Trieloff M. and Turner G. (2003) Resolving atmospheric contaminants in mantle noble gas analyses. *Geochem. Geophys. Geosyst.* **4** 1-17.

Hashizume K., Kase T., Matsuda J. and Sato H. (1997) On the siderophile behaviour of nitrogen and carbon: Implications for their inventory in the Earth. *Kazan* **42** S293.

Hawkesworth C., Kempton P.D., Rogers N.W., Ellam R.M. and Calsteren P.W. (1990) Continental mantle lithosphere, and shallow level enrichment processes in the Earth's mantle. *Earth. Planet. Sci. Lett*. **96** 256-268.

Helffrich G.R. and Wood B.J. The Earth's mantle. *Nature* **412** 501-507.

Hofmann A.W. (1997) Mantle geochemistry: the message from oceanic volcanism. *Nature* **385** 219-229.

Honda M. and Mcdougall I. (1998) Primordial helium and neon in the Earth- A speculation on early degassing. *Geophys. Res. Lett.* **25** 1951-1954.

Honda M. and Patterson D.B. (1999) Systematic elemental fractionation of mantle-derived helium, neon, and argon in mid-oceanic ridge glasses. *Geochim. Cosmochim. Acta.* **63** 2863-2874.

Honda M., Macdougall I., Patterson D., and Doulgeris A. and Clague D. (1991) *Nature* **349** 149.

Honda M., Phillips D., Harris J. W. and Yatsevich I. (2004) Unusual noble gas compositions in polycrystalline diamonds: preliminary results from the Jwaneng kimberlite, Botswana. *Chem. Geol*. **203** 347-358.

Hunemohr H. (1989) Edelgase in U- und Th-reichen Mineralen und die Bestimmung der ^{21}Ne-Dicktarget-Ausbeute der $^{18}O(\alpha,n)^{21}Ne$ -kernreaktion in Bereich 4.0-8.8 MeV. *Ph.D. thesis* 159 pp., Johannes Gutenberg-Univ. Mainz, Mainz Gemany.

Ingle S., Weis D., Doucet S. and Mattielli N. (2003) Hf isotope constraints on mantle sources and shallow level contaminants during Kerguelen hot spot activity since ~120 Ma. *Geochem. Geophys. Geosyst.* **4** 1-28.

Jambon A., Weber H.W. and Begemann F. (1985) Helium and argon from an Atlantic MORB glass: concentration, distribution and isotopic composition. *Earth. Planet. Sci. Lett*. **73** 255-267.

Javoy M. (1997) The major volatile elements of the Earth: Their origin, behaviour, and fate. *Geophys. Res. Lett.* **24** 177-180

Javoy M. (1998) The birth of the Earth's atmosphere: the behaviour and fate of its major elements *Chem Geol* **147** 11-25.

Javoy M. (1999) Chemical Earth models. *Earth. Planet. Sci.* **329** 537-555.

Javoy M. and Pineau F. (1983) Stable isotope constraints on a model Earth from a study of the mantle nitrogen. *Meteoritics* **18** 320-321.

Javoy M. and Pineau F. (1991) The volatile record of a popping rock from the Mid-Atlantic ridge at 14°N: chemical and isotopic composition of gas trapped in the vesicles. *Earth. Planet. Sci. Lett*. **107** 598-611.

Javoy M., Pineau F., Staudacher T., Cheminee J.L. and Krafft M. (1989) Mantle volatiles sampled from a continental rift: The 1988 eruption of Oldoinyo Lengai (Tanzania). *Terra* **1** 324 (abstr.).

Kale V.S. (1998) Proterozoic Geohistory of Indian peninsula in the perspective of supercontinental regimes. In The Indian Precambrian (ed. B.S. Paliwal) Scientific Publishers (India) 128-141.

Kaneoka I. (1998) Noble gas signatures in the Earth's interior-coupled or decoupled behaviour among each isotope systematics and problems related to their implication. *Chem. Geol*. **147** 61-76.

Kaneoka I., Takaoka N. and Upton B.G.J. (1986) Noble Gas Systematics in Basalts and a Dunite Nodule from Reunion and Grand Comore Islands, Indian ocean. *Chem. Geol*. **59** 35-42.

Kellogg L.H., Hager B.H. and Hilst R.D. (1999) Compositional Stratification in the Deep Mantle. *Science* **283** 1881-1884.

Kennedy B.M., Hiyagon H., and Reynolds J. H. (1990) Crustal neon: a striking uniformity. *Earth. Planet. Sci. Lett*.. **98,** 277-286.

Kent R.W., Storey M. and Saunders A.D. (1992) Large igneous provinces: Site of plume impact or plume incubation? Geology 20 891-894.

Komiya T., Maruyama S., Masuda T., Nohda S., Hayashi M. and Okamoto K. (1999) Plate tectonics at 3.8-3.7 Ga: field evidence from the Isua accretionary complex, southern west Greenland. *J. Geol.* **107** (1999) 515-554.

Kramm U. and Kogarko L.N. (1994) Nd and Sr isotopic signatures of the Khibina and Lovozero agpaitic centres, Kola alkaline province, Russia. *Lithos* **32**, 225-242.

Krishnamurthy P. (1988) Carbonatites of India. *Expl. Res. Atomic Min.* **1** 81-115.

Kumar A. and Gopalan K. (1991) Precise Rb-Sr age and enriched mantle source of the Sevattur carbonatites, Tamil Nadu, South India. *Current Science* **60** 653-655.

Kumar A., Charan S.N., Gopalan K. and Macdougall J.D. (1998) A long-lived enriched mantle source for two Proterozoic carbonatite complexes from Tamil Nadu, Southern India. *Geochim. Cosmochim. Acta.* **62** 515-523.

Kumar D., Mamallan R. and Dwivedy K.K. (1996) Carbonatite magmatism in northeast India. *J. Southeast Asian Earth Sci.* **13** 145-158.

Kwon S-T., Tilton G.R. and Grunenfelder M.H. (1989) Lead isotope relationships in carbonatites and alkalic complexes: An overview. In *Carbonatites: Genesis and evolution* (ed. K Bell) Unwin Hyman Ltd, London 360-387.

Leya I. and Wieler R. (1999) Nucleogenic production of Ne isotopes in Earth's crust and upper mantle induced by alpha particles from the decay of U and Th. *J. Geophys. Res.* **104(B7)** 15439-15450.

Libourel G., Marty B. and Humbert F. (2003) Nitrogen solubility in basaltic melt. Part I. Effect of oxygen fugacity. *Geochim. Cosmochim. Acta* .**67** 4123-4135.

Lippolt H.J., Leitz M., Wernicke R.S. and Hagedorn B. (1994) (U+Th)/He dating of apatite: experience with samples from different geochemical environments. *Chem Geol.* **112** 179-191.

Martin H. (1986) Effect of steeper Archean geothermal gradient on geochemistry and subduction-zone magmas. *Geology* **14** 753-756.

Marty B. (1995) Nitrogen content of the mantle inferred from N2-Ar correlation in oceanic basalts. *Nature* **377** 326-329.

Marty B. and Dauphas N. (2003) 'Nitrogen isotopic compositions of the present mantle and the Archean biosphere": Reply to comment by Pierre Cartigny and Magali Ader *Earth. Planet. Sci. Lett*. **216** 433-439.

Marty B. and Humbert F. (1997) Nitrogen and argon isotopes in oceanic basalts. *Earth. Planet. Sci. Lett*. **152** 101-112.

Marty B., Gunnlaugsson E., Jambon A., Oskarsson N., Ozima M., Pineau F. and Torssander P. (1991) Gas geochemistry of geothermal fluids, the Hengill area, southwest rift zone of Iceland. *Chem Geol* **91** 207-225.

Marty B., Lenoble M. and Vassard N. (1995) Nitrogen, helium and argon in basalt: a static mass spectrometry study. *Chem. Geol.* **120** 183-195.

Marty B., Zashu S. and Ozima M. (1983) Two noble gas components in a Mid-Atlantic Ridge basalt. *Nature* **302** 238-240.

Marty M., Tolstikhin I., Kamensky I. L., Nivin V., Balaganskaya E. and Zimmermann J.L. (1998) Plume-derived rare gases in 380 Ma carbonatites from the Kola region (Russia) and the argon isotopic composition in the deep mantle. *Earth. Planet. Sci. Lett*. **164** 179-192.

Mason B. and Moore C.B. (1982) Principles of Geochemistry 4th ed., J. Wiley New York.

Matsumoto T., Chen Y. and Matsuda J. (2001) Concomitant occurrence of primordial and recycled noble gases in the Earth's mantle. *Earth. Planet. Sci. Lett*. **185** 35-47.

Matsumoto T., Honda M., McDougall I., Yatsevich I. and O'Reilly S.Y. (1997) Plume-like neon in a metasomatic apatite from the Australian lithospheric mantle. *Nature* **388** 162-164.

Meshik A.P., Kehm K. and Hohenberg C.M. (2000a) Anomalous xenon in zone 13 Okelobondo. *Geochim. Cosmochim. Acta* .**64** 1651-1661.

Meshik A.P., Lippolt H.J. and Dymkov Yu. M. (2000b) Xenon geochronology of Schwarzwald pitchblendes. *Mineralium Deposita* **35** 190-205.

Miyazaki A., Hiyagon H., Sugiura N., Hirose K. and Takahashi E. (2004) Solubilities of nitrogen and noble gases in silicate melts under various oxygen fugacities: Implications for the origin and degassing history of nitrogen and noble gases in the Earth. *Geochim. Cosmochim. Acta* .**68** 387-401.

Mohapatra R. (1998) Study of the abundance and isotopic composition of nitrogen in Earth's mantle. *Ph.D. Thesis.* Maharaja Sayajirao University of Baroda, Baroda India.

Mohapatra R. and Murty S.V.S. (2004) Nitrogen isotopic composition of the MORB mantle: A reevaluation. *Geochem. Geophys. Geosyst.* **5** 1-9.

Mohapatra R.K. and Murty S.V.S. (2000a) Origin of air like noble gases in oceanic basalts. *Geophys. Res. Lett.* **27** 1583-1586.

Mohapatra R.K. and Murty S.V.S. (2000b) search for mantle nitrogen in the ultramafic xenoliths from San Carlos, Arizona. *Chem. Geol.* **164** 305-320.

Moreira M. and Sarda P. (2000) Noble gas constraints on degassing processes. *Earth. Planet. Sci. Lett*. **176** 375-386.

Moreira M., Kunz J. and Allegre C. (1998) Rare Gas Systematics in popping Rock: Isotopic and Elemental Composition in the Upper Mantle. *Science* **279** 1178-1181.

Murty S.V.S and Mahajan R.R. (2003) Vacuum Crushing Technique for the Study of Trapped Noble Gases in Planetary Samples. ISMAS 2003 *ISMAS Silver Jubilee. Symp. Mass. Spectr.* 570-573.

Nelson D.R., Chivas A.R., Chappell B.W. and McCulloch M.T. (1988) Geochemical and isotopic systematics in carbonatites and implications for the evolution of the ocean-island sources. *Geochim. Cosmochim. Acta* .**52** 1-17.

Ozima M. and Alexander Jr. C. (1976) Rare Gas Fractionation Patterns in Terrestrial Samples and the Earth-Atmosphere Evolution Model. *Rev. of Geophys.* **14** 385-390.

Ozima M. and Podosek F. A. (2002) In *Noble Gas Geochemistry* Cambridge University Press (second edition).

Pandit M.K., Sial A.N., Sukumaran G.B., Pimentel M.M., Ramaswamy A.K. and Ferreira V.P. (2002) Depleted and enriched mantle sources for Paleo- and Neoproterozoic carbonatites of Southern India: Sr, Nd, C-O isotopic and geochemical constraints. *Chem. Geol.* **189** 69-89.

Patterson D.B., Honda M. and Mcdougall I. (1994) Atmospheric, MORB-Like, and Crustal-Derived Noble Gas Components in Subduction-Related Samples. In *Noble Gas Geochemsitry and Cosmochemistry* (ed. J. Matsuda) Terra Scientific Publishing Company, Tokyo 147-158.

Pearson D.G., Shirey S.B., Harris J.W. and Carlson R.W. (1998) Sulphide inclusions in diamonds from the Koffiefontein kimberlite, S Africa: Constraints on diamond ages and mantle Re-Os systematics. *Earth. Planet. Sci. Lett*. **160** 311-326.

Peters K.E., Sweeney R.E. and Kaplan I.R. (1978) Correlation of carbon and nitrogen stable isotope ratios in sedimentary organic matter. *Limnol. Oceanogr.* **23** 598-604.

Pinti D.L., Hashizume K. and Matsuda J. (2001) Nitrogen and argon signatures in 3.8 to 2.8 Ga metasediments: Clues on the chemical state of the Archean ocean and the deep biosphere. *Geochim. Cosmochim. Acta* **65** 2301-2315.

Porcelli D. and Ballentine C.J. (2002) Models for the Distribution of Terrestrial Noble Gases and Evolution of the Atmosphere. In *Reviews in Mineralogy and Geochemistry* (ed. Porcelli D., Ballentine C.J. and Wieler R) The Mineralogical Society of America 411-480.

Prombo C. A. and Clayton R. N. (1993) Nitrogen isotopic compositions of iron meteorites. *Geochim. Cosmochim. Acta*.. **57,** 3749-3761.

Proussevitch A.A., Sahagian D.L. and Anderson A.T. (1993) Dynamics of diffusive bubble growth in magmas: isothermal case. *J. Geophys. Res*. **98** 22283-22307.

Ray J.S. and Pande K. (1999) Carbonatite alkaline magmatism associated with continental flood basalts at stratigraphic boundaries: cause for mass extinctions *Geophys. Res. Lett.* **26,** 1917-1920.

Ray J.S., Ramesh R. and Pande K. (1999) Carbon isotopes in Kerguelen plume-derived carbonatites: evidence for recycled inorganic carbon. *Earth. Planet. Sci. Lett*. **170** 205-214.

Ray J.S., Trivedi J.R. and Dayal A.M. (2000) Strontium isotope systematics of Amba Dongar and Sung Valley carbonatite-alkaline complexes, India: evidence for liquid immiscibility, crustal contamination and long-lived Rb/Sr enriched mantle sources. *J. of Asian Earth Sci.* **18** 585-594.

Reiners P.W. and Farley K.A. (1999) Helium diffusion and (U-Th)/He thermochronometry of titanite. *Geochim. Cosmochim. Acta.* **63** 3845-3859.

Reiners P.W. and Farley K.A. (2001) Influence of crystal size on apatite 9U-Th)/He thermochronology: an example from the Bighorn Mountains, Wyoming. *Earth. Planet. Sci. Lett*. **188** 413-420.

Richardson S. H., Shirey S.B., Harris J.W. and Carlson R.W. (2001) Archean subduction recorded by Re-Os isotopes in eclogite sulphide inclusions in Kimberley diamonds. *Earth. Planet. Sci. Lett*. **191** 257-266.

Richet P., Bottinga Y. and Javoy M. (1977) A Review of Hydrogen, Carbon, Nitrogen, Oxygen, Sulphur, and Chlorine Stable isotope Fractionation among Gaseous Molecules. *Ann. Rev. Earth Planet. Sci.* **5** 65-110.

Saasada T., Hiyagon H., Bell K. and Ebihara M. (1997) Mantle derived noble gases in carbonatites. *Geochim. Cosmochim. Acta.* **61** 4219-4228.

Sano Y., Takahata N., Nishio Y., Fischer T.P. and Williams S.N. (2001) Volcanic flux of nitrogen from the Earth. *Chem. Geol*. **17** 263-271.

Sarda P., Staudacher T. and Allegre C. J. (1988) Neon isotopes in submarine basalts *Earth. Planet. Sci. Lett*. **91** 73-88.

Sarda P., Staudacher T. and Allegre C.J. (1985) $^{40}Ar/^{36}Ar$ in MORB glasses: constraints on atmosphere and mantle evolution. *Earth. Planet. Sci. Lett*. **72** 357-375.

Schleicher H., Kramm U., Pernicka E., Schidlowski M., Schmidt F., Subramanian V., Todt W. and Viladkar S. (1998). Enriched subcontinental upper mantle beneath southern India: evidence from Pb,Nd, Sr, and C-O isotopic studies on Tamil Nadu carbonatites. *J. Petrol.* **39** 1765-1785.

Secher K. and Larson L.M. (1980) Geology and mineralogy of the Sarafartoq carbonatite complex, southern West Greenland. *Lithos* **13**, 199-212.

Shukolyukov Y.A., Jessberger E.K., Meshik A.P., Minh D.V. and Jordan J.L. (1994) Chemically fractionated fission xenon in meteorites and on the Earth. *Geochim. Cosmochim. Acta.*. **58,** 3075-3092.

Simonetti A., Goldstein S.L., Schmidberger S.S. and Viladkar S.G. (1998) Geochemical and Nd, Pb, and Sr Isotope Data from Deccan Alkaline Complexes- Inferences for Mantle Sources and Plume-Lithosphere Interaction. *J. Petrol.* **39** 1847-1864.

Sparks R.S.J. (1978) The dynamics of bubble formation and growth in magmas: a review and analysis, *J. Volcanol. Geotherm. Res.* **3** 1-37.

Sparks R.S.J., Barclay J., Jaupart C., Mader H.M. and Phillips J.C. (1994) Physical aspects of magma degassing I: Experimental and theoritical constraints on vesciculation. In *Volatiles in Magmas, Reviews in*

*Mineralogy **30*** (ed. M.R. Carroll and J.R. Holloway) Mineralogical Society of America, Washington, DC 414-445.

Staudacher T. and Allegre C. J. (1988) Recycling of oceanic crust and sediments: the noble gas subduction barrier. *Earth. Planet. Sci. Lett*. **89** 173-183.

Stuart F., Turner G. and Taylor R. (1994) He-Ar Isotope Systematics of Fluid Inclusions: Resolving Mantle and Crustal Contributions to Hydrothermal fluids. In *Noble Gas Geochemistry and Cosmochemistry* (ed. J. Matsuda) Terra scientific Publishing Company Tokyo 261-277.

Subramanian V., Viladkar S.G. and Upendran R. (1978) Carbonatite alkalic complex of Samalpatti, Dharampuri district, Tamil Nadu. *J. Geol. Soc. India* **19** 206-216.

Tolstikhin I.N. and Marty B. (1998) The evolution of terrestrial volatiles: a view from helium, neon, argon and nitrogen isotope modelling. *Chem Geol.* **147** 27-52.

Tolstikhin I.N., Kamensky I.L., Marty B., Nivin V.A., Vetrin V.R., Balaganskaya E.G., Ikorsky S.V., Gannibal M.A., Weiss D., Verhulst A. and Demaiffe D. (2002) Rare gas isotopes and parent trace elements in ultrabasic-alkaline-carbonatite complexes, Kola Peninsula: Identification of lower mantle plume component. *Geochim. Cosmochim. Acta.* **66** 881-901.

Tonks W.B. and Melosh H.J. (1990) The Physics of Crystal Settling and Suspension in a Turbulent Magma Ocean. In Newsom H.E. and Jones J.H. (Eds) *Origin of the earth.* Oxford Univ. Press, New York.151-174.

Trieloff M., Kunz J. and Allegre C.J. (2002) Noble gas systematics of the reunion mantle plume source and the origin of primordial noble gases in Earth's mantle. *Earth. Planet. Sci. Lett*. **200** 297-313.

Trieloff M., Kunz J., Clague D.A., Harrison D. and Allegre C.J. (2000) The nature of pristine noble gases in mantle plumes. *Science* **288** 1036-1038.

Turekian K.K. (1990) The parameters controlling planetary degassing based on based on ^{40}Ar systematics. In From mantle to meteorites. (ed. Gopolan K., Gaur V.K., Somayajulu B.L.K. and Macdougall J.D. Indian Acad Sci, Bangalore 147-152.

Veena K., Pandey B.K., Krishnamurthy P. and Gupta J.N. (1991) Pb, Sr and Nd isotopic systematics of Sung Valley, Meghalaya, India: Implication for contemporary sub-crustal upper mantle characterisation. *5th Ntl. Symp. Mass. Spectr.* EPS-19/1-EPS-19/4.

Veena K., Pandey B.K., Krishnamurthy P. and Gupta J.N. (1998) Sr and Nd isotopic systematics of Sung Valley, Meghalaya, Northeast India: Implication for contemporary plume-related mantle source characteristics. *J. Petrol.* **39** 1975-1984.

Viladkar S.G. (1981) The carbonatites of Ambadongar, Gujarat, India. *Bull. Geol. Soc. Finland*. **53** 17-28.

Viladkar S.G. and Subramanian V. (1995) Mineralogy and geochemistry of the carbonatites of the Sevathur and Samalpatti complexes, Tamil Nadu. *J. Geol. Soc. India* **45** 379-398.

Viladkar S.G. and Schidlowski M. (2000) Carbon and Oxygen Isotope Geochemistry of the Amba Dongar Carbonatite Complex, Gujarat, India. *Gond. Res.* **3** 415-424.

Vlaar N.J., Keken P.E. and Berg A.P. (1994) Cooling of the Earth in the Archaean: Consequences of pressure-release melting in a hotter mantle. *Earth. Planet. Sci. Lett*. **121** 1-18.

Warnock A.C.,Zeitler P.K., Wolf R.A. and Bergman S.C. (1997) An evaluation of low-temperature apatite U-Th/He thermochronometry. *Geochim. Cosmochim. Acta.* **61** 5371-5377.

Wetherill G.W. (1954) Variations in the isotopic abundances of neon and argon extracted from radioactive minerals. *Phys. Rev.* **96,** 679-683.

Williams-Jones A.E. and Palmer D.A.S. (2002) The evolution of aqueous-carbonic fluids in the Ambadongar carbonatite, India: Implications for fenitisation. *Chem. Geol*. **185** 283-301.

Wolf R.A., Farley K.A. and Silver L.T. (1996) Helium diffusion and low-temperature thermochronometry of apatite. *Geochim. Cosmochim. Acta.* **60** 4231-4240.

Wyllie P.J. (1989) Origin of carbonatites: evidence from phase equilibrium studies. In *Carbonatites: Genesis and evolution* (ed. K. Bell) Unwin Hyman Ltd, London 500-545.

Wyllie P.J. and Lee W.J. (1998) Model system controls on conditions for formation of magnesiocarbonatites and calciocarbonatite magmas from the mantle. *J. Petrol.* **39** 1885-1893.

Yatsevich I. and Honda M. (1997) Production of nucleogenic neon in the Earth from natural radioactive decay. *J. Geophys. Res* **102** 10291-10298.

Zeitler P.K., Herczig A.L., Mcdougall I. and Honda M. (1987) U-Th-He dating of apatite: a potential thermochronometer. *Geochim. Cosmochim. Acta.* **51** 2865-2868.